UNCLASSIFIED

AD NUMBER

AD827295

NEW LIMITATION CHANGE

TO

Approved for public release, distribution unlimited

FROM

Distribution authorized to U.S. Gov't. agencies and their contractors; Critical Technology; JAN 1968. Other requests shall be referred to Commanding General, U.S. Army Electronics Command, Attn: AMSEL-KL-PE, Fort Monmouth, NJ.

AUTHORITY

USAEC ltr, 16 Jun 1971

THIS PAGE IS UNCLASSIFIED

AD827295

AD

Research and Development Technical Report
ECOM- 87341-1

DEVELOPMENT OF A

GASOLINE FIRED THERMIONIC POWER SUPPLY

SUMMARY REPORT

D D C
RECEIVED
FEB 26 1968
D

by

L. J. Lazaridis and P. G. Pantazelos

January 1968

U.S. Army Electronics Command, Fort Monmouth, New Jersey

ECOM

UNITED STATES ARMY ELECTRONICS COMMAND · FORT MONMOUTH, N.J.

Contract No. DA36-039-SC-87341(E)

THERMO ELECTRON CORPORATION
Waltham, Massachusetts

DISTRIBUTION STATEMENT

This document is subject to special export controls and each transmittal to foreign governments or foreign nationals may be made only with prior approval of CG, U.S. Army Electronics Command, Fort Monmouth, N. J.

Attn: AMSEL-KL-PE

169

ACCESSION for
CFSTI WHITE SECTION ☐
DDC BUFF SECTION ☐
UNANNOUNCED ☐
JUSTIFICATION
BY
DISTRIBUTION/AVAILABILITY CODES
DIST. AVAIL. and/or SPECIAL
2

NOTICES

Disclaimers

The findings in this report are not to be construed as an official Department of the Army position, unless so designated by other authorized documents.

The citation of trade names and names of manufacturers in this report is not to be construed as official Government indorsement or approval of commercial products or services referenced herein.

Disposition

Destroy this report when it is no longer needed. Do not return it to the originator.

ECOM-87364-1 January 1968

DEVELOPMENT OF A GASOLINE-FIRED THERMIONIC POWER SUPPLY

SUMMARY REPORT

November 1961 to July 1966

Contract No. DA36-039-SC-87341(E)

Project No. 1T6-22001-A-053, Task No. 01, Subtask No. 09

Prepared by

L. J. Lazaridis and P. G. Pantazelos

Thermo Electron Corporation
Waltham, Massachusetts

For

U. S. Army Electronics Command, Fort Monmouth, N. J.

DISTRIBUTION STATEMENT

This document is subject to special export controls and each transmittal to foreign governments or foreign nationals may be made only with prior approval of CG, U. S. Army Electronics Command, Fort Monmouth, N. J.

Attn: AMSEL-KL-PE

ABSTRACT

This report summarizes the work performed by Thermo Electron Corporation to develop a gasoline-fired thermionic power supply. The work is divided into three phases:

1. The development of a gasoline burner capable of providing the high temperatures and high heat fluxes required by the thermionic converters.

2. The development of a thermionic converter with the required power output, efficiency, weight and life.

3. The design of a power supply utilizing the above two components and including power conditioning, controls and packaging.

The development of suitable oxidation protection for the converter's refractory-metal emitter is described, as well as the experimental evaluation of a variety of materials under conditions simulating a flame-heated thermionic converter. The development work on a flame-heated thermionic converter culminated in the recently completed Series VI-S Converter. The design, construction, and test of the potassium heat pipe used for collector cooling are also described. Test data is given, and a system design is presented.

TABLE OF CONTENTS

		Page
I.	INTRODUCTION AND SUMMARY	1
II.	EMITTER SHELL	5
	SHELL FABRICATION	24
	Tungsten Coating	24
	Silicon Carbide Coating	25
	Resistance-Heated Unit for Deposition of SiC	33
	SURFACE FINISHING OF TUNGSTEN	39
	Mechanical Finishing	39
	Electropolishing	41
III.	THERMIONIC CONVERTER	45
	SERIES VI-S DIODE	81
	DIODE CONSTRUCTION	83
	PREASSEMBLY COMPONENT TESTING	84
	TESTING OF SERIES VI-S DIODES	96
	HEAT-PIPE COLLECTOR	99
	TEST RESULTS	100
	IMPROVED SERIES VI DIODES	111
IV.	COMBUSTION SYSTEM	119
APPENDIX A	SYSTEM ANALYSIS	137
APPENDIX B	SINGLE-DIODE 45-WATT ENGINE DESIGN	155

LIST OF ILLUSTRATIONS

Figure		Page
II-1	Two Emitter Shells Under Test in Methane-Air Burners. .	16
II-2	Vacuum Profile of Silicon Carbide Shell.	19
II-3	Vacuum Profile of Another Silicon Carbide Shell.	20
II-4	Resistance-Heated Apparatus for Deposition of Tungsten.	26
II-5	Resistance-Heated Apparatus for Deposition of Tungsten. (dismantled condition)	28
II-6	Resistance-Heated Apparatus for Deposition of Tungsten. (assembled condition)	29
II-7	Induction-Heated Unit Assembled for SiC-Coating Run . . .	30
II-8	View of Induction-Heated Coating Unit Showing Rotating Seal Assembly (Upper-Left Quadrant), Induction Lead-Through (Left Center), and Coating Reactant-Feed Line (Foreground).	31
II-9	Induction-Heated Unit with Monel Bell Jar in Place for SiC-Coating Run.	32
II-10	Induction-Heated Unit for Deposition of SiC or Tungsten. .	35
II-11	Resistance-Heated Unit for Deposition of SiC.	36
II-12	Apparatus for Electropolishing Tungsten-Coated Shells. .	43
III-1	Cross Section of Series II Hydrocarbon-Fueled Thermionic Diode.	47
III-2	Exploded View of Hydrocarbon-Fueled Thermionic Diode.	48
III-3	Hydrocarbon-Fueled Thermionic Diode After Test in a Hydrocarbon Flame.	49
III-4	Outgassing Profile for Diode II-23.	61
III-5	Watt-Hour Profile for Diode II-23.	62

LIST OF ILLUSTRATIONS (continued)

Figure		Page
III-6	Performance Curves for Diode II-23	63
III-7	Outgassing Profile for Diode II-29	64
III-8	Watt-Hour Profile for Diode II-29	65
III-9	Performance Curves for Diode II-29	66
III-10	Model III Burner Driving Diode II-29	67
III-11	Power Density versus Time for Two Output Voltages for Diode II-31	68
III-12	Performance Curves for Diode II-31	69
III-13	Cross Section of Series III Diode	71
III-14	Series V Hydrocarbon-Fired Thermionic Diode Design	72
III-15	Series VI Hydrocarbon-Fired Thermionic Diode Design	75
III-16	Schematic Layout of Burner and Shell Under Test	79
III-17	Detail Drawing of Experimental Hydrocarbon-Fired Thermionic Converter, Series VI-S	85
III-18	Series VI-S Hydrocarbon-Fired Thermionic Converter	86
III-19	Exploded View of Diode VI-S	87
III-20	Cracked Shell as Recieved and Zygloed	89
III-21	Emitter Depth Gauge	90
III-22	Measuring Emitter Depth	91
III-23	Collector Length Gauge	92
III-24	Collector Length Measurement	93
III-25	Collector Concentricity Measurement	94
III-26	Diode Shell Temperature Profile	97
III-27	Collector Heat Pipe Test Data	98
III-28	Components and a Complete Heat Pipe	101
III-29	Schematic of Precalibrated Calorimeter	102

LIST OF ILLUSTRATIONS (continued)

Figure		Page
III-30	Calorimeter Set-Up	103
III-31	Calorimeter Calibration	104
III-32	Heat through Heat Pipe versus ΔT	105
III-33	Complete Heat Pipe - Collector Structure	106
III-34	Typical Life Test Set-Up	109
III-35	Diode I-V Curves from VI-5	110
III-36	Diode 66FL-08 After 170 Hours Test	112
III-37	Area of Jet Erosion of Diode 66FL-08 Resulting in Failure	113
III-38	Cratering on One Side of Diode	114
III-39	Flame-Heated Diode I-V Curves for 74FL-17	116
III-40	Envelope of 74FL-17 Curves Compared with Curves Obtained in 1966	117
IV-1	Experimental Set-Up for Evaluation of Model I Burners	121
IV-2	Heat Flux Density versus Simulated Emitter Temperature	122
IV-3	Emitter Temperature versus Ideal Air Power per Unit Heated Area	123
IV-4	Combustion System Pressure Drop	124
IV-5	Model II Burner Before Initial Test	125
IV-6	Model II Burner Under Test	126
IV-7	Emitter Temperature versus Combustion Chamber Exhaust Gas Temperature	127
IV-8	Model III Burner Driving Diode II-29	129
IV-9	Model IV Burner on Test	130
IV-10	Combustion Efficiency versus Emitter Temperature	133

LIST OF ILLUSTRATIONS (continued)

Figure		Page
IV-11	Model V Burner with Jet-Impingement Heat Exchanger	134
IV-12	Effectiveness versus Pounds per Hour	135
A-1	Schematic Diagram of Possible Hydrocarbon-Fired Thermionic Engine Configurations	139
A-2	Individual Diode Weight vs Gross Generated Diode Power for 1963	142
A-3	1963 Diode Efficiency vs Gross Generated Diode Power	143
A-4	Diode Weight vs Gross Generated Diode Power for 1965 Diodes	144
A-5	Diode Efficiency vs Gross Generated Diode Power for 1965 Diodes	145
A-6	1963 Dc-Dc Converter Efficiency vs Weight by Vendor	149
A-7	1965 Dc-Dc Converter Efficiency vs Weight by Vendor	150
A-8	Total System Weight vs Number of Diodes	153
B-1	Cross Section of Complete 45-Watt Generator	157

LIST OF TABLES

		Page
II-1	EMITTER SHELL MATERIAL REQUIREMENTS	[illegible]
II-2	RESULTS OF VACUUM ENCLOSURE MATERIALS EVALUATION	[illegible]
III-1	TEST CONVERTER SUMMARY, SERIES I DIODE	50
III-2	CONVERTER CHARACTERISTICS	53
A-1	WEIGHT AND EFFICIENCY OF 1463 HYDROCARBON-FIRED DIODE	141
A-2	WEIGHT AND EFFICIENCY OF 1463 HYDROCARBON-FIRED DIODE	141
A-3	WEIGHT AND EFFICIENCY OF 1463 DC-DC CONVERTER	147
A-4	WEIGHT AND EFFICIENCY OF 1463 DC-DC CONVERTER	148

1. INTRODUCTION AND SUMMARY

This report describes the progress to date of a program, sponsored by the U.S. Army Electronics Command, to develop a gasoline-fueled, 45-watt, 6-volt thermionic power supply. The work is being conducted at Thermo Electron Engineering Corporation and at the Battelle Memorial Institute.

The thermionic energy conversion principle, being static, offers the potential of silent operation. Furthermore, since it is capable of operation at high power densities, the thermionic converter, for a given power requirement, promises to be very light-weight. Finally, the devices can be made of conventional materials and, because they are small, promise to be low in cost. All of these characteristics are important in military field equipment and have justified a continuing effort to develop the conversion process and to apply it to various power requirements.

At the outset of this program, the thermionic converter had already exhibited adequate performance and life to be considered a practical device. Thermo Electron, with some sponsorship by the American Gas Association, had also developed a usable high-temperature recuperative burner that operated on natural gas and air, and had conducted numerous experiments to find a barrier material to protect the converter from the flame. The program described here was therefore aimed at increasing burner temperatures and efficiency, adapting the burner to leaded gasoline, extending the work on the barrier material to obtain longer life, and integrating the burner, the converter and the barrier into a usable power source.

Shortly after the program's initiation, gasoline was successfully used in the burner by first vaporizing the fuel. This test was accomplished with a laboratory setup, but it showed that usable hardware could be designed. Burner development then concentrated on a suitable high-temperature material and means of fabricating the material. Self-bonded silicon carbide was found satisfactory. Finally, additional recuperation was added to the burner, which resulted in higher efficiency.

Work on a barrier material was initially concentrated on protective non-ceramic coatings. These proved incapable of operation beyond 150 hours. The effort was then shifted to the use of pyrolytically deposited silicon carbide, and a test barrier reached nearly 1000 hours. Problems of chemical reactions between the barrier and the converter's emitter were encountered, but these were solved. Finally the barrier was integrated with a converter, and flame-heated converter test data was obtained.

In this report the work on the burner, barrier, and converter is described in separate sections. A system analysis was conducted to compare a multi-converter system with a single-converter system, and the latter was considered best. Thus, in the body of the report a change will be observed from a 12-diode approach with all diodes in series to a single diode and a dc-dc converter. The system analysis is included as Appendix A. The design of the complete 45-watt power source is described in Appendix B.

For military applications, where high performance and low weight are essential, further work is required to improve the performance and life of the converter. In addition, the ancillaries of a

complete system such as the fuel pump and controls remain to be designed.

II EMITTER SHELL

Thermo Electron recognized the emitter protective shell material as a major problem area well before the burner program, described in Section IV, had yielded significant results. When it became clear that the fundamental problems associated with the burner had been solved, emphasis was placed on finding an adequate emitter shell material. Up to that time, only a small amount of work could be expended in this direction.

In May of 1961, a major effort was launched to find a long-lived material to protect the diode from its flame environment. At first, the emphasis was placed on the oxide ceramics, because they seemed to combine in a unique and highly desirable manner all of the properties needed by a good emitter shell material (see Table II-1). As the program proceeded, the search was progressively widened to include all materials with a melting point over 1400°C. Available literature was searched, and known sources of high-temperature materials were approached for speciments of materials as well as data on their physical, chemical, and electrical characteristics. The materials procured ranged from hexaboron silicide and molybdenum coated with "Valcoat 12," both of which proved essentially unsuitable, to tantalum coated with R-505C and pyrolytically deposited silicon carbide, both of which demonstrated potential or long lives as diodes or simulated diode parts

The first step in the testing procedure was a room-temperature helium permeability check. If the sample proved impermeable under these circumstances, it was subjected to air firing at emitter temperature. As an additional check of the suitability of the material in the event that it might also be used as a "membrane" to separate the

oxidizing environment from the vacuum environment required inside the converter, some of the samples were also vacuum-fired. Furthermore, in the course of the assembly (brazing, outgassing, etc.) of a thermionic converter it becomes necessary to subject the components to temperatures of 1000 to 1200°C in vacuum. Therefore it was necessary to check the stability of the protectiveness of the coating under similar conditions. Weight change and helium permeability were checked after vacuum-firing periods ranging from 4 to 10 hours.

TABLE II-1

EMITTER SHELL MATERIAL REQUIREMENTS

Material should be:

1. Vacuum-tight or highly impermeable to the products of combustion at thermionic temperatures.*
2. Resistant to oxidation at thermionic temperatures in atmospheres containing up to 2% oxygen.**
3. Resistant to high thermal gradients and thermal shock.
4. Highly involatile at thermionic temperatures.
5. Resistant to erosion by high-velocity gases at thermionic temperatures.
6. Easy to fabricate.

* Thermionic temperatures were assumed to be in the range 1200°C to 1700°C.

** The ambient atmosphere considered was that resulting from the near-stoichiometric combustion of leaded gasoline and air.

Some samples were subjected to repeated vacuum-firing if the data indicated this was desirable. Samples which passed these tests were given oxidation tests in stagnant air, as well as in a less-oxidizing but relatively fast-moving stream of gas from a propane-oxygen welding torch. The samples were also thermally shocked. The materials tested, their chemical composition, and the results of the above tests are listed in Table II-2.

Of the materials that were tested, the first type that showed promise of achieving the life requirement of 500 hours was the Sylcor aluminum-tin coating. Extensive testing of this coating applied on tantalum, both on complete diodes and on components, proved conclusively that this material could, at best, average 100 hours of life. Figure II-1 shows two emitter shells under test in methane-air burners.

Failure of this coating occurred in virtually all cases in areas that were of the order of a few square millimeters in magnitude. The exact failure mechanism could not be determined, partly because of the small area and partly because, after coating failure, the substrate oxidized very rapidly and obscured the region. General depletion of the coating over large areas, either in the hot or cold region, as might occur from erosion or gradual chemical attack of the coating, was not observed.

Concurrent with the tests of the above coating, pyrolytically deposited silicon carbide samples were procured, and two were tested. The results were very encouraging, and work thereafter was concentrated on this material.

TABLE II-2

RESULTS OF VACUUM ENCLOSURE MATERIALS EVALUATION

PART A - NON-METALLICS

Manufacturer and Designation	Material	Test Results
Morganite Refractories Triangle H-T	59% Al_2O_3 38% SiO_2 3% Impurities	Overly sensitive to thermal gradients.
Mac Danel AV33	98% Al_2O_3 2% Impurities	Overly sensitive to thermal gradients.
Raytheon Manufacturing Co. R-95	95% Al_2O_3	Overly sensitive to thermal gradients.
Raytheon Manufacturing Co. R-100	99.9% Al_2O_3	Sensitive to thermal gradients. Impermeable at room temperature.
General Electric Company Quartz	99.97% SiO_2	Poor thermal gradient characteristics. Impermeable at room temperature after severe thermal shock. Devitrifies above 1100°C.
Carborundum "KT" silicon carbide +8 modifications	95% SiC	Good resistance to thermal gradients. Impermeable at room temperature as received.
Thermal Dynamics Inc. Plasma jet-sprayed and plasma jet-remelted molybdenum disilicide	98% $MoSi_2$	Porous at room temperature. Poor oxidation and thermal gradient resistance.

THERMO ELECTRON

National Beryllia Corporation Berlox hot-pressed	99.5% BeO	Good resistance to thermal gradient 40% of sample porous at room temperature. Attacked by water vapor above 1200°C with the evolution of toxic residue.
Berlox isostatically pressed and sintered	99.5% BeO	All samples vacuum-tight at room temperature. Vacuum-tight at room temperature after vacuum firing at 1400°C.
Berlox coated with Pt	99.5% BeO + Pt	Platinum coating peels off after sustained high-temperature torch-firing.
Carborundum Company Graphite coated with boride "Z"		Inconsistent oxidation resistance.
Graphite coated with silicon carbide	C + SiC	Inconsistent oxidation resistance.
Zirconium Corp. of America Lime-stabilized zirconia (nuclear grade)	ZrO_2 CaO	Porous. Fair to poor thermal gradient resistance.
Corning Glass Company Yttrium-stabilized zirconia	ZrO_2 Y	Not tested. Vendor claims poor thermal gradient characteristics.
New England Materials Laboratory Nickel-alumina cermet isostatically pressed and sintered and hot-pressed	Ni + Al_2O_3	Porous. Poor thermal gradient characteristics.

THERMO ELECTRON ENGINEERING CORPORATION

TABLE II-2 (continued)

PART A - NON-METALLICS

Manufacturer and Designation	Material	Test Results
High Temperature Materials, Inc.	Pyrolytically deposited boron-silicon in unknown proportions.	Two samples burned rapidly under propane-oxygen torch firing at 1400°C.
	Pyrolytically deposited graphite	Vacuum-tight at room temperature as received and after vacuum-firing. Needs oxidation protection.
	Pyrolytic silicon carbide on pyrolytic tungsten	Vacuum-tight at 1400°C after 882 hours. Highly resistant to oxidation at 1400°C. Excellent resistance to high thermal gradients and thermal shock. Highly resistant to erosion by flame.
A. D. Little, Inc.	Pyrolytic silicon carbide	Two samples lost approximately 10% of weight after 150 hours of firing. Samples were vacuum-tight at room temperature after vacuum-firing. Good resistance to thermal shock.
Brigham Young University Fused silicon carbide	Raw stock 99.5% SiC	Permeable after vacuum-firing. Essentially the same as "KT" Silicon carbide.
Corning Glass Works	Pyroceram 960X (proprietary compound)	Fair thermal shock resistance. Impermeable before and after vacuum-firing. Devitrification after approximately 20 hours at 1400°C under torch-firing.

THERMO ELECTRON

Diamonite Products Mfg. Co.	50% Silicon carbide 50% Aluminum oxide	Specimen vacuum-tight at room temperature as received from vendor, but permeable after high-temperature vacuum-firing. Fair to good thermal shock resistance.
	8% Silicon carbide 92% Aluminum oxide	Specimen vacuum-tight as received from vendor and after short-time high-temperature firing. Specimen failed in thermal shock under torch and after slow cooling in vacuum.
Allis-Chalmers Company, Research Division Hexaboron silicide	B_6Si	Good thermal gradient resistance-30% of sample vacuum-tight at room temperature. Crumbles to powder after vacuum-firing at 1400°C. Good oxidation resistance at 1400°C in air.
Boeing Aircraft Corporation	$C + MoSi_2 + TiB$	Porous at room temperature. Excellent thermal gradient resistance. Poor oxidation resistance.

THERMO ELECTRON ENGINEERING CORPORATION

TABLE II-2 (continued)

PART B - COATED REFRACTORY METALS

NOTE: The refractory metals (molybdenum, tantalum, columbium and tungsten) meet all the requirements for a vacuum enclosure except for oxidation resistance and high-temperature permeability. There is, therefore, only the question of finding a coating for these materials which will resist the oxidation and erosion conditions which the burner imposes on the vacuum enclosure, preventing the absorption of combustion gases by the substrate.

The remainder of this tabulation will, therefore, list and comment only on the oxidation and erosion characteristics of the various refractory metal coatings. Data generated during a torch-firing test is the most meaningful, since it represents the simultaneous imposition of erosion and oxidation conditions.

Manufacturer	Coating Designation	Comments
	TANTALUM	
Chromalloy Corporation	W-2	Data scattered badly. The coating was edge-sensitive.
	Tantalum Disilicide	Afforded fair oxidation protection to substrate. Coating was edge-sensitive.
Sylvania Electric Products Corp., Sylcor Division	S-34	This organization originated S-34. Data indicates poor oxidation protection of substrate for samples tested. Vendor claims samples non-representative compared with same coating prepared by National Research Corp. Coating applied at 1800°F vacuum (10^{-4} mm Hg).

THERMO ELECTRON CORPORATION

National Research Corp.	S-34	Coating afforded superior oxidation protection of substrate. Maximum time to failure - 167 hrs. Minimum time to failure - 20 hrs. Coating had fair to good edge characteristics. Vacuum-tight at 2550°F. Coating near failure after 53.2 hrs of torch-firing during high-temperature permeability test.
Chance Vought Corp.	Vought "G"	Coating afforded poor oxidation protection of substrate. Maximum time to failure - 2.5 hrs. Minimum time to failure - 1.0 hr.
Sylvania Electric Products Corp., Sylcor Division	R-505 (derivative of S-34)	Coating afforded excellent oxidation protection to substrate under the most severe test (torch-firing). Maximum time to failure - 81 hrs. Minimum time to failure - 60 hrs. Coating applied at 1800°F in vacuum (10^{-4} mm Hg).
New England Materials Laboratory, Inc.	Platinum coating	Specimen tested at 2905°F (1600°C) in helium. Brittle intermetallic formed. Severe spalling after 10 hours.
Thompson Ramo Woolridge, Tapco Group	TRW-1 on Tantalloy	All torch-fired samples failed before 60 hours. Two of five air-furnace-fired samples were still intact at end of 150 hours of cyclic testing.
	TRW-1 on tantalum	All torch-fired samples failed before 50 hours. Four of five air-furnace-fired samples failed before 75 hours. One remaining air-furnace-fired sample was intact at the end of 98 hours.

THERMO ELECTRON CORPORATION

TABLE II-2 (continued)

PART B - COATED REFRACTORY METALS

Manufacturer	Coating Designation	Comments
GT and E Bayside Laboratories, Sylvania Division	R-505 on tantalum	All samples torch-fired; all samples failed between 60 and 90 hours.
	R-505 on Tantalloy 90% Ta 10% W	All samples torch-fired. Six out of seven samples failed between 70 and 130 hours. Remaining sample failed at 25 hours.
	R-505A on Tantalloy	Five samples torch-fired. All samples failed between 75 and 120 hours.
	TUNGSTEN	
Poly Cote Corporation	Platinum Silicon monoxide Silicon carbide	These coatings were of micro-inch thicknesses and were applied by vapor-deposition. None of these coatings afforded any significant oxidation or erosion protection to the substrate.
Chance Vought Corp.	Vought "C"	Coating afforded only poor to fair oxidation resistance to substrate.
	Vought "D"	Coating afforded fair oxidation protection to substrate.
Sylvania Electric Products Corp., Sylcor Division	S-34	Coating did not afford significant protection to substrate.
Chromalloy Corporation	T-2	Coating afforded fair to good oxidation resistance to substrate.
Sylvania Electric Products Corp., Sylcor Division	R-505	Coating afforded no significant oxidation resistance to the substrate.
Chromalloy Corporation	$W Si_2$	Coating afforded no significant oxidation resistance to substrate.

THERMO ELECTRON INSTRUMENTS CORPORATION

	MOLYBDENUM	
Value Engineering Corporation	Valcoat 12	Coating afforded no significant protection to substrate
American Machine and Foundry Company	AMFKOTE-2	Fair
Chromalloy Corporation	W-2	Results were unusually consistent and indicated fair protection.
	W-3	Fair protection.
Sylvania Electric Products Corp., Sylcor Division	S-34	Fair to good protection.
Chance Vought Corporation	Vought "A"	Coating afforded only slight protection to the substrate.
	Vought "B"	Coating afforded fair oxidation resistance to substrate.
Sylvania Electric Products Corp., Sylcor Division	R-505	No significant protection under torch-firing; good protection in air furnace.
Pfaulder Permatile Corp.	PFR-6	Poor.
	COLUMBIUM	
Chance Vought Corporation	Vought "E"	Coating afforded good oxidation protection to substrate under both air- and torch-firing
	Vought "F"	Coating afforded fair oxidation protection to substrate.
Thompson Ramo Woolridge, Tapco Group	TRW-1	All seven samples failed before 75 hours.

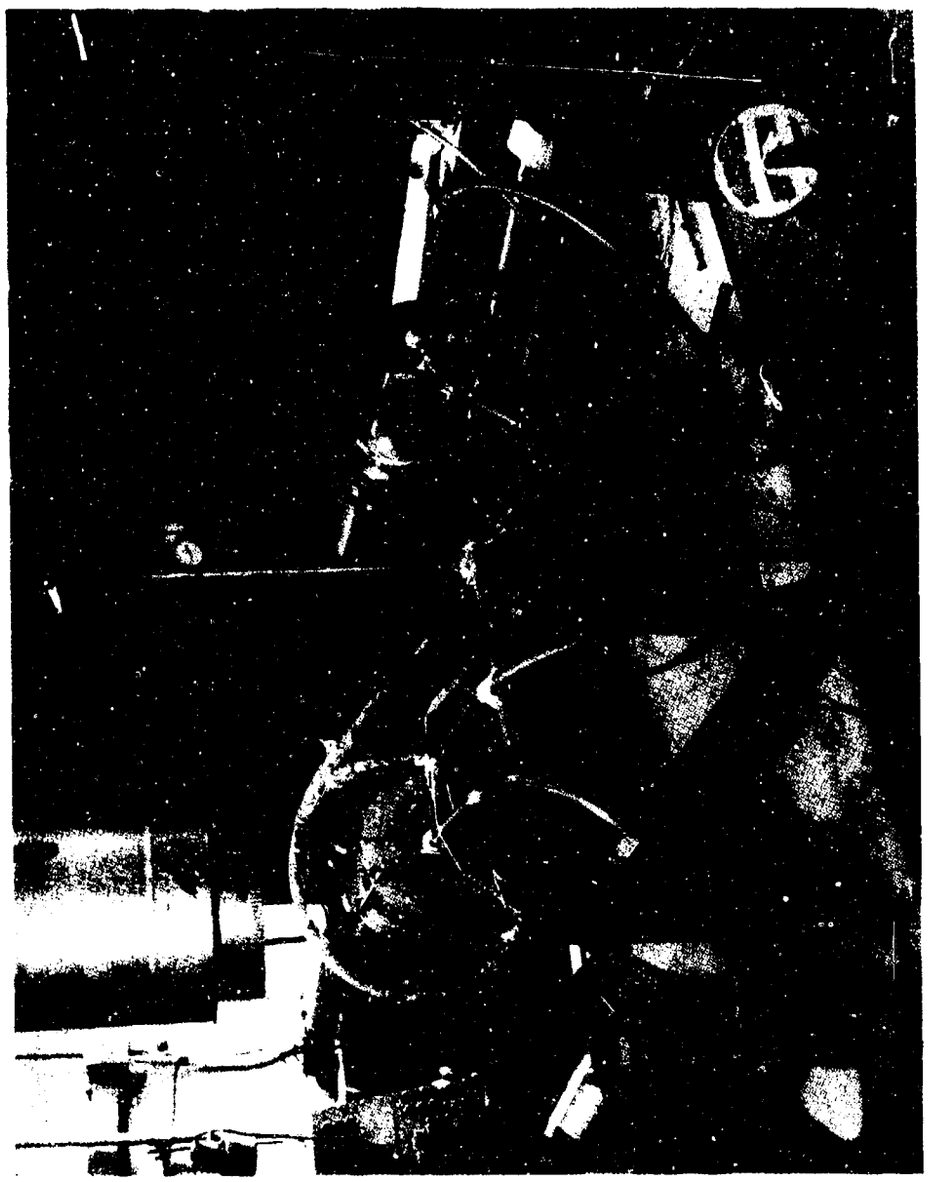

Figure II-1. Two Emitter Shells Under Test in Methane-Air Burners.

There are many variables which can affect this process, but its basic simplicity and the controls which can be brought into play have resulted in very high levels of purity, and virtually theoretical density of the so-deposited compound or element. Among these process variables are the composition of the feed compound, the flow rates, the carrier gas composition (if used), the aerodynamics in the immediate region of the mandrel, the chamber pressure, the temperature of the mandrel, and the mandrel material. The mechanical finish and the geometry of the mandrel also affect both the maximum rate of deposition and the crystallographic structure of the deposited material.

The experimental apparatus used to test the high-temperature permeability and oxidation resistance of the silicon carbide emitter shells is similar to that shown in Figure II-1. This photograph shows the high-temperature test burners each heating a "dummy" diode, i. e., the emitter shell portion of the diode without collector shell, insulator, cooling ducts, etc. The tests consisted of attaching a copper tube to each shell, connecting the tube to an ion pump and heating the sample in a natural-gas burner. Tested this way, one sample ran for 882 hours at temperatures between 1275°C and 1400°C, and underwent three thermal cycles during this time period. Figure II-2 shows a graph of the measured getter ion pump pressure versus time. Another shell logged 519 hours at thermionic temperatures and underwent 101 thermal cycles, approximately half of which were imposed as quickly as the burner would allow. A plot of ion pump pressure versus time is shown in Figure II-3. Both of these samples consisted of closed-end tubes with a diameter of 5/8 inch and a length of 3 inches of silicon carbide deposited on a tungsten substrate. The

tungsten provided the emitting surface. Tungsten rather than any other refractory metal was chosen because its thermal expansion matched closely that of silicon carbide.

Following the test of these two silicon carbide shells, more samples were obtained from several vendors. These were again shells of silicon carbide on tungsten and were of a size and shape to fit the Series VI diode. Tests of these showed two principal problems:

(1) When heated at 1400°C for about 100 hours, the silicon carbide separated from the tungsten substrate.

(2) In some samples thermal shock caused cracking.

A program was therefore undertaken with the Battelle Memorial Institute to understand better the reasons contributing to the noticed type of failure and also to find a means of fabricating sound and long-lived samples. This program began with the coating of both tungsten and molybdenum emitters with silicon carbide. Two types of shells were formed and showed promise for the intended application. The first was based on a tungsten coating deposited by hydrogen reduction of WF_6 on a graphite mandrel. After the tungsten was formed, SiC was deposited on the tungsten. The vapor-formed SiC-tungsten shell was separated from the graphite at Thermo Electron. To accomplish this, one end of the mandrel was cut away to expose the graphite which was leached out by an acid treatment in a subsequent step. Difficulties encountered with this type of shell were (1) cracking of the composite during the cutting to expose the graphite, and (2) failure of the bond between the SiC and W after only a few (10 - 50) hours at operating temperature. The cracking

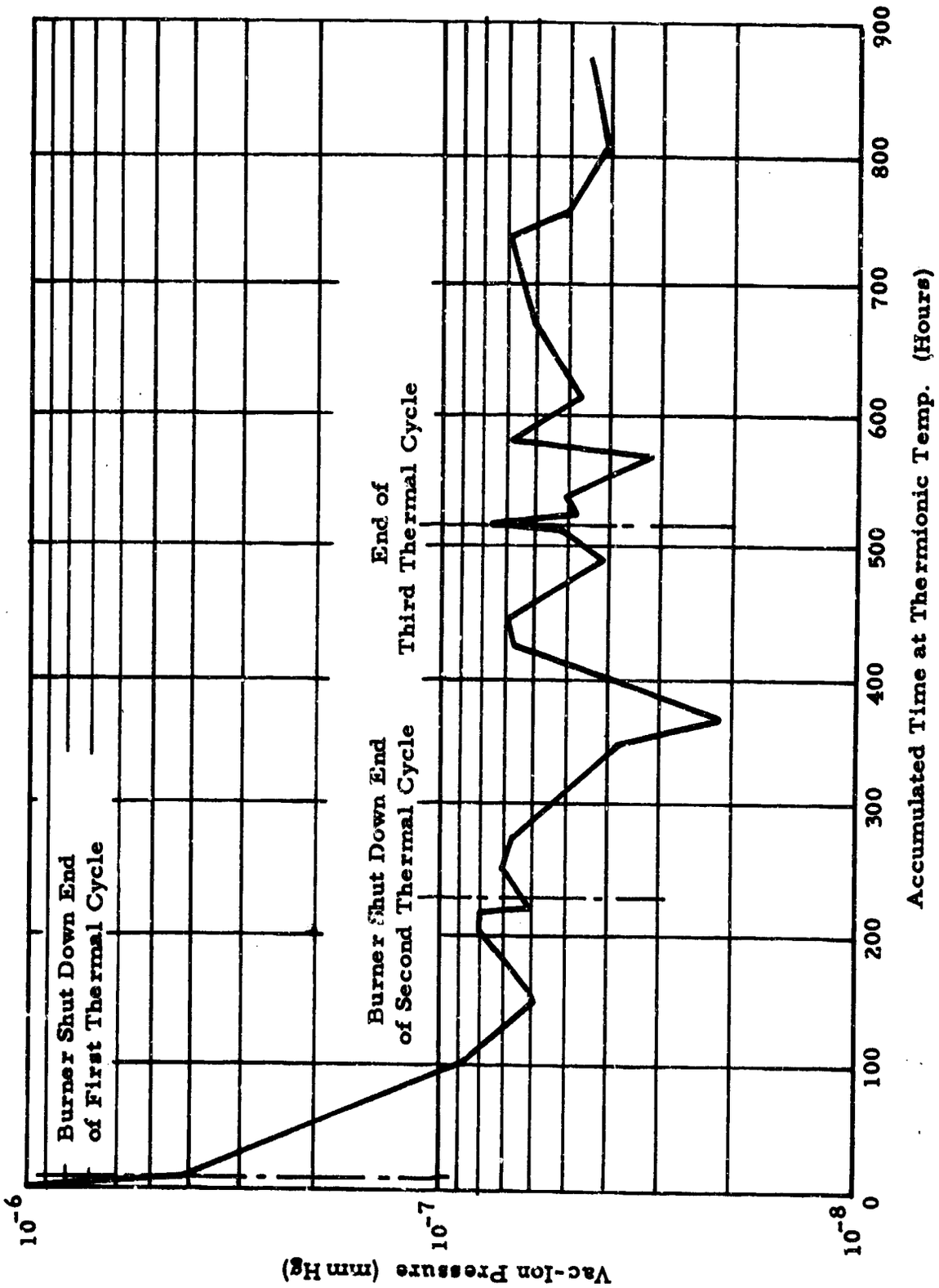

Figure II-2. Vacuum Profile of Silicon Carbide Shell.

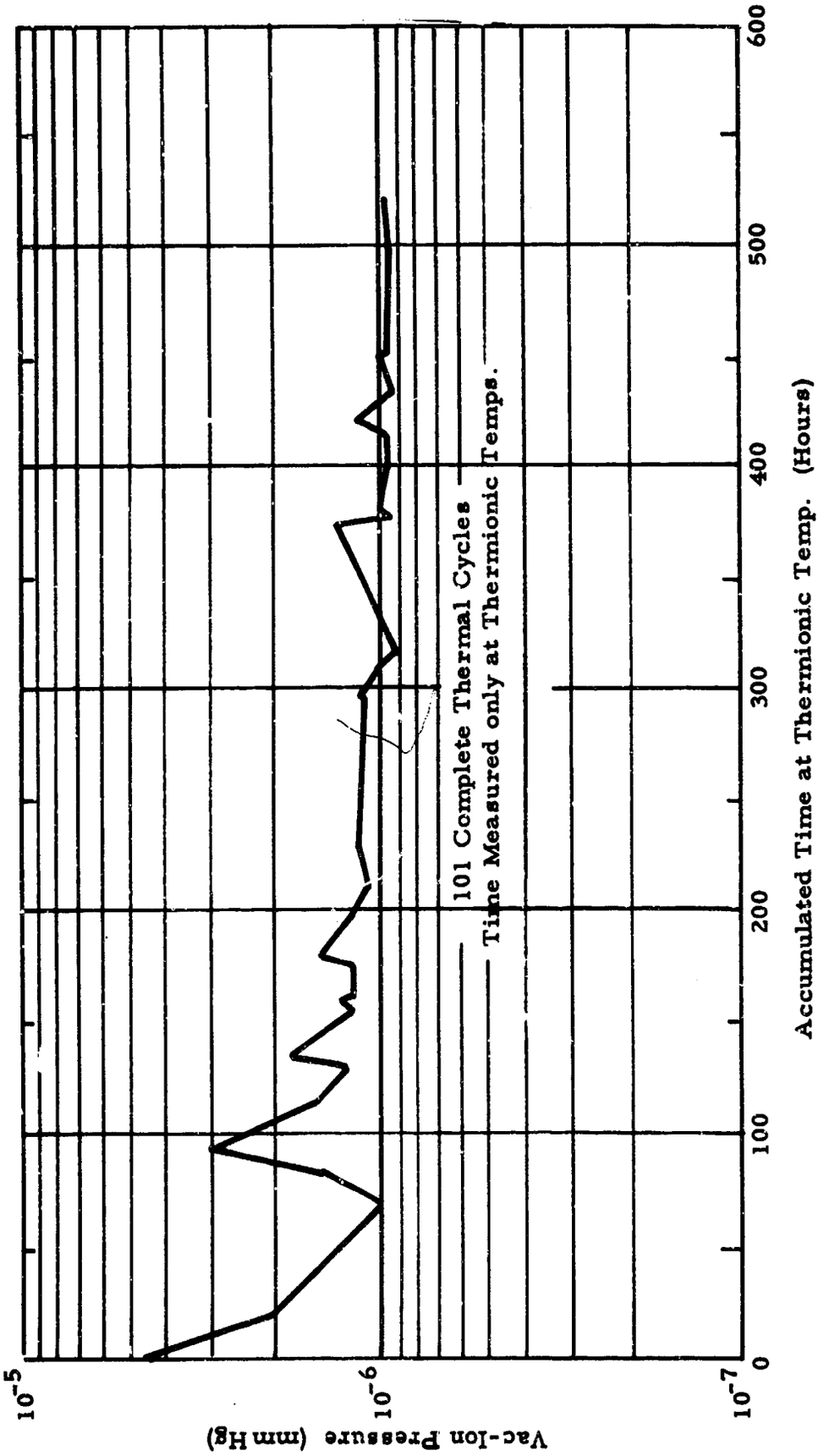

Figure II-3. Vacuum Profile of Another Silicon Carbide Shell.

problem was then circumvented by deposition of SiC on a machined molybdenum shell which became part of the diode. The adherence of SiC to molybdenum was very poor, so a barrier of tungsten was applied initially to the molybdenum and then overcoated with SiC. After preparation, the Mo-W-SiC assembly was extremely rugged. However, after about 25 to 50 hours under the burner separation of SiC would occur. It was thought that the separation problem could be avoided by improvement of the SiC deposition process. SiC-tungsten composites were formed on molybdenum tubes to simplify the geometry for the vapor-forming process. Various amounts of carbon as methane were added along with the coating reactant CH_3SiCl_3, with the hope that a more favorable stoichiometry of the SiC could be obtained which would remain bonded to the tungsten for longer periods of time under the burner. Electron-microprobe analyses indicated that SiC coatings were nearly stoichiometric, and that a reaction zone consisting of tungsten carbide and tungsten silicide formed in the region exposed to the burner. To determine whether or not stoichiometric SiC would ever be compatible for long periods of time at 1400°C, tungsten was deposited on transparent single crystals of SiC. These couples were then heated at 1400°C for 25 to 50 hours. Metallographic examination established that the pure single-crystal SiC and the tungsten had reacted, and separation of the two materials had occurred as a result of a volume change at the interface. Subsequent studies on precarburization of the tungsten prior to the deposition of SiC revealed that a tungsten carbide barrier layer of about 1 mil in thickness would not stop the interaction leading to early failure. This prompted the development of the present type of shell, which consists of a machined graphite

body 40 mils thick with tungsten deposited on the inside and SiC deposited on the outside so that the graphite is completely encapsulated and provides (1) a surface on which to vapor-form the SiC and tungsten, and (2) a reaction barrier between the SiC and tungsten in the area heated by the burner. Fourteen such composites had been vapor-formed and the coating techniques were developed to a considerable extent. Composite shells tested under the burner at Thermo Electron showed considerable promise. However, the shell characteristics differed widely, which was attributed to inadequate control of the deposition variables, and the tungsten surface was granular, thus preventing the achievement of accurate interelectrode spacing and presenting excessive radiation losses. An effort was then initiated to improve the shell fabrication equipment and to find means of polishing the tungsten surface.

Thirty-four thermionic converter hot shells were formed in induction-heated and resistively heated equipment. The shells, 3.095 inches in length and 1.69 inches inside diameter adjacent to a closed hemispherical end and 1.79 inches inside diameter at the other end, consisted of a machined graphite body with a 40-mil-thick wall having about 12 mils of tungsten deposited on the inside and about 12 mils of SiC deposited on the outside. The graphite served a dual purpose in that it provided a substrate for deposition of the tungsten and SiC, and it became a reaction barrier between the SiC and tungsten.

The tungsten was deposited by hydrogen reduction of tungsten hexafluoride (WF_6), while the SiC was deposited by pyrolysis and/or hydrogen reduction of methyl trichlorosilane (CH_3SiCl_3).

In addition to the preparation of shells, (1) a resistively heated unit for the deposition of tungsten was designed, constructed, and operated, (2) the feasibility of using a resistance-heated unit for the preparation of SiC coatings was evaluated, and (3) a cursory investigation of surface finishing of the tungsten coatings by grinding and electropolishing was carried out.

The new resistively heated unit for the preparation of tungsten coatings was used successfully in the preparation of 15 of the shells, while inductively heated equipment developed previously under the sponsorship of Thermo Electron was used for tungsten coating in the earlier portion of the work. This equipment is also still in use for the SiC deposition phase.

The development of the resistance-heated unit for the preparation of SiC coatings is not so advanced as that of the tungsten-coating unit. Three shells were coated in the unit with promising results. However, the unit requires additional development before it can be operated on a routine basis.

Work on surface finishing of the tungsten included evaluation of the use of (1) electrical-discharge machining, (2) surface grinding with a small hand grinder, (3) surface grinding with a brass or rubber ball-shaped mandel in a slurry of 100-grit SiC and water, and (4) electropolishing with NaOH-water solution. The grinding operations appear to be satisfactory to remove protrusions on the surface of the tungsten, if performed prior to the SiC-coating step. Electropolishing after deposition of the SiC is effective for a final finishing step.

Of 34 shell-preparation experiments, 17 yielded shells which were judged to be suitable for use by Thermo Electron for testing

under the burner and/or for use in fabrication of diodes. The remaining 17 reject shells included three prepared in the resistance-heated SiC-coating unit with poorly distributed SiC, and 14 which developed cracks in the tungsten and/or SiC after the SiC coatings were applied.

SHELL FABRICATION*

The preparation of the SiC-graphite-tungsten composite shell involves numerous steps. As is the case in most development programs, techniques are improved as the work progresses. Therefore, the final procedure usually differs somewhat from that used in the earlier stages of the program. The procedure given in this section describes the latest techniques. To provide an overall picture for the reader, an outline of the procedure is given and then a detailed description follows:

(a) A shell is machined from a graphite cylinder.

(b) The shell is baked in hydrogen for 10 minutes.

(c) Tungsten is deposited from WF_6.

(d) SiC is deposited from CH_3SiCl_3.

(e) Surface contaminants are removed electrochemically from the tungsten.

(f) The tungsten and SiC are checked for cracks with a dye penetrant.

Tungsten Coating

The shell is inserted in a holder, where it is held by friction. The holder containing the shell is attached to a Monel rod, as shown in Figure II-4. The end of the Monel rod is threaded to accommodate a second shaft to facilitate the insertion of the hardware into the

*Conducted by the Battelle Memorial Institute under contract to Thermo Electron Engineering Corporation.

coatin unit. The shell-holder assembly is inserted from the open-flanged end of the coating unit shown in Figures II-4, II-5 and II-6. The one end of the Monel rod attached to the shell holder protrudes through an "O"-ring seal and roller-bearing supports, as shown in Figure II-4. A drive gear is attached to the end of the Monel rod and is driven by a synchronous motor. The motor and drive gear are coupled with a ladder chain. The flange, which carries the coating nozzle, is then put into place, and connections for water cooling and gas flows are made. Hydrogen is injected at Point N, as shown in Figure II-4, to purge the shaft housing of air and coating reactants. Hydrogen is fed through the nozzle for purge as the unit is heated to a wall temperature of 650°C (shell temperature of 540°C). The nozzle temperature is thermostated with hot tap water. WF_6 is then added to the hydrogen steam fed through the nozzle. The hydrogen flows are maintained through the support-shaft housing and through the nozzle. The WF_6 flow, fed from the tank and line heated to hold a pressure of 10 to 15 psig tank and line pressure, is controlled by the Monel valve and monitored by the weight change of the WF_6 cylinder. A 12- to 15-mil-thick coating is obtained in 85 minutes. When the desired amount of WF_6 has been fed, the WF_6 flow is discontinued and the wall temperature is increased to stress-relieve the tungsten. At this point, the tungsten-graphite shell is set on a rubber-gasketed fixture, evacuated, and helium leak-checked.

Silicon Carbide Coating

The shell, placed on a mandrel, is supported on an Alundum tube (see Figure II-7) which projects through a rotating seal, as shown in Figure II-8. The Monel bell jar is put in place (see Figure II-9) and the coating chamber is evacuated to exclude air.

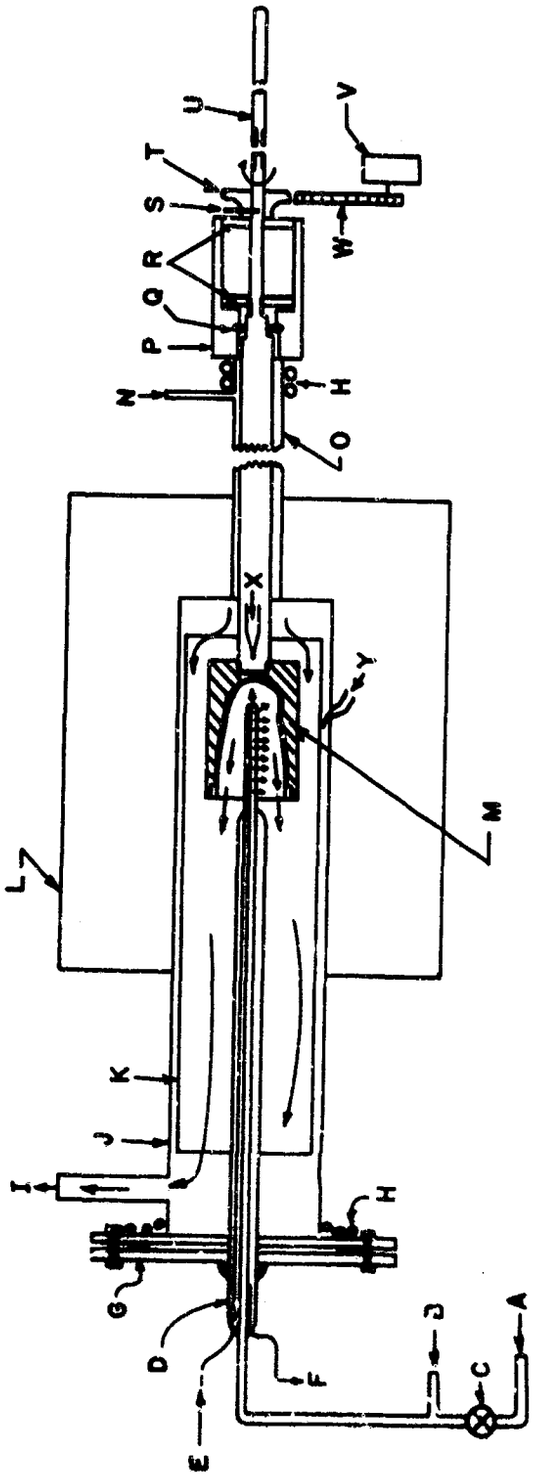

Figure II-4. Resistance-Heated Apparatus for Deposition of Tungsten.

Legend for Figure II-4

A - WF_6 inlet.

B - Hydrogen inlet for reduction of WF_6 in hot zone.

C - WF_6 feed control.

D - WF_6-H_2 feed nozzle with a jacket of copper tubing to contain hot tap water to thermostat temperature of nozzle.

E - Hot tap-water inlet.

F - Water outlet.

G - Monel flanges.

H - Cold tap water cooling coils.

I - Exhaust to hood.

J - Reaction zone housing.

K - Removable molybdenum cylinder.

L - Clamshell oven.

M - Thermionic hot-shell holder.

N - Hydrogen inlet for purge between rotating-support shaft and housing.

O - Housing for rotating support shaft.

P - Nickel housing for seal and bearing support.

Q - "O"-ring seal.

R - Roller bearings.

S - Set screw.

T - Sprocket.

U - Removable handle for moving the shell holder and rotating shaft beyond the opening at the flanged end of the reactor housing.

V - Motor.

W - Chain.

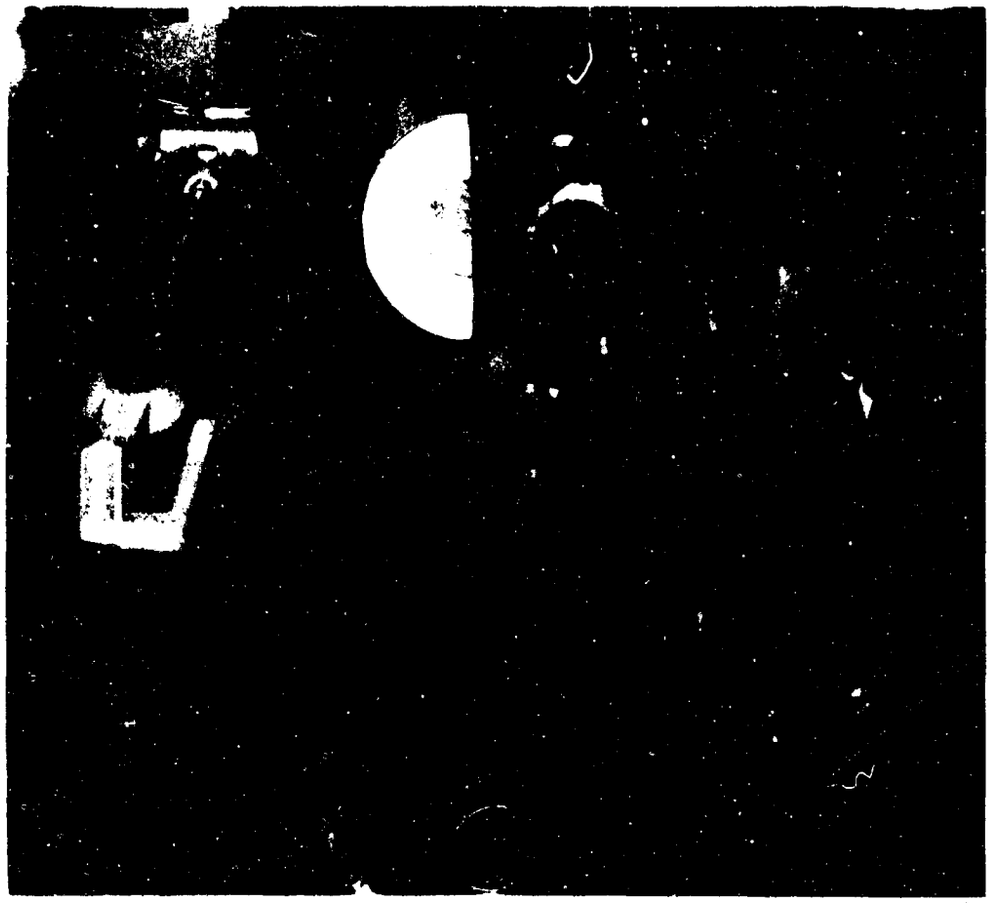

Figure II-5. Resistance-Heated Apparatus for Deposition of Tungsten (dismantled condition).

Figure II-6. Resistance-Heated Apparatus for Deposition of Tungsten (assembled condition).

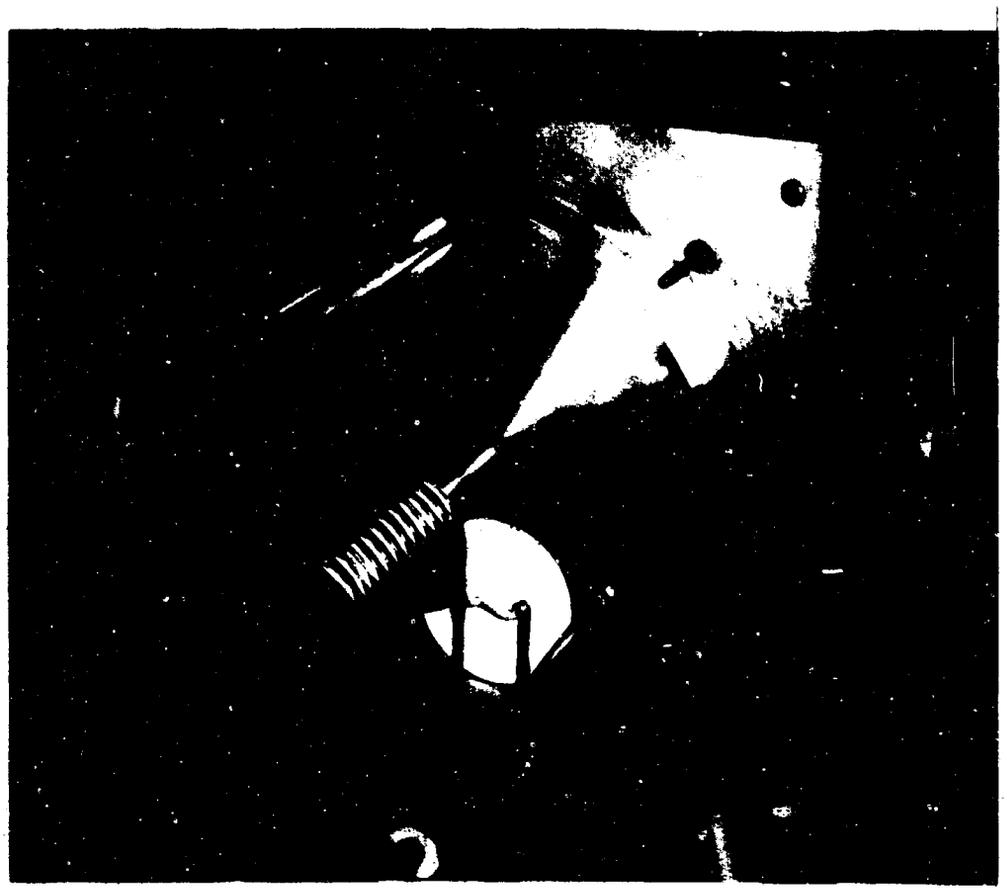

Figure II-7. Induction-Heated Unit Assembled for SiC-Coating Run.

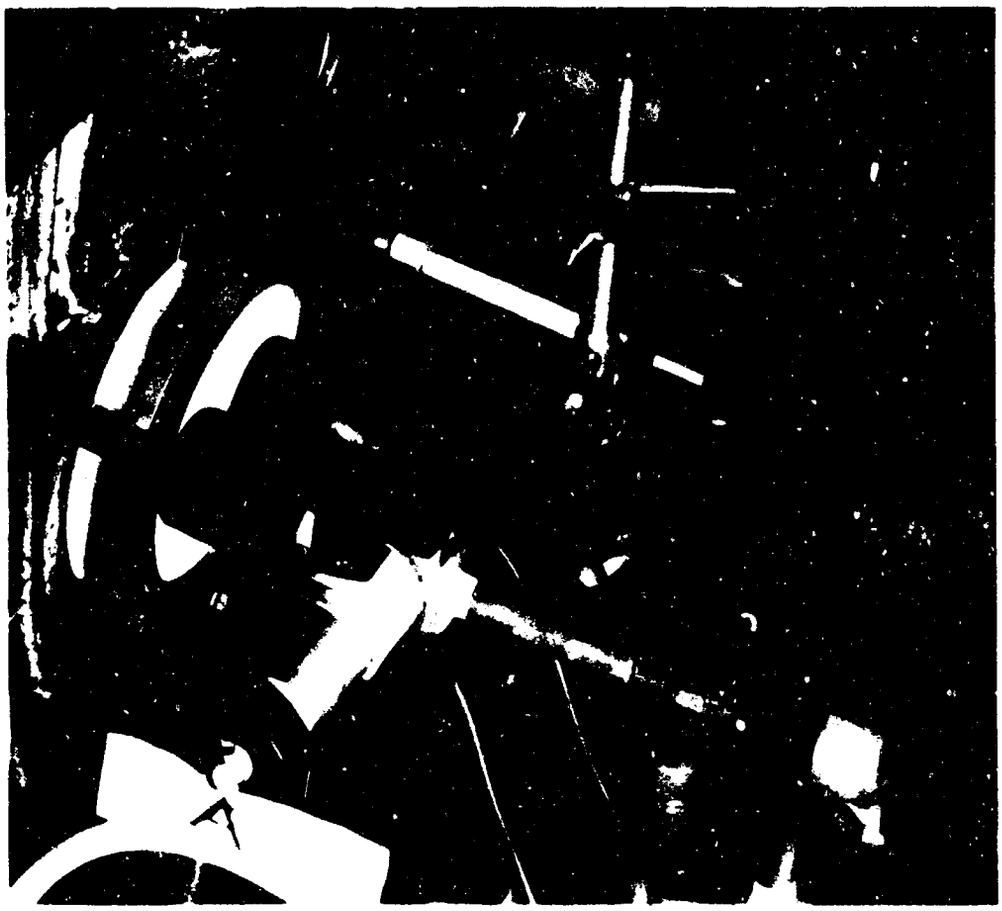

Figure II-8. View of Induction-Heated Coating Unit Showing Rotating-Seal Assembly (Upper-Left Quadrant), Induction Lead-Through (Left Center), and Coating Reactant-Feed Line (Foreground).

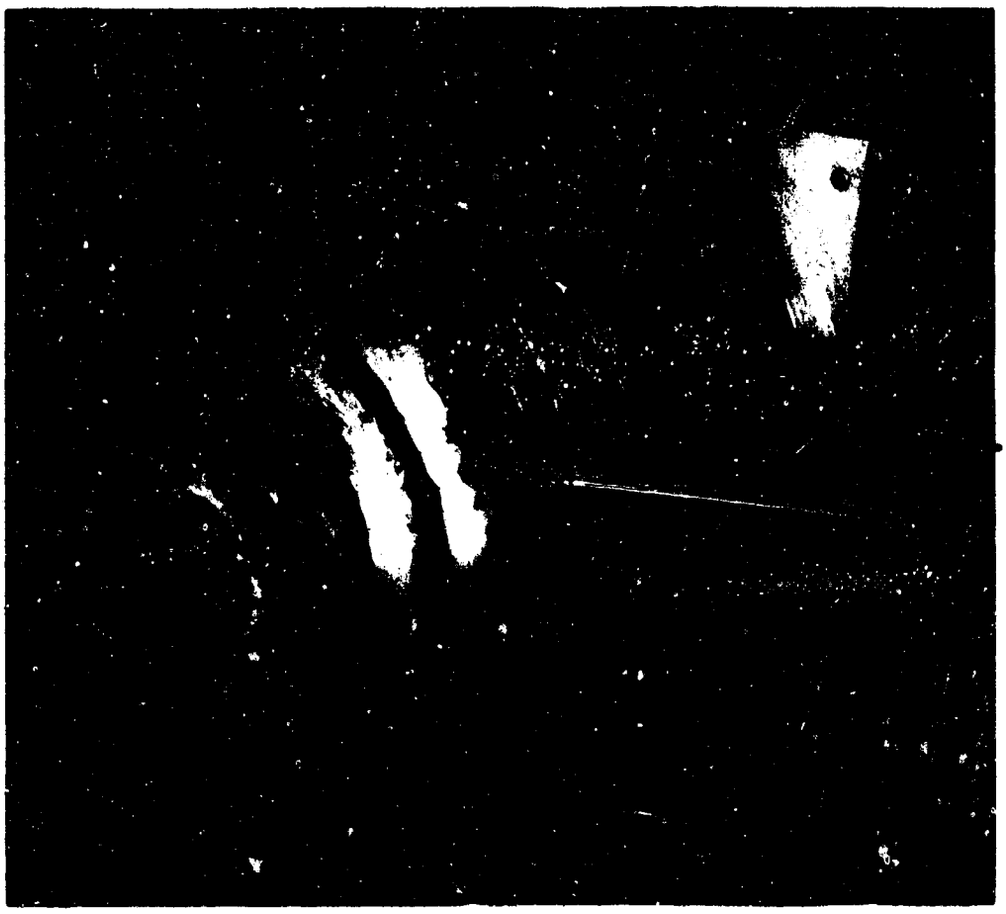

Figure II-9. Induction-Heated Unit with Monel Bell Jar in Place for SiC-Coating Run.

After evacuation the unit is filled with hydrogen through Valve A, shown in Figure II-10. The coating unit is pressurized for a precautionary pressure check, bled down to atmospheric pressure by opening a valve on the exhaust line, and then hydrogen flow is initiated. The shell is inductively heated to 1200 to 1260°C. While the shell temperature is being adjusted, the CH_3SiCl_3 is purged with hydrogen. When temperatures are steady and the system is well purged, the CH_3SiCl_3 is admitted. The mixture passes through Valve A connected to a feed line visible in Figure II-8. The gases flow past the heated rotating shell, and are then exhausted.

When the desired amount of SiC has been deposited, Valve F is closed (see Figure II-10) to stop the CH_3SiCl_3 feed. The shell is then cooled.

Resistance-Heated Unit for Deposition of SiC

Development of a resistance-heated unit for deposition of SiC is not so far advanced as the development of a unit for deposition of tungsten. Three shells were coated with SiC by resistance-heating. It was demonstrated that the desired temperature levels could be maintained. However, the coating uniformity was poor for all three of the shells. The reason for the poor uniformity was improper gas-flow patterns.

It was intended to develop a unit which would coat the shell in an upright position and without rotation. If successful, the principle could be readily used in a multiple-shell coater for commercial production. Inclusion of a mechanism for rotation and the use of a horizontal-shell support would undesirably complicate the assembly of a multiple-shell unit.

The resistance-heated unit, with the latest design modifications shown in Figure II-11, was used to coat a shell. In order to protect the heater element from the coating reactants, the assembly was continuously purged with hydrogen. With the apparatus used for Shells 1R and 2R, the hydrogen purge of the heater assembly was exhausted at the base of the shell. It appeared that the upward convective flow of the hydrogen exhausted at the base of the shell caused the coating to be thin and non-uniform around the circumference at the base. Therefore, provision was made for removal of the purge gas further downstream from the coating zone. The change was ineffective. However, the fact that the interior of the shell and the heater assembly were coated with silica, as a result of the reaction of the Alundum with the coating reactants, indicated that the area between the shell and the support was not adequately sealed. Thus, an appreciable fraction of the hydrogen purge could have been exhausted at th base. Incorporation of a better seal may improve the coating uniformity.

It is interesting to note that the rate of deposition of the SiC is two to three times that obtained in the induction-heated unit at nearly the same temperature and coating-reactant concentration. The higher SiC-deposition rate can at least be partially explained. With the induction unit, a condensate of viscous liquid reaction product forms on the water-cooled induction coil and drips off from the coil. The condensation depletes the SiC available for deposition. No condensate is formed in the resistance-heated unit.

With the resistance-heated unit, the hemispherical ends of the shells have a glassy smooth deposit, while the straight sections

Figure II-10. Induction-Heated Unit for Deposition of SiC or Tungsten.

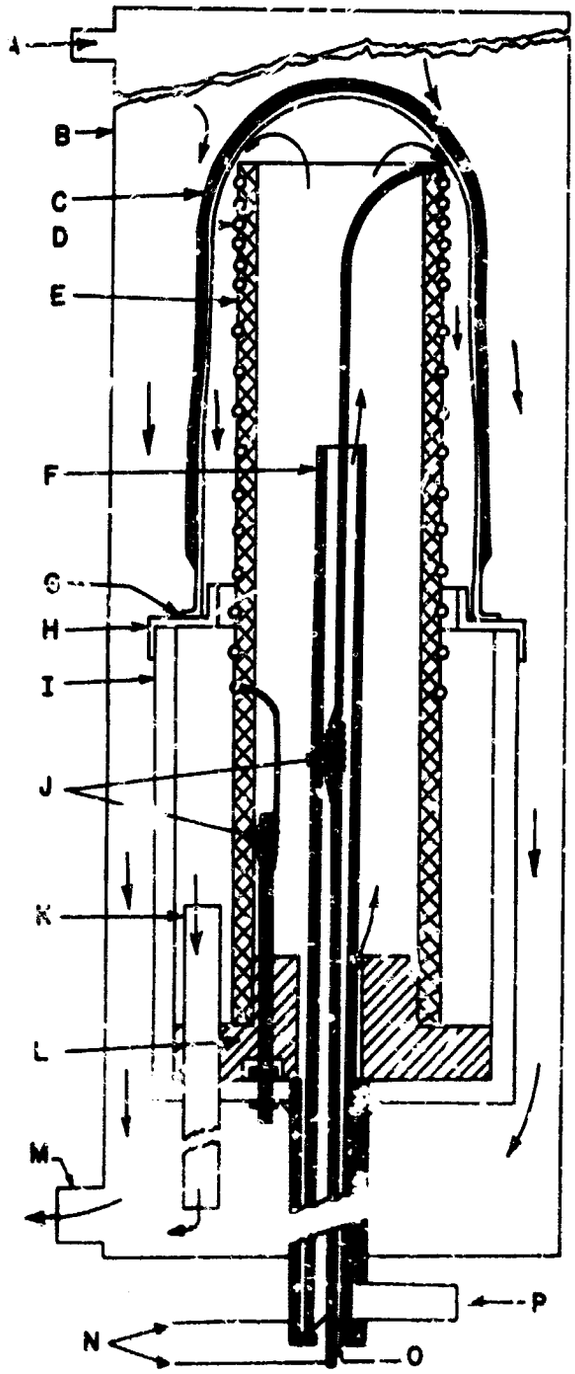

Figure II-11. Resistance-Heated Unit for Deposition of SiC.

Legend for Figure II-11

A - Coating reactant gas inlet.

B - Vycor tube housing.

C - Tungsten-coated graphite shell to be coated with SiC.

D - Molybdenum-heater wire.

E - Alundum tube.

F - Alundum tube.

G - Molybdenum disc.

H - Nickel fitting.

I - Nickel support and housing.

J - Molybdenum rod.

K - Internal H_2 purge exhaust line.

L - Alundum spacer.

M - Exhaust line to hood.

N - Electrical-power leads.

O - Rubber or Teflon insulator.

P - Internal purge-gas inlet.

resemble the inductively heated deposits in color and texture, i. e., dull gray to black and somewhat rough. The difference in surface appearance on the resistance-heated shells is apparently due to changes in coating-reactant concentrations as the gas is forced along the length of the shell.

In any future work on the development of the resistance-heated unit for the deposition of SiC, the following changes are recommended:

(1) Improve the seal between the base of the shell and the support by use of a machined close-fitting molybdenum fixture in place of the nickel fitting (H) shown in Figure II-11.

(2) Increase the diameter of the Vycor housing (b).

(3) Decrease the diameter of the housing (I) shown in Figure II-11.

(4) Include a thin-walled molybdenum shell (≈ 10 mils in thickness) between the heating element and the tungsten-coated-graphite shell to provide additional protection for the heater element, and to provide a support for possible horizontal operation.

(5) If the only alternative is to support the shell in a horizontal position with rotation, a cross-shaped Vycor housing fabricated from 90-mm-OD tubing with the shell located in the center of the cross is recommended.

SURFACE FINISHING OF TUNGSTEN

Work on the surface finishing of the tungsten included evaluation of the use of (1) electrical-discharge machining, (2) surface grinding with a small hand grinder, (3) surface grinding with a brass or rubber ball-shaped mandrel in a slurry of 100-grit SiC and water, and (4) electropolishing with NaOH-water solution. It appears that the most promising procedure, judged on the basis of quality and cost, is to cut off the tungsten protrusions with a small hand grinder prior to the deposition of the SiC and follow with an electropolish subsequent to the deposition of SiC. Without the SiC coating, the shell is able to survive the considerable vibration inherent in the grinding operation. The ability of the shell to withstand vibrational shock of the same order of magnitude after coating with SiC has not been established. However, it is considered to be a good practice to do any grinding prior to application of the SiC, since if breakage inadvertently occurs less preparation time is wasted. For the electropolishing, it is necessary to treat the final coated product, since a carbide film is deposited on the tungsten in the SiC-preparation step. Thus, an electropolish prior to the deposition of SiC would be fruitless.

Mechanical Finishing

A tungsten-coated graphite shell (later coated with SiC and numbered 39FS) was surface-finished in the hemispherical end and adjacent straight section by electrical-discharge machining. A flat surface was obtained which was considered to be in excellent condition for a final electropolish. Although the electrical-discharge machining produced a desirable product, the time required (1 hour)

and electrode replacement (a result of excessive erosion) were considered too costly for the intended application. Two spherical brass electrodes were used for machining one shell. Other electrode materials are available which may have a longer life. However, the time required for the electrical-discharge machining would be essentially unchanged.

The spherical brass electrodes which were used in the electrical-discharge machining experiment were 20 mils less in diameter than the inside diameter of the shells. These mandrels were then used to evaluate grinding with a 100-grit SiC-water slurry. A 1/2-in.-diameter shank, attached to the brass sphere, was chucked and driven by a drill press. Finished shells that had cracked were used as test pieces. About 2 cc of 100-grit SiC and 10 cc of water were placed in the shell. The shell, held manually, was moved up against the rotating brass mandrel. Grinding to a level surface required 15 to 30 minutes. With proper jigs, the use of the slurry may be practical on a production basis. Mandrel wear would not be expected to be a serious problem, since the radius of the mandrel should stay reasonably constant with wear.

The fastest removal of surface protrusions was accomplished with a small grinder, held manually, operating at 18,000 rpm. About 5 minutes was required to complete the operation with a 3/4-in.-diameter grinding wheel. Since the tungsten-coating process at its present stage of development involves the formation of about 6 objectionable protrusions, extensive grinding is not required. Therefore, use of the hand-held grinder could be a practical method for mass production of such shells.

A cast rubber mandrel with and without SiC inclusions was also used with a 100-grit SiC-water slurry for grinding. However, the resilient mandrel produced a polished surface without satisfactory leveling of the protrusions.

Electropolishing

The removal of tungsten in electropolishing depends on oxidation and dissolution of the oxidation product. Therefore, the electrolyte for rapid removal of tungsten would be one in which the oxidation products would be readily soluble. A caustic solution meets the requirement, while nitric-acid solutions, for example, do not dissolve all of the oxidation products. It was demonstrated that an adherent insulating oxide film can be readily formed with 5-v/o HNO_3 and 20-v/o HNO_3, which stops further tungsten removal. Although rapid removal of tungsten occurred with caustic concentrations of 120 g/liter and current densities up to 6.5 A/in.^{2}, no polishing was obtained; i.e., the surface appearance of the tungsten was unchanged. Still higher current densities would probably result in polishing. However, as the current density is increased, control of the electrolyte temperature becomes a major problem. For this and following experiments, the shell was set in a graphite holder, as shown in Figure II-12. A hemispherical graphite cathode was used.

With a concentration of 50 g of NaOH per liter, a bright reflective polish could be obtained. However, the polishing was sensitive to (1) the spacing between the cathode and tungsten, (2) the flow pattern of the electrolyte, and (3) the current density.

Although a bright reflective finish was obtained, complete leveling of protrusions was not accomplished. On continued

electropolishing, the protrusions became pits. It is suspected that removal of tungsten was more rapid at grain boundaries surrounding the protrusions and, as a result, the protrusions lifted out.

The use of a rotating cathode provided with a wiper cut from 1/8-in. -thick rubber sheet was also evaluated. The wiping action was definitely beneficial in leveling protrusions. However, the beneficial result was sensitive to pressure exerted by the wiper, and it was not established that uniform results could be obtained on the entire surface desired to be polished.

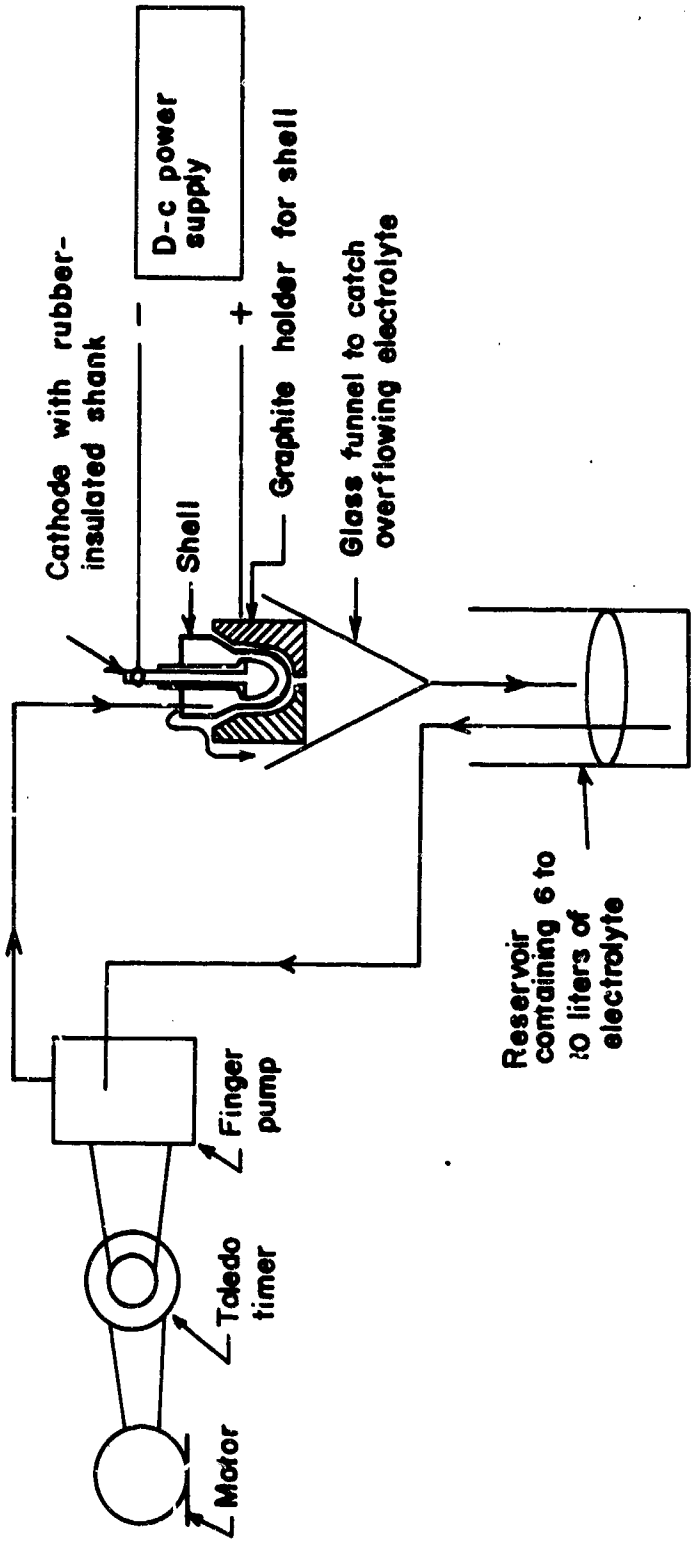

Figure II-12. Apparatus for Electropolishing Tungsten-Coated Shells.

III. THERMIONIC CONVERTER

Thermo Electron began work on hydrocarbon thermionic power systems in 1958. After the completion of preliminary systems analyses, combustion system development, and materials investigations, actual converter development (diode) was started. Since diode technology had progressed well as a result of Thermo Electron's comprehensive thermionic research program and hardware development projects, the program described here began immediately with the fabrication of a relatively large number of converters for testing under operating conditions that closely approximated those expected in a hardware generator. A unique high-temperature, high-heat-flux burner previously developed by Thermo Electron, and described in Section IV of this report, was used for this purpose. The objective of this effort was to approach the requirements established for the converters as closely as possible and to obtain enough experimental data to provide a sound basis for design modifications which would eliminate the problems encountered during test operation.

The first thermionic diode designed and built for a hydrocarbon-fueled thermionic engine, designated as Series II, is shown in cross section in Figure III-1. This diode had a tantalum emitter and spacer tube protected with an aluminum-tin coating developed by the General Telephone and Electronics Company's research laboratory. (The basis for the selection of this material is discussed in Section II of this report.) Figure III-2 shows the parts of the diode in exploded view, and Figure III-3 shows one of these diodes after test in a hydrocarbon flame. The diode fitted into an aluminum-oxide cylinder in the burner and was held in place by a packing gland. Each diode was tested by heating the emitter to a temperature of 1300 to 1430°C,

monitoring performance at this temperature for approximately 6 hours, taking performance curves, and then shutting down overnight. This testing was continued until the output of the diode dropped to zero. Each diode was then dissected and a study made of all determinable changes in geometry and material. A total of 43 converters were built, and most of them were tested in this manner. A small number of these diodes, however, were tested in vacuum to provide standards for comparison of diode performance (see Table III-1). The significant test results are described below:

(1) One major difficulty was the weld which held the emitter backing plate to the emitter shell (see Figure III-1). Study of failed units indicated that during fast heating of the converter, the thin side wall increased in temperature much faster than the more massive emitter disc and, as a result, the wall expanded faster than the disc. This resulted in high stresses in the spacer tube at this point and caused failure. Furthermore, the weld region was difficult to coat evenly. The oxidation-resistant coating had to diffuse into the hot-shell material to be effective, and the diffusion layer was two to three mils. Therefore the coating could diffuse completely through thin sections causing shorts in the interelectrode space. In the development of the next series of converters (Series III), both problems were circumvented by use of a deep-drawn sheet for fabrication of the hot shell, which eliminated welds at the hot end.

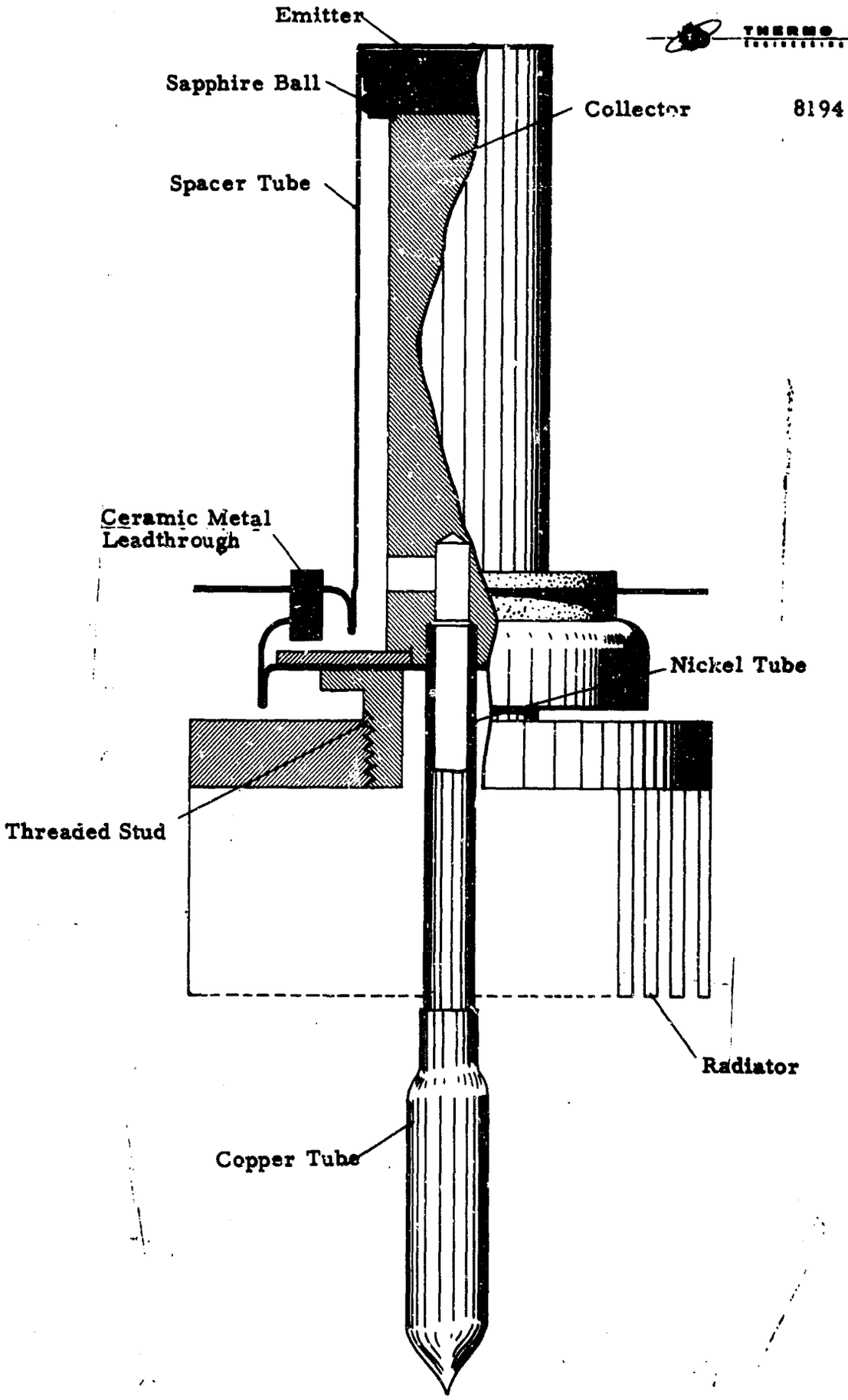

Figure III-1. Cross Section of Series II Hydrocarbon-Fueled Thermionic Diode.

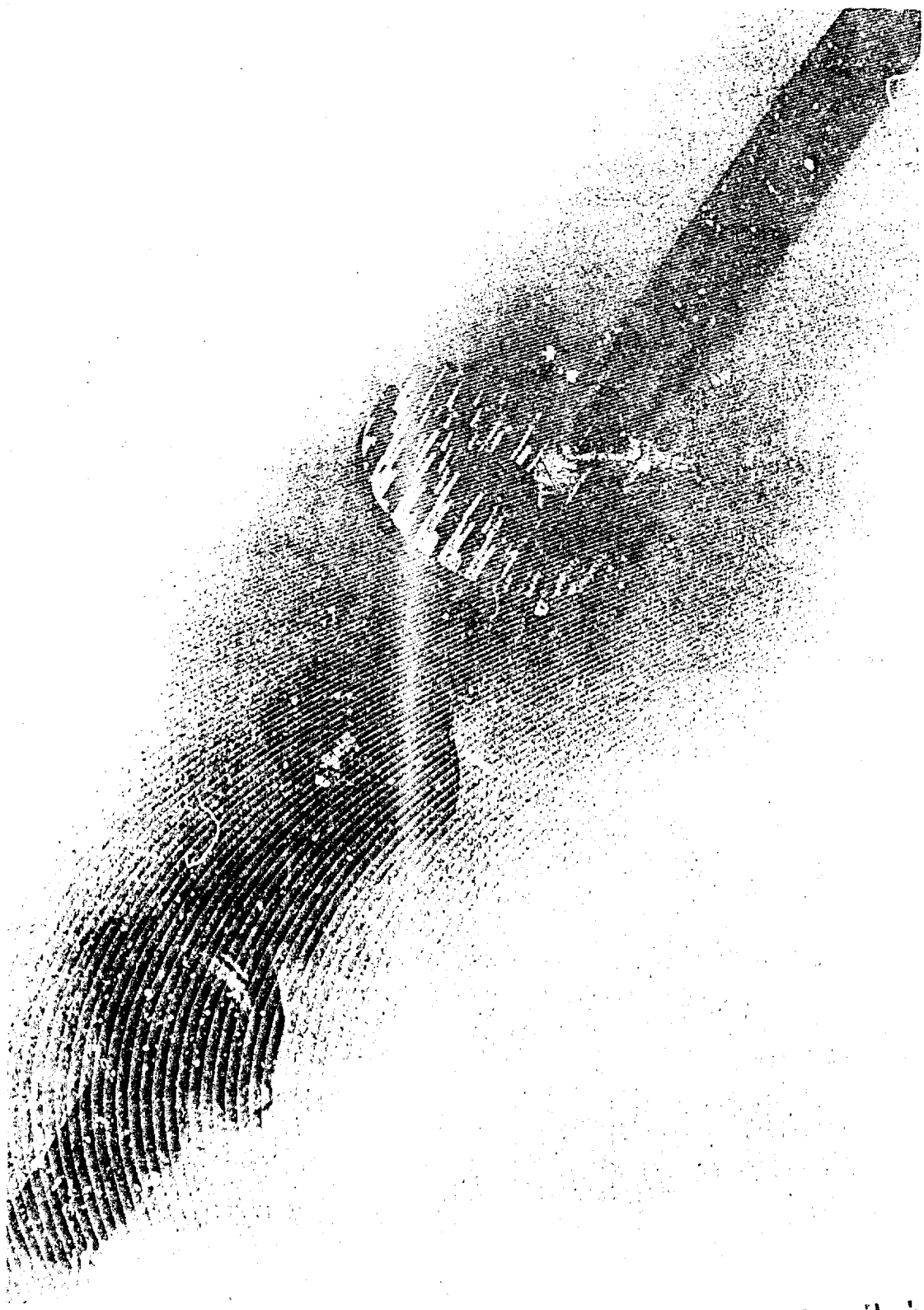

Figure III-2. Exploded View of Hydrocarbon-Fueled Thermionic Diode.

Not Available On

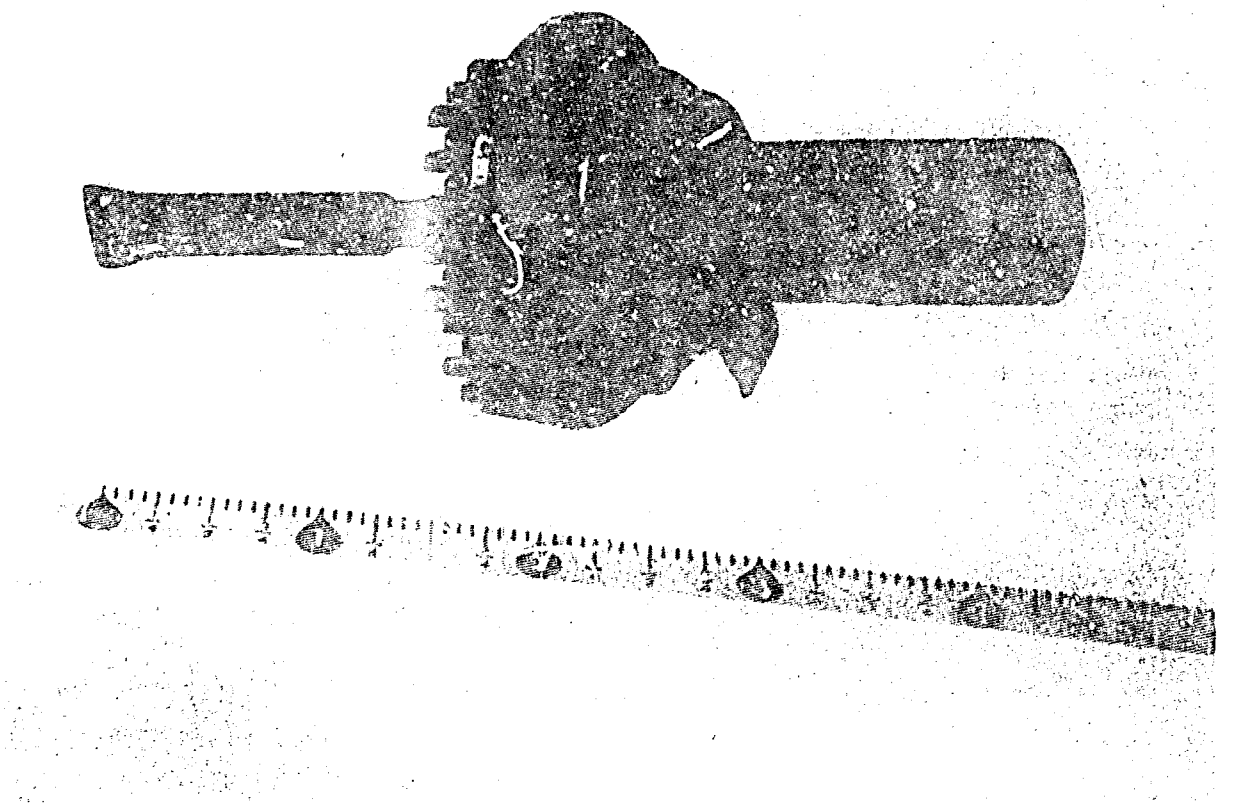

Figure III-3. Hydrocarbon-Fueled Thermionic Diode After Test in a Hydrocarbon Flame.

TABLE III-1

TEST CONVERTER SUMMARY, SERIES II DIODE

Diode No.	Design and Fabrication Features	Primary Cause of Failure	Comments
I-1	Uncoated Mo emitter Mo collector		Unable to make leadthrough hot-shell weld.
I-2	Uncoated Mo emitter Mo collector		Unable to make leadthrough hot-shell weld.
I-3	Coated Mo emitter Mo collector	Hot-end electron-bombardment weld failed.	Outgassed using RF coil as heat source. Five rapid thermal cycles before failure.
I-4	Uncoated Mo emitter Mo collector	Leadthrough metallizing failure.	160 hours of life in vacuum. 1.48 w/cm^2 at T_e = 1430°C at 0.5 volt.
I-5	Uncoated Mo emitter Tungsten oxide collector		Performance very low after 30 hours.
I-6	Coated Mo emitter Mo collector	Failed during outgassing on burner. Coating attacked by impurities in protecti sleeve.	
I-7	Coated Mo emitter Mo collector	Leadthrough - hot shell weld contaminated by coating material.	

THERMO ELECTRON
ENGINEERING CORPORATION

I-8	Coated		Not built. Coated hot shell used to check effect of rapid heating of emitter end.
I-9	Coated Mo emitter Mo collector		Leadthrough - hot shell weld unsuccessful.
I-10	Coated		Not built. Coated hot shell used to check effect of rapid heating of emitter end.

All the following diodes were fitted with rhenium emitters and molybdenum collectors:

II-1	Uncoated		Tube retired after 24 hours of very low performance in vacuum.
II-2	Coated	Reaction of coating with alumina protection sleeve.	Diode generated power for 100 continuous hours. Maximum power density 1.11 w/cm^2 at 0.3 v and T_e = 1280°C.
II-3	Coated Increased clearance between hot shell and protection sleeve.	Badly oxidized side walls of hot shell.	Failed after 5-1/2 hours of outgassing and 8 hours of running time at 1330°C.
II-4	Coated Increased clearance between hot shell and protection sleeve	Badly oxidized side walls of hot shell.	Failed in essentially the same manner as II-3 after 5 hours of outgassing and 3 hours of running time.

THERMO ELECTRON
ENGINEERING CORPORATION

TABLE III-1 (continued)

Diode No.	Design and Fabrication Features	Primary Cause of Failure	Comments
II-5	Coated Same radial clearance as II-2	Oxidation of hot shell at cooler end.	Improper machining methods caused cracking of coating which could not heal. Failure after 4 hours of outgassing and 6-1/2 hours of power generation at 1330°C.
II-6	Coated Same radial clearance as II-2	Oxidation of hot shell at cooler end.	Improper machining methods caused cracking of coating which could not heal. Failure after 4 hours of outgassing and 1-1/3 hours of power generation at 1360°C.
II-7	Coated		Tube not built because of same machining treatment as diodes II-5 and II-6.
II-8	Uncoated		Tube not completed - final electron-bombardment weld failed.
II-9	Uncoated		Tube not completed - final electron-bombardment weld failed.
II-10	Coated after diode assembly; outgassed in vacuum	Reaction between hot shell and alumina sleeve.	Diode produced power for 22-1/2 hours. Maximum power density 1.15 w/cm^2 at 0.20 v and T_e = 1330°C.

THERMO ELECTRON CORPORATION

II-11	Uncoated Outgassed for 34 hours at temperatures up to 1700°C in vacuum	No failure; tube retired after 100 hours.	Very low performance. Testing indicated collector face temperature approximately 100°C too high.
II-12	Uncoated Outgassed for 13 hours at temperatures up to 1700°C	No failure; tube retired after 366 hours of power generation.	Maximum power density = 4.1 w/cm^2 at 0.4 volt and 1420°C.
II-13	Coated Increased diameter collector stem to decrease collector face temperature. All further diodes have larger-diameter collector stem. Coating thickness = 38.7 mg/cm^2		Final electron-bombardment weld unsuccessful - could not be salvaged.
II-14	Coated with R-505A Thickness = 38.7 mg/cm	Oxidation of hot shell 1-1/4" from hot end.	Outgassed for 6 hours on burner operated as a diode for 23-1/2 hours. Maximum power density = 1.19 w/cm^2 at 0.38 v and T_e = 1330°C.
II-15	Coated with R-505A Thickness = 45 mg/cm^2	Oxidation of hot shell 1-14" from hot end.	Outgassed for 9-1/3 hours at temperatures up to 1360°C. Generated power for 7.80 hours. Maximum power density = 0.57 w/cm^2 at 0.17 v and T_e = 135[illegible]°C.

THERMO ELECTRON ENGINEERING CORPORATION

TABLE III-1 (continued)

Diode No.	Design and Fabrication Features	Primary Cause of Failure	Comments
II-16	Coated with R-505A Thickness = 52 mg/cm	Sapphire spheres pushed through hot shell wall.	Outgassed for 11 hours at temperatures up to 1330°C. Operated as diode for 2 hours. Maximum power density = 1.25 w/cm^2 at 0.28 v and T_e = 1328°C.
II-17	Coated with R-505A modified with titanium Coating thickness = 45 mg/cm^2	Hot end electron-bombardment weld oxidation.	Outgassed for 9-1/2 hours at temperatures up to 1345°C. Virtually no power output. One burst of 2.5A at 0.38 v and T_e = 1315°C.
II-18	Coated with R-505A modified with titanium Coating thickness = 43 mg/cm^2	Hot and electron-bombardment weld oxidation.	Outgassed for 7 hours at temperatures up to 1368°C. Generated power for 6-1/3 hours. Maximum power density = 1.26 w/cm^2 at 0.33 v and T_e = 1407°C.
II-19	Coated after diode assembly with R-505C Coating thickness cannot be determined; attempted to apply 50 mg/cm^2.	Cesium reservoir failed apparently during coating operation. Could not be salvaged. Leadthrough flanges attacked by coating vapor; lead-through porous.	Outgassed in vacuum for 12 hours at temperatures up to 1600°C. Substantial amount of grain growth in hot shell at emitter end. No power generated.
II-20	Coated after diode assembly with R-505C. Coating thickness cannot be determined; attempted to apply 50 mg/cm^2.	Coating material corroded leadthrough flange. Tube beyond repair.	Outgassed in vacuum for 14 hours at temperatures up to 1700°C. Substantial amount of grain growth in hot shell at emitter end. No power generated.

THERMO ELECTRON ENGINEERING CORPORATION

II-21	Coated after diode assembly with R-505C Coating thickness cannot be determined; attempted to apply 50 mg/cm^2.	Hot end electron-bombardment weld oxidation.	Outgassed in vacuum for 18-2/3 hours at temperatures up to 1600°C. Was fired as diode but generated essentially no power before failure.
II-22	Coated after diode assembly with R-505C Coating thickness cannot be determined; attempted to apply 50 mg/cm^2.	Embrittlement of hot shell near hot end electron-bombardment weld. Coating material shorted electrodes after 1/2 hour of heating on burner up to 1200°C.	Outgassed in vacuum for 8-1/2 hours at temperatures up to 1600°C. Substantial amount of grain growth in hot shell at emitter end.
II-23	Coated with R-505C Coating thickness = 56 mg/cm^2	Hot end electron-bombardment weld oxidation.	Outgassed using natural gas-air burner as a heat source for 9-1/2 hours at temperatures up to 1340°C. Generated electrical power for 127.1 hours. Maximum power density = 1.92 w/cm^2 at 0.365 v and T_e = 1365°C.
II-24	Coated with R-505C Coating thickness = 54 mg/cm^2	Oxidation of hot shell 0.4" from emitter end.	Outgassed using natural gas-air burner as a heat source for 13-1/4 hours at temperatures up to 1340°C. Generated electrical power for a total of 31-1/2 hours. Maximum power density = 1.0 w/cm^2 at 0.21 v and T_e = 1350°C.

THERMO ELECTRON ENGINEERING CORPORATION

TABLE III-1 (continued)

Diode No.	Design and Fabrication Features	Primary Cause of Failure	Comments
II-25	Coated with R-505C Coating thickness = 54 mg/cm^2	Oxidation of emitter backing plate close to electron-bombardment weld.	Outgassed for 10-1/2 hours on natural gas-air burner at temperatures to 1370°C. Generated electrical power for 3-1/2 hours at low power density.
II-26	Coated with R-505C Coating thickness 55 mg/cm^2	Oxidation of hot shell 0.35" from hot end.	Outgassed for 14 hours on the natural gas-air burner at temperatures up to 1335°C. Generated power for 12.2 hours. Maximum power density = 1.51 w/cm^2 at 0.3 v and T_e = 1363°C.
II-27	Coated with R-505C Coating thickness = 61 mg/cm^2	Oxidation of hot shell 1-1/2" from emitter end.	Outgassed on natural gas-air burner for 11-1/4 hours at temperatures up to 1350°C. Generated electric power for 83-1/3 hours. Maximum power density = 0.61 w/cm^2 at 0.26 v and T_e = 1370°C.
II-28	Coated with R-505C Coating thickness = 58 mg/cm^2		Coated hot shell improperly machined. Diode could not be built.

THERMO ELECTRON

II-29	Coated with R-505C	Hot end electron-bombardment weld oxidation.	Outgassed on natural gas-air burner for 11-2/3 hours at temperatures up to 1470°C. Tube generated power for a total of 43-1/3 hours; maximum power density = 2.85 w/cm^2 at 0.381 v and T_e = 1450°C.
II-30	Coated with R505C Coating thickness = 55 mg/cm^2	Hot end electron-bombardment weld oxidation	Outgassed on natural gas-air burner for 13 hours at temperatures up to 1500°C. Tube generated power for a total of 5-1/4 hours. Maximum power density occurred at 1.81 w/cm^2 at 0.34 v and T_e = 1440°C.
II-31	Uncoated	Tube retired after 2071-1/2 hours of vacuum firing	Outgassed in vacuum for 23 hours at 1660°C. Maximum power density = 4.0 w/cm^2 at 0.44 v and T_e = 1400°C.
II-32	Uncoated		Final electron-bombardment weld unsuccessful. Salvage unsuccessful. No power.
II-33	Coated		Collector flange improperly jigged. Tube not completed.

THERMO ELECTRON ENGINEERING CORPORATION

(2) A number of failures of the hot shell occurred about 1/4" from the hot end. Some of these were associated with interaction of the oxidation-resistant coating and the alumina sleeve which surrounded the entire hot shell. This problem was overcome by replacing the 96% pure alumina sleeve with one of recrystallized 99.5% pure alumina. Also, in this area the maximum rate of chemical reaction occurred between the substrate and the coating, causing the coating to diffuse through the hot shell particularly rapidly in this region. Two steps were taken to alleviate these problems: First, the substrate thickness was increased from 0.010" to 0.025", and second, the substrate material was changed to 90% tantalum, 10% tungsten.

(3) The sapphire spheres which centered and insulated the collector stem from the hot shell were another problem. One type of failure involved the mechanical clearances between the spheres and the inside of the hot shell. If the clearance was insufficient, the collector with the embedded spheres could still be pressed into place. This pressing caused distortion of the coated hot shell and cracking of the somewhat brittle intermetallics formed during the coating process. The coating was self-healing, provided that there was a supply of aluminum present and that the temperatures were high enough for the distribution mechanism to be operative. However, at the collector end of the diode (about 1 to 1-1/2" from the emitter) the temperature was low, and this healing mechanism did not occur. As a result, failures occurred at the cooler end in the form of straight lines spaced 120° apart circumferentially. Immediately after removing the mechanical interference between the hot shell and the spheres, this type of failure ceased. Another problem with the spheres occurred during diode operation. The force of atmospheric pressure caused

the collector support flange to bend. This forced the collector stem to assume a position at an angle to the axis of the hot shell and thus applied a force to these spheres, which pushed through the hot and relatively weak tantalum. This problem was eliminated in the subsequent design by replacing the sapphire spheres with split sapphire sleeves, which reduced bearing stress by several orders of magnitude.

(4) The performance of the diodes tested under this program was better than any ever demonstrated before using a hydrocarbon flame, but it fell short of that predicted by Thermo Electron's research data. One of the main reasons for this discrepancy was the elastic and plastic deformation of the collector support flange, which resulted in changes of the interelectrode spacing. The part was too heavily loaded by atmospheric pressure for its designed thickness. This problem was eliminated in the next series of diodes, Series III, by strengthening the member and also by reducing the load on the part. This diode was smaller in diameter, and consequently atmospheric loading of the diaphragm was less. Another reason for poorer-than-predicted performance was the fact that the collector stem had a relatively large portion of its cross-sectional area removed to allow passage of the cesium vapor. Therefore the heat-rejection path had low conductance, and the collector face overheated. This problem was circumvented in the Series III diode by designing the collector stem so that the cross-sectional area removed for the cesium passage was compensated for by an increase in the diameter of the stem. The collector face temperature also tended to be excessively high because the pin-finned radiator was in relatively poor thermal contact with the collector stem. In the Series III design the collector and cooling fins were machined from one integral piece of stock.

The best performance achieved with the Series II diode was typified by the test results of the following three converters:

The first was converter II-23, which generated electric power for 127.1 hours, exclusive of 9 hours of flame-heated outgassing. Figure III-4 shows the outgassing profile of this tube. Figure III-5 is a plot of gross power output versus time for the cyclic flame-heated testing to which diode II-23 was subjected. A group of performance curves taken during the life ot this diode is shown in Figure III-6.

The life history of diode II-29 is documented in Figures III-7 through III-9. This diode was outgassed at temperatures up to 1450°C and operated as a diode at 1440°C. Its outgassing profile is shown in Figure III-7. The change in pressure between the hot and cold condition after outgassing was small, indicating that the tube was well outgassed. Figure III-8 shows the power production history of this diode, and Figure III-9 is a composite of several curves of power density versus output voltage. This diode was tested at its rated design voltage (0.5v) during virtually its entire life. Figure III-10 is a photograph of diode II-29 on test.

A third converter, II-31, was operated in vacuum to evaluate the materials (other than the emitter shell coating) and construction techniques used in the diode. Figure III-11 is a plot of power density versus time at 0.4v and 0.5v outputs for converter II-31. The test temperature was 1400°C, and all data was taken with the cesium reservoir temperature optimized for the different voltages. Figure III-12 shows several I-V curves generated during the life of the tube. After 2000 hours of operation at 1400°C and after 85 thermal cycles, the diode continued to produce power.

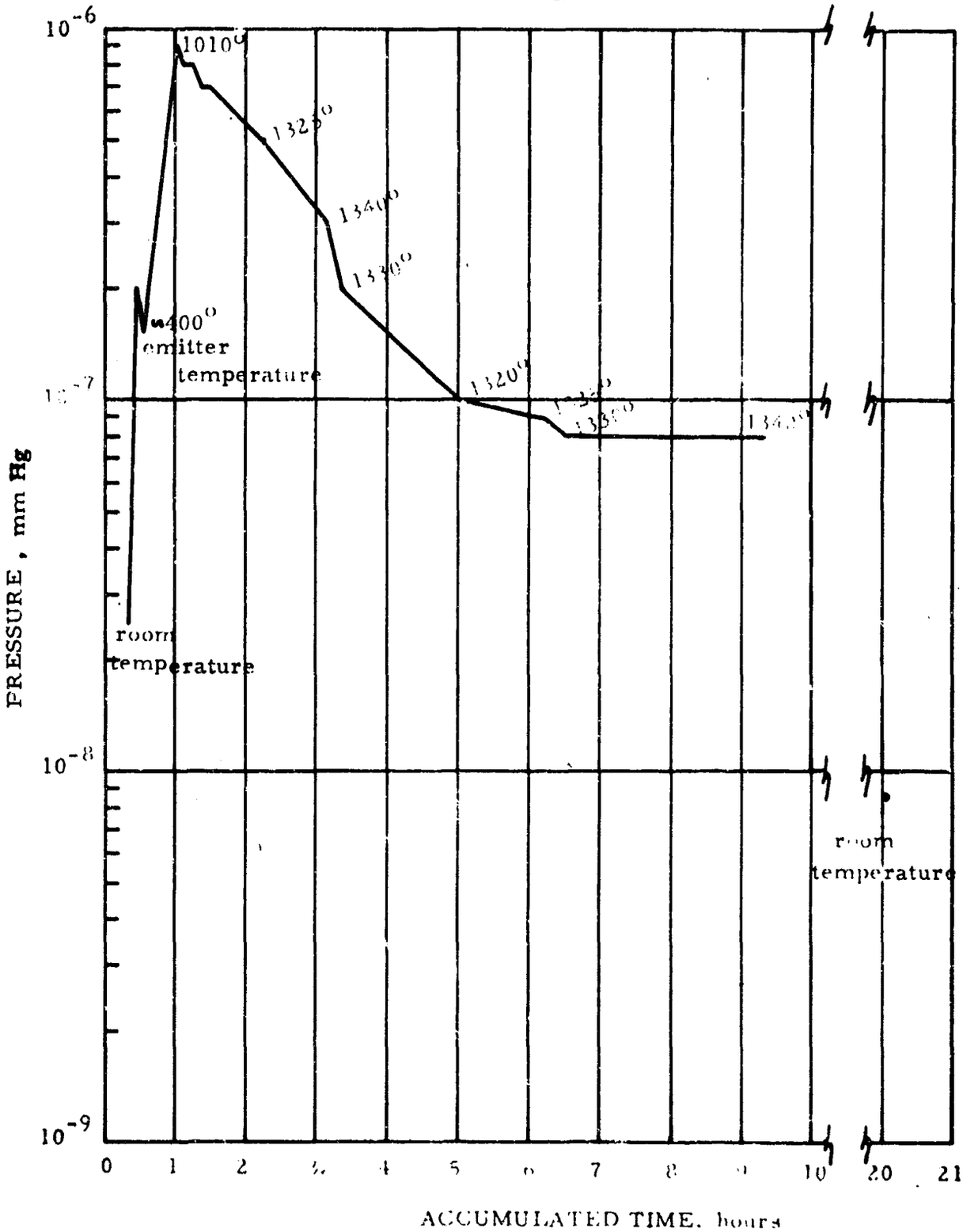

Figure III-4. Outgassing Profile for Diode II-23.

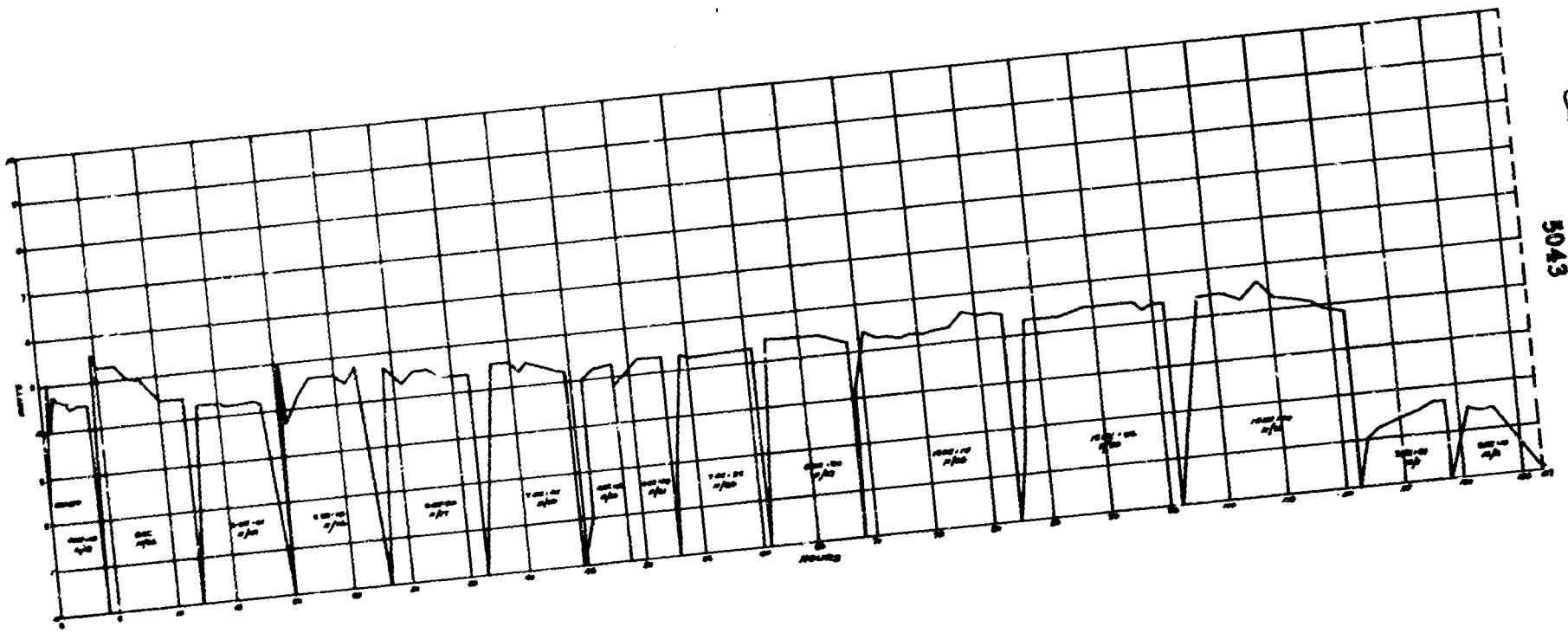

Figure III-5. Watt-Hour Profile for Diode II-23.

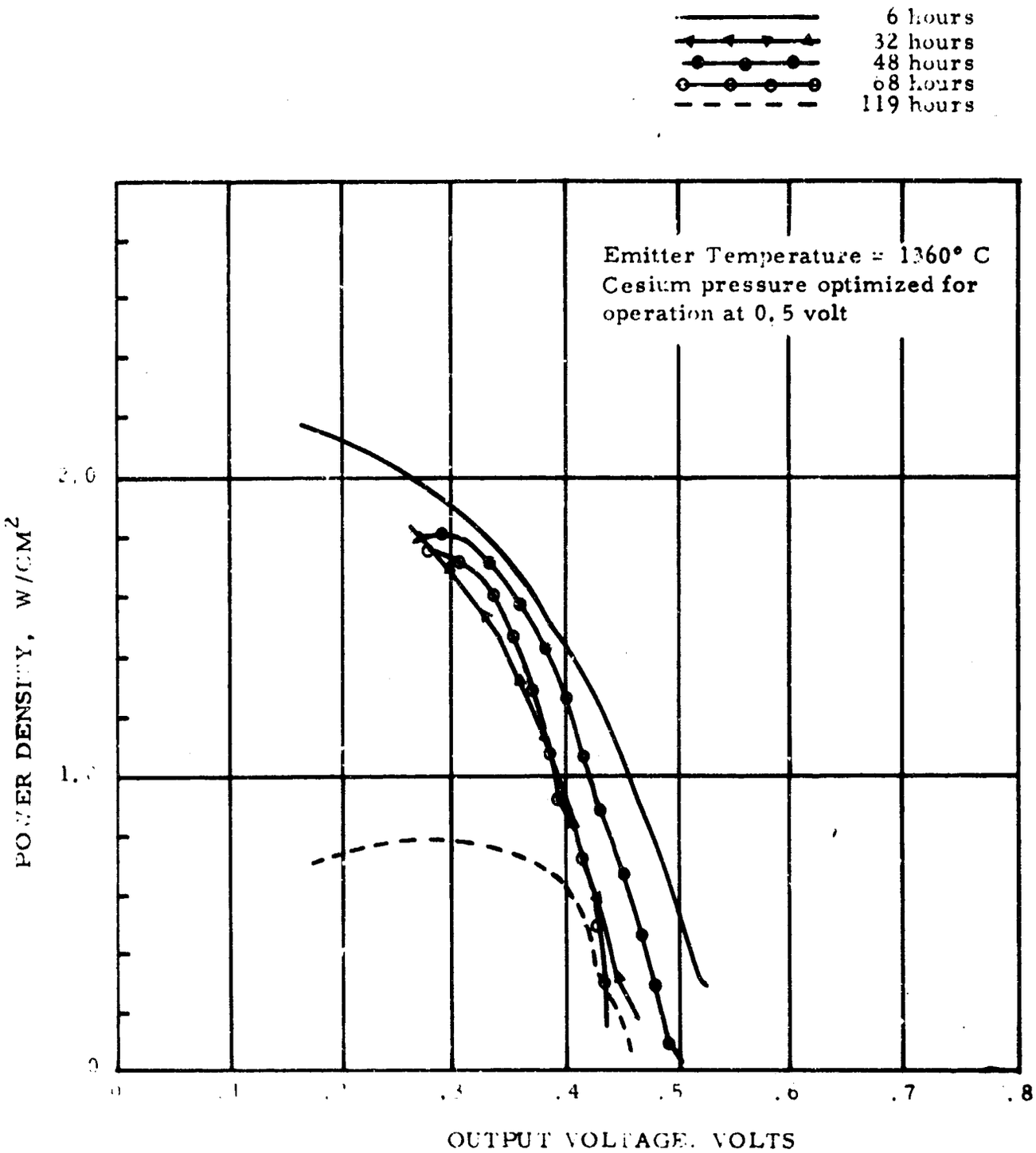

Figure III-6. Performance Curves for Diode II-23.

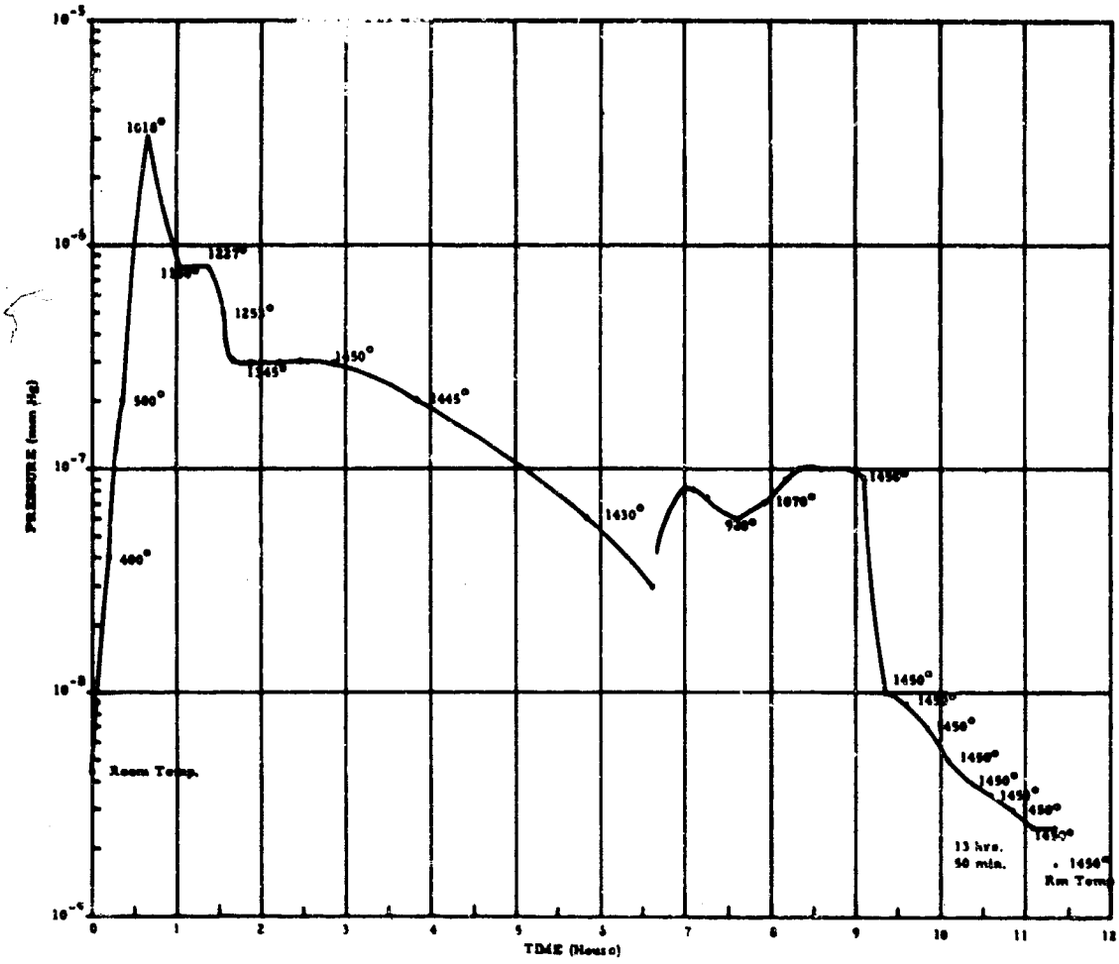

Figure III-7. Outgassing Profile for Diode II-29.

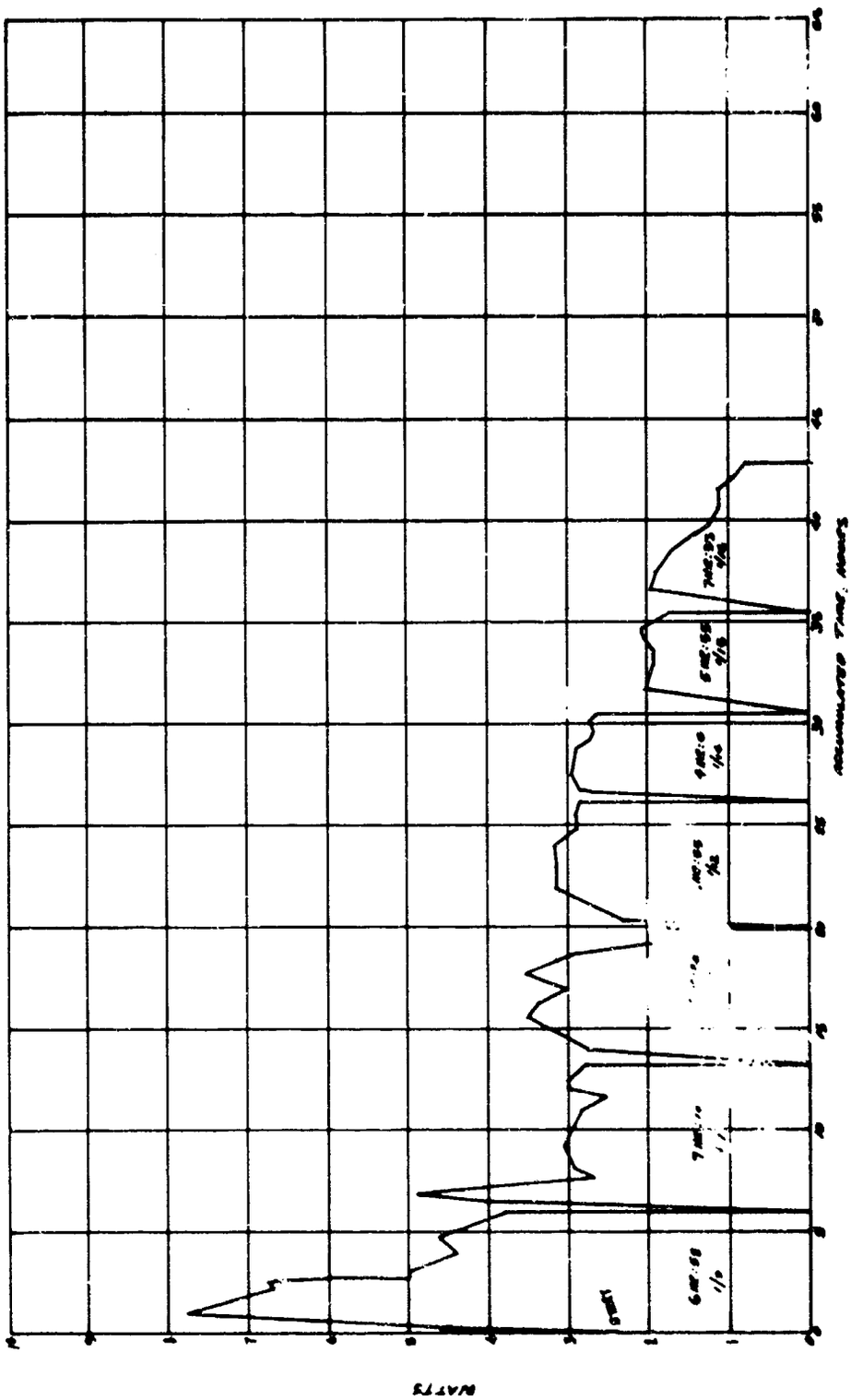

Figure III-18. Series VI-S Hydrocarbon-Fired Thermionic Converter.

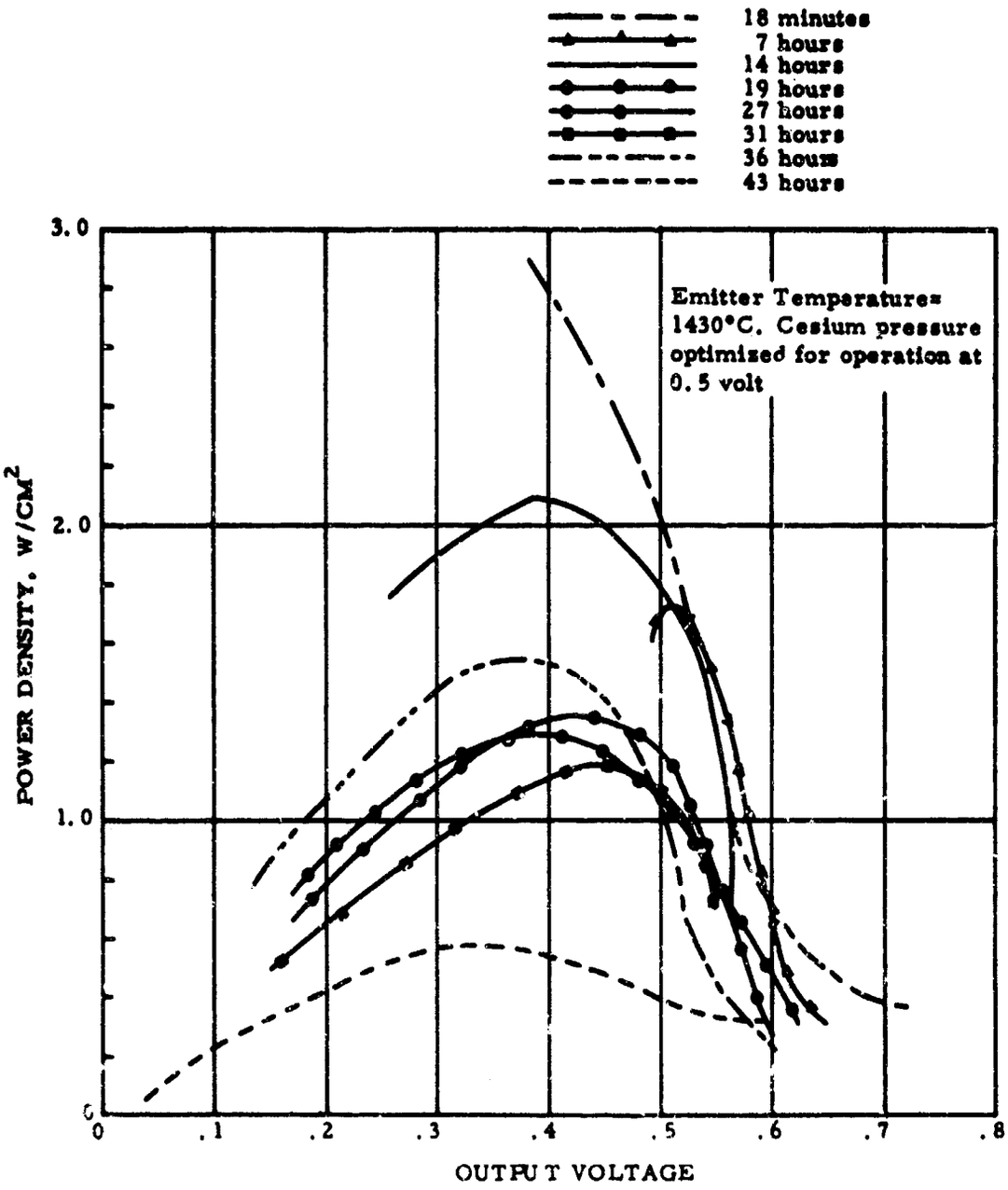

Figure II-9. Performance Curves for Diode II-29.

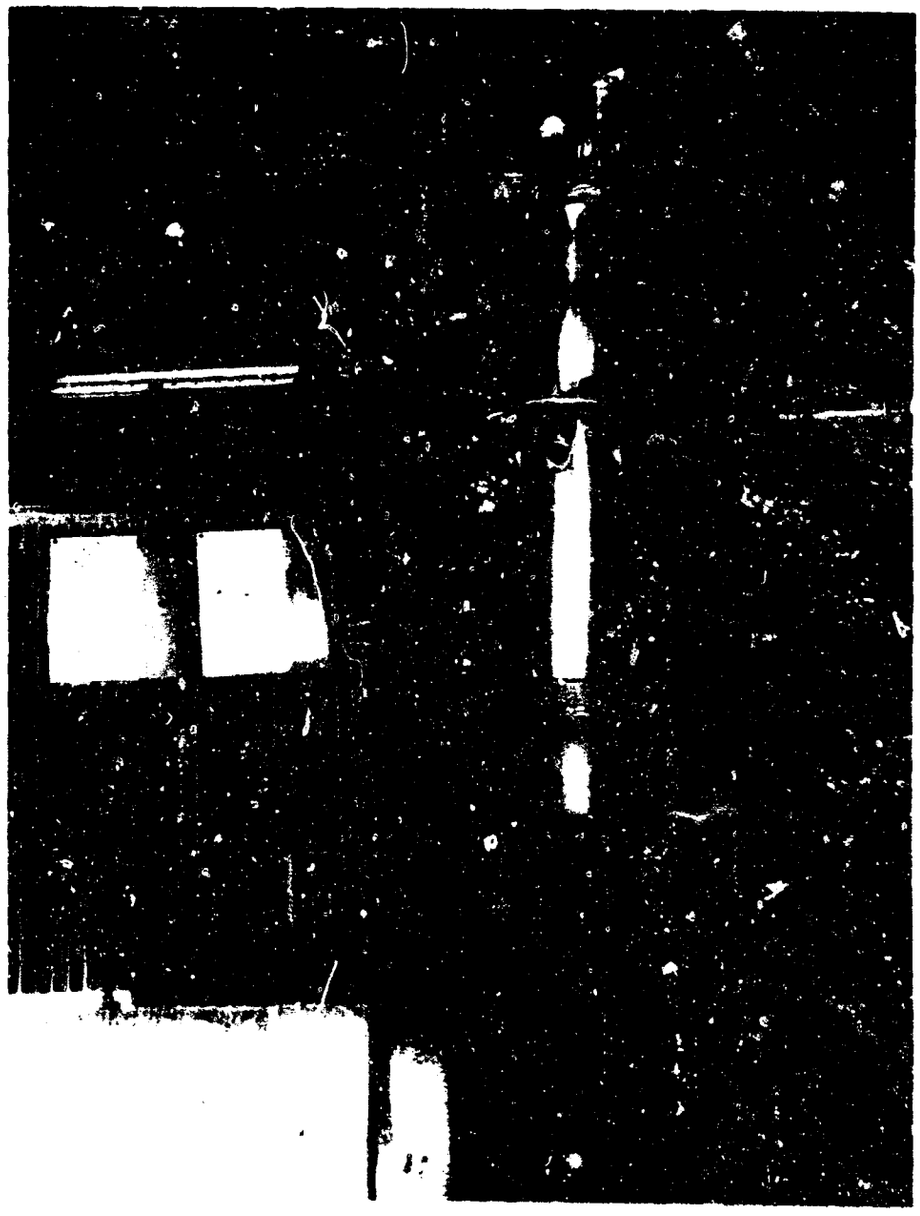

Figure III-10. Model III Burner Driving Diode II-29.

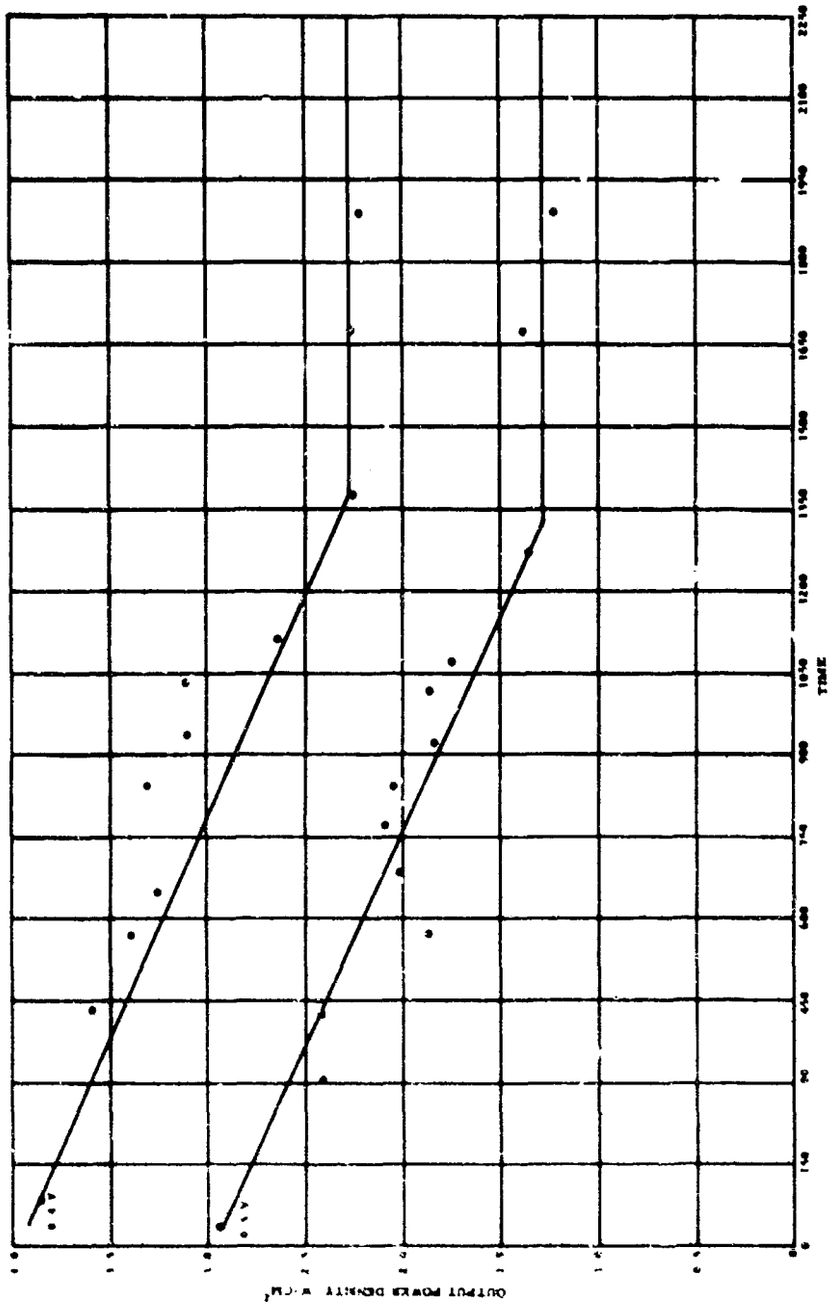

Figure III-11. Power Density versus Time for Two Output Voltages for Diode II-31.

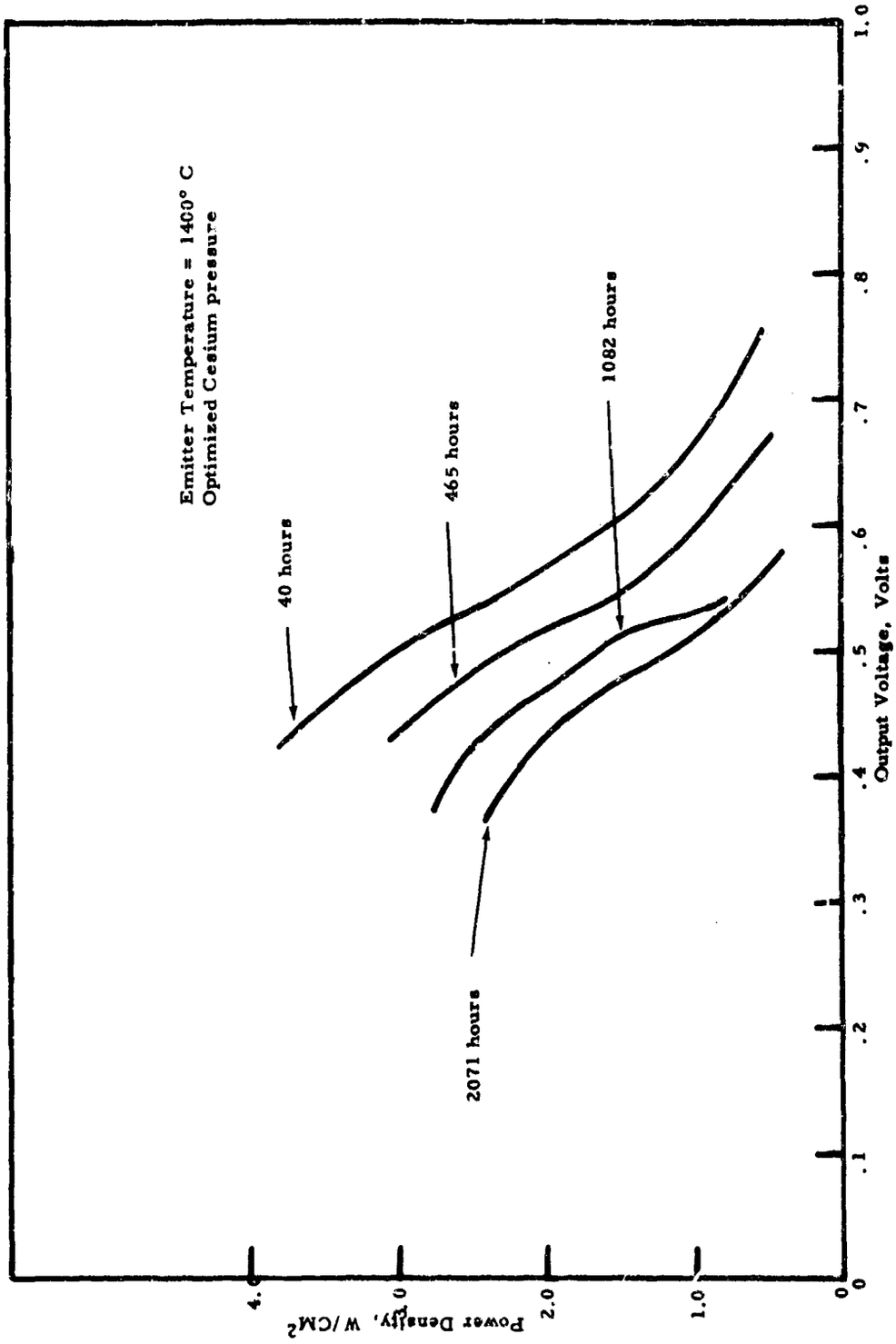

Figure III-12. Performance Curves for Diode II-31.

The experience gained in developing the Series II diode was used in designing the next series of diodes, designated as Series III. This series of diodes incorporated structural improvements over the Series II and also used an improved version of General Telephone and Electronic's aluminum-tin mixture for oxidation protection. The Series III diode is shown in Figure III-13.

During the early stages of the Series III development program oxidation-resistant emitter shells (hot shells) made of pyrolytic silicon carbide on tungsten, described in Section II, became available and showed promise of greatly improved resistance to combustion products. Work was therefore stopped on the Series III, and a diode was designed incorporating a hot shell of this latter material. This diode, designated Series V, incorporated all the mechanical improvements of the Series III plus the silicon carbide hot shell.

The Series V diode is shown in Figure III-14. The hot shell assembly consisted of the shell and a molybdenum adapter which was brazed to the open end of the hot shell. An adapter of this type served a dual purpose: to join the shell to the diode outer structure, and to minimize the effect of differential thermal expansion between the shell and the diode structure. These differential thermal expansions were present during diode fabrication, assembly and cycling. The adapter-to-hot-shell braze joint was so designed that the braze material was ductile enough to yield and absorb the differential thermal expansion. The hot shell tip was hemispherical to allow maximum area utility for a given diameter hot shell and to make it easier to fabricate by pyrolytic deposition. The emitter surface was cleaned and polished by electro-polishing.

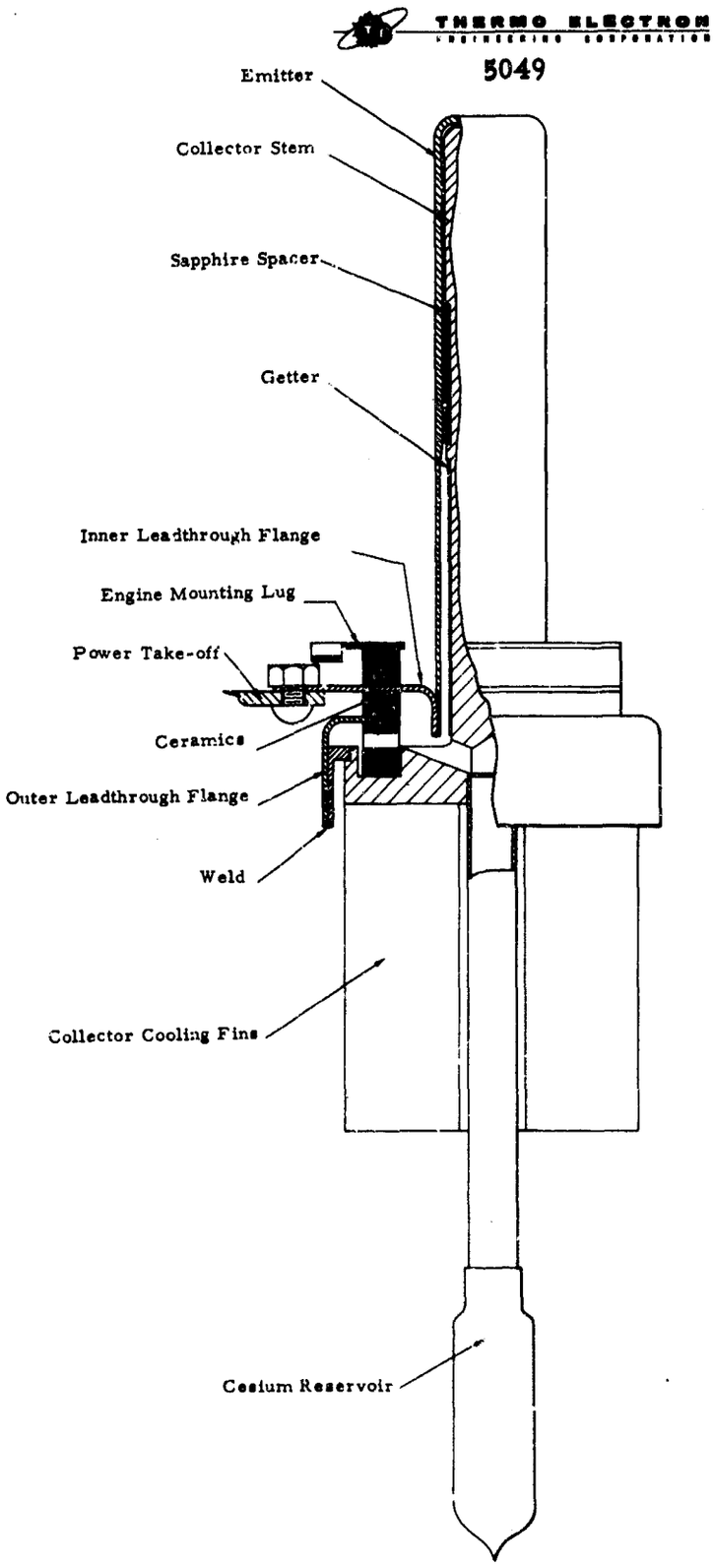

Figure III-13. Cross Section of Series III Diode.

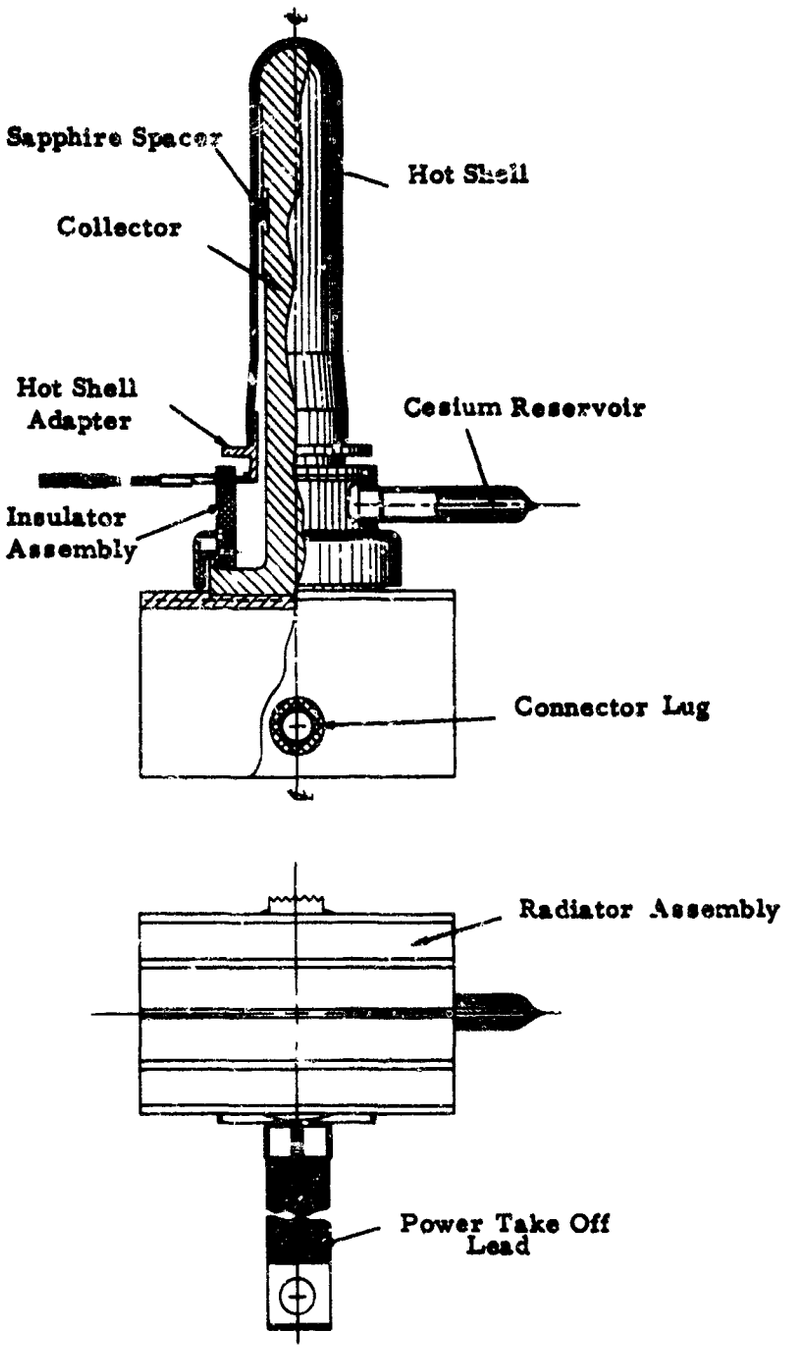

Figure III-14. Series V Hydrocarbon-Fired Thermionic Diode Design.

The insulator assembly was a stacked structure of metallized high-alumina ceramic rings and Kovar parts, one of which was a stamped cup, the other a cylindrical part having an integral flat flange. The flanged section of the latter part comprised part of the stacked-butt seal section and was backed by a ceramic ring to equalize thermal stresses on both sides of the flange. The cylindrical section provided a surface to which the hot shell assembly could be brazed. A 3/16"-diameter nickel tube was provided to serve as an outgassing tubulation and as a cesium reservoir.

The concentricity of the long collector stem with respect to the hot shell was maintained by three small sapphire spacers. These spacers were designed to have sufficient surface area to minimize bearing stresses on the hot shell wall while not adversely restricting pumping paths within the diode during outgassing. The spacer design was such that yielding would occur at the collector base before the bearing stresses on the hot shell wall became significant. The finned radiator assembly was brazed to the outside surface of the collector base. This radiator assembly was designed to dispose of the rejected heat from the diode and to maintain the critical thermal balance of the diode.

Power take-off from the diode was accomplished with a flexible cable extending from the top cylindrical Kovar piece of the insulator assembly.

As a result of the system analysis performed in 1963, it became apparent that a larger diode could be used in designing the 45-watt thermionic engine, shown in Appendix A. Such a unit, with a design output of 100 watts, was designated the Series VI diode and is described next.

The Series VI diode, shown in cross section in Figure III-15, is a larger version of a Series III diode using the same basic concept (that is, two concentric cylinders with one end hemispherically closed). The emitter and collector are formed by the two hemispheres, and the cylindrical section forms a heat choke, so that the emitter temperature gradually drops to the maximum allowable seal temperature, which is 500°C. A ceramic-to-metal seal provides the required electrical insulation between emitter and collector. The cooling of the collector was accomplished with forced convection by jets of inert gas through a specially provided cooling probe.

Before proceeding with the actual construction of the Series VI diodes, effort was concentrated on establishing sources of supply for the Series VI type of hot shell. For the temperature range of 1350 to 1450°C, where these diodes were planned to operate, the W-Mo emitter-collector system was chosen, as was a spacing of approximately 10 mils. Various suppliers of hot shells made with pyrolytically-deposited silicon carbide on tungsten were contacted. In addition, a contact was established with the Battelle Memorial Institute, Columbus, Ohio, regarding the possibility of manufacturing pyrolytically-deposited silicon carbide shells on tungsten and at the same time providing the project with consulting and investigative services.

By the middle of 1964 several shells were received from these suppliers. The first ones were made with the use of copper mandrels to which tungsten was first deposited, and then silicon carbide after the copper mandrels were removed. Other shells were made on graphite mandrels. The discontinuation of the tungsten deposition operations at the research facilities of the first supplier led to concentrated efforts with the others. Orders were placed for pyrolytically-deposited tungsten

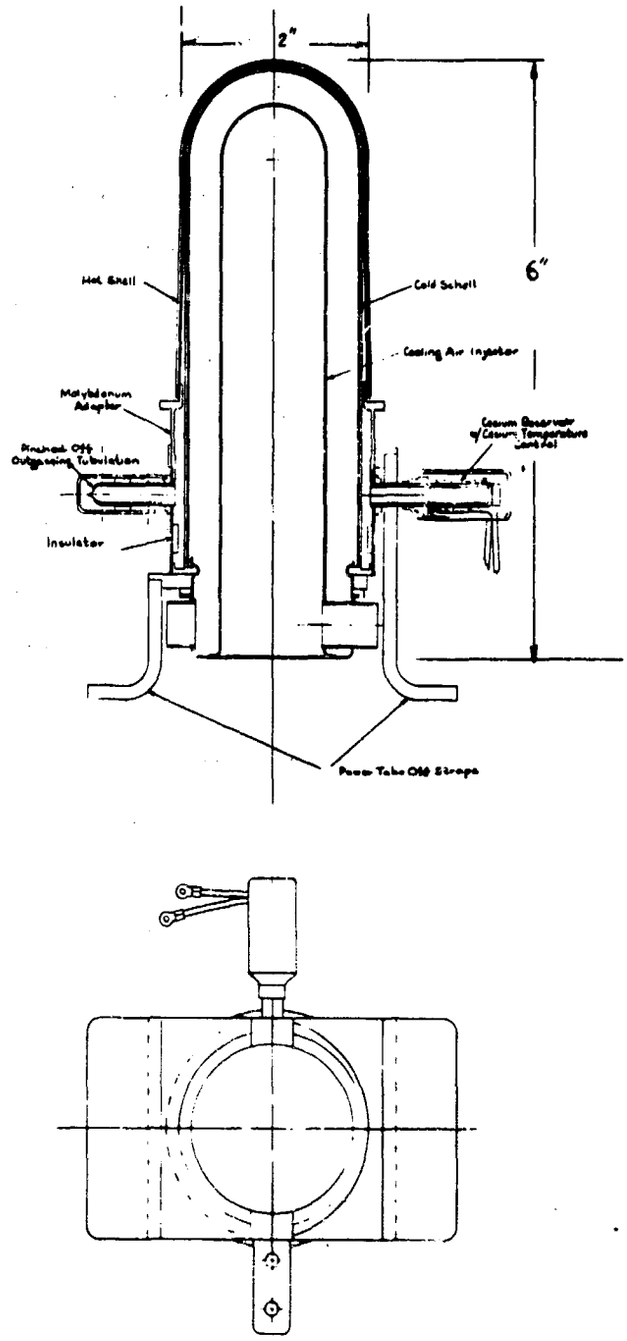

Figure III-15. Series VI Hydrocarbon-Fired Thermionic Diode Design.

shells which would then be coated with silicon carbide by other vendors, and a number of experimental shells were received. None, however, were satisfactory. In July of 1964 the first three experimental shells were received from Battelle Memorial Institute. Examination and tests gave evidence of poor adherence between silicon carbide and tungsten, and the shells failed at various stages of preparation before they could be used for tests under the burner. Work continued with Battelle Memorial Institute with the construction of complete shells, including the deposition of tungsten and of silicon carbide. Several problems had to be solved involving improvement of deposition techniques, mandrel removal procedure, and processing of the shells before they could be assembled in a diode, and they are described in detail in Section II of this report.

By October 1964 progress in all these areas had reached the point where a complete diode could be assembled with confidence. Such a diode was first assembled and tested during the month of November. This diode, VI-1, was tested with a methane-air burner.

Before the diode was placed on test, the best burner had been calibrated with a dummy shell in order to correlate shell temperature with the burner parameters. In this burner the shell surface was not visible during operation. Consequently pyrometric measurements could not be taken during the test. After outgassing for 16 hours at 1450°C, pinch-off, and cesium distillation, Diode VI-1 was placed on test in the burner and was run at an estimated emitter temperature of 1350°C. The diode produced 21 watts and ran for 3.4 hours. At the end of that time the diode temperature began to fall off, and pressure measurements on the burner indicated that one of the fuel injectors was plugged. The burner

was examined, and it was established that a temperature difference of more than 200°C existed circumferentially on the emitter area because of the plugged injectors. In addition, craters and erosion were evident on the protective silicon carbide coating .

To allow observation of the emitter shell during testing and the performance of pyrometric temperature measurements, a methane-oxygen burner was designed. In the absence of preheated air and to achieve the high heat fluxes and temperatures required by the thermionic converters, a mixture of methane and oxygen was used. The burner consists of a flame arrestor and mixing chamber of an oxyacetylene torch connected to a plenum, which in turn has orifices to direct the flames at the hemisphere. The burning occurs after the mixed oxygen and methane have passed through the orifice, in a manner similar to a gas burner in a stove. The jets of burning gas strike the shell and heat it. The plenum forming the burner head is water-cooled. A schematic layout of the burner and the shell under test is given in Figure III-16. Of course, there is a tendency for the part of the shell being struck by the flame to be hotter than surrounding areas. The first burner had an insufficient number of orifices, and temperatures between 1300°C and 1450°C were observed. The high-temperature spots constituted about 1/20 of the total hemispherical area. To heat the diode evenly and over the bulk of its hemispherical surface, a larger burner, with smaller orifices spaced closer to each other, was constructed and was used successfully.

A second diode, VI-2, was placed on life-test. After 40 hours the cooling of the collector was accidentally interrupted, and the collector overheated, expanded, and pressed through the hot shell, destroying the diode. The shell was examined, and it showed no signs of erosion or oxidation.

From the tests performed up to that time on individual shells, as well as on complete diode assemblies, two conclusions could be drawn:

1. The silicon carbide coating of tungsten was preventing the oxidation of tungsten at temperatures up to 1450°C. It was also forming an impervious barrier to the gaseous environment of the diode, as evidenced by the stable thermionic performance that was obtained.

2. In the structures obtained by pyrolytic deposition of silicon carbide, lifetimes of from 100 to 150 hours were achieved.

The heating was interrupted every 20 hours, and the shell was allowed to cool to room temperature. Several shells were tested, and invariably the mode of failure was the fracture and spalling of silicon carbide from the tungsten substrate. This occurred during the cooling-down cycle at a temperature below the visible range, estimated at 400 to 500°C. A number of controlled tests were then performed with composite vapor-formed structures. It was then noticed that the presence of a carburized layer of tungsten was improving the bond between the silicon carbide and tungsten. It was also noticed, through electron probe analysis and metallographic examination of these structures, that a layer of tungsten disilicide was formed after the tungsten-silicon carbide structure had remained at the test temperature (1400 to 1450°C) for a period of over 10 hours. An exact relationship has not been established between the

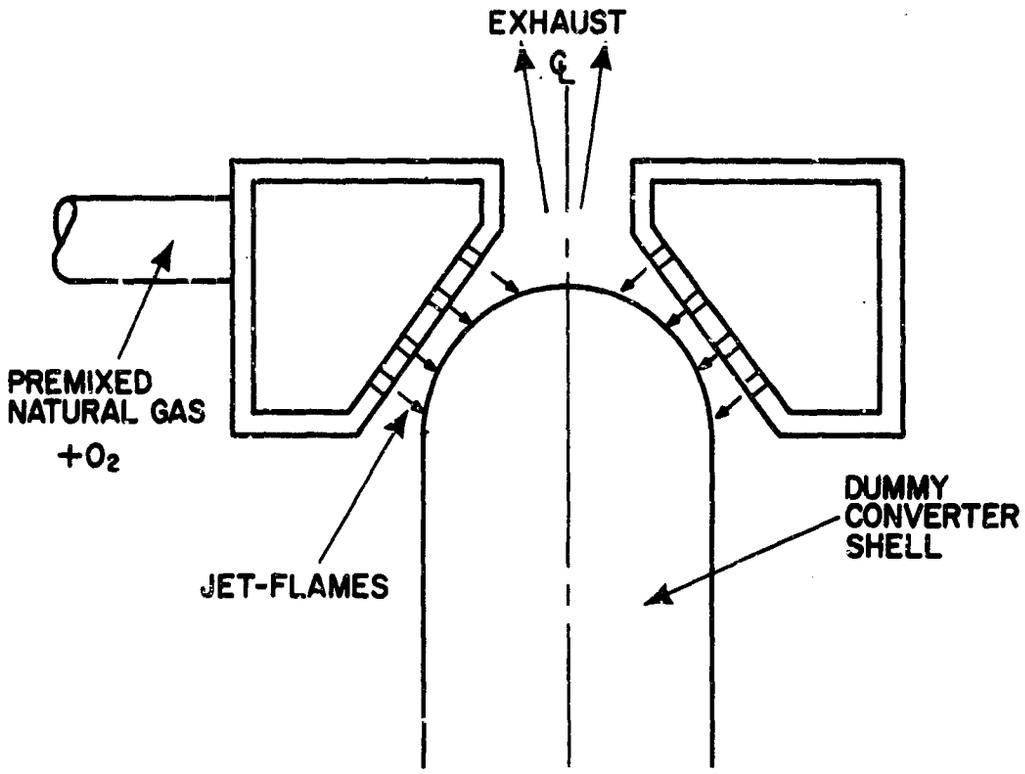

Figure III-16. Schematic Layout of Burner and Shell Under Test.

thickness of tungsten disilicide and the time at temperature, but a thickness of 1 to 2 mils could be measured at the end of a test period of 200 hours at temperatures exceeding 1100°C.

The encouraging results which were obtained with structures of a strongly carburized layer of tungsten led to the conclusion that carbon was an inhibitor to the formation of tungsten disilicide, acting as a barrier to the interdiffusion of W and Si. Structures were next manufactured in which a carbon interlayer, acting also as a deposition mandrel, was placed between the tungsten and the silicon carbide. Cylindrical structures were first manufactured for simplicity, and the carbon mandrel was coated on one side with tungsten and on the other side with silicon carbide. The thickness of the carbon was kept to the minimum that structural strength would allow, which was approximately 40 mils. Such structures were tested at Battelle Memorial Institute, under controlled atmospheres in furnaces, where the temperature was uniform and closely controlled. This type of testing was chosen to avoid the possibility that the strength of the bond might be affected by the action of elements other than temperature, such as an environment of an oxidizing or reducing atmosphere. Under identical conditions, tests without the carbon interface showed SiC spalling from W after 100 to 150 hours in the temperature range of 1400 to 1475°C at a brittle interface between the tungsten and the vapor-deposited silicon carbide, which was identified as tungsten disilicide.

To summarize the observations and conclusions of the controlled tests and the tests with the new barrier-equipped shell:

1. 1,000 hours of cyclic operation of the new type of shell specimen were completed. This test, performed at the BMI Laboratories, proved beyond

a doubt the value of the barrier material between the protective SiC layer and the W emitter material. It has been stated elsewhere in this report that exposure to high temperatures causes chemical interactions between the SiC and the W substrate and results in the deterioration of the bond and separation in 100 to 150 hours. Examination of this last test specimen after completion of 1000 hours and 10 cycles showed excellent bond strength. Metallographic examination of the interphase on both sides of the carbon barrier confirmed the reliability of the barrier material. Testing was continued on a portion of the same test specimen under the same conditions (inert gas environment 1400°C, 100-hour cycle), and it was re-examined after the completion of a total of 4000 hours without showing spalling or cracking.

2. After the 1000-hour test, two shells of the diode geometry were manufactured at BMI, and were sealed into vacuum-tight assemblies. Techniques and materials used were identical to those used in construction of the diode.

SERIES VI-S DIODE

These last emitter shell developments and improved methods of collector cooling were used to arrive at a new type of Series VI diode which will be called the Series VI-S.

The new ideas and improvements included in the design of the Series VI-S diode are listed below:

1. Barrier-equipped composite hot shell consisting of pyrolytically-deposited tungsten on a carbon mandrel protected by vapor-deposited silicon carbide.

2. A configuration of the end of the "hot shell" (emitter shell) such that the carbon interlayer is protected from exposure to air.

3. A nickel collector, so that the high coefficient of expansion of nickel, requiring large initial spacing (0.025" approx.) which decreases to 0.010" when the rated operating temperatures are reached, prevents ramming of the emitter by the collector in the event of fast heating or cooling of the converter. This improvement allows the fast cycling of the converter without the danger of emitter-to-collector contact.

4. In order to allow free convection cooling of the collector, a finned structure, specifically designed for that purpose, was attached to the collector.

5. Heat-pipe cooling of the collector allowed the achievement of a light-weight, free-convection-cooled diode. The use of the heat pipe allows the raising of the fin structure temperature so that large quantities of heat can be dissipated with fewer fins. Also the heat pipe makes possible the efficient heat transfer from collector tip to collector base without temperature drop and without the use of solid sections of high-thermal-conductivity materials (such as copper) which would have increased the weight of the unit considerably.

A detailed drawing of this new converter series is presented in Figure III-17. The actual diode is shown in Figure III-18 with the finned structure arranged for flow of air axially. Figure III-19 shows an exploded view with the main subassemblies completed. The general characteristics of the Series VI-S converter are as follows:

TABLE III-2

CONVERTER CHARACTERISTICS

Emitter	Tungsten
Collector	Nickel
Emitter Area	27 cm^2
Spacing (operating)	0.010"
Spacing (cold)	0.026"
Emitter Temperature	1450°C (max.)

DIODE CONSTRUCTION

Diode VI-S-01 was the first of this series to be completely assembled and outgassed successfully, but it failed because of a leak which developed on the last pinch-off after the diode was cesiated.

Diode VI-S-02 was outgassed and placed under test. Four test runs were completed with satisfactory performance before structural failure occurred on the emitter shell of the diode. The maximum performance obtained from this diode was 100 amperes at a voltage of 0.35 volt. The structural failure was the result of excessive expansion of the collector structure and insufficient expansion of the emitter

structure. This resulted in progressively smaller spacing than the calculated 0.010". As tests were performed at higher and higher current densities, yielding higher electron cooling, the collector temperature was raised to the point where it expanded beyond the calculated amount and contacted the emitter. Analysis of the data obtained from the test of this diode indicated the need for a re-evaluation of the temperature distribution both on the emitter and on the collector structures. The cooling by free convection and the lower thermal conductivity of the shell composite (SiC-C-W), a material for which accurate data on physical properties were not available, resulted in temperature patterns on the emitter and collector structures significantly different from the calculated ones.

PREASSEMBLY COMPONENT TESTING

Because of the developmental stage of the construction of the diode components, an elaborate procedure was established to check their quality and dimensional accuracy before assembly. The components requiring testing were the emitter shell, the heat pipe, the ceramic-to-metal seal, and the complete emitter and collector assemblies.

For the emitter shell a detailed procedure of leak-checking had to be set up for the following reasons:

The shell composite consists of three structures: the silicon carbide, the carbon mandrel, and the tungsten shell. Since the carbon mandrel is porous and subject to oxidation when exposed to oxidizing atmosphere, it has to be protected completely from exposure to atmospheric air or combustion products. For that purpose it is essential

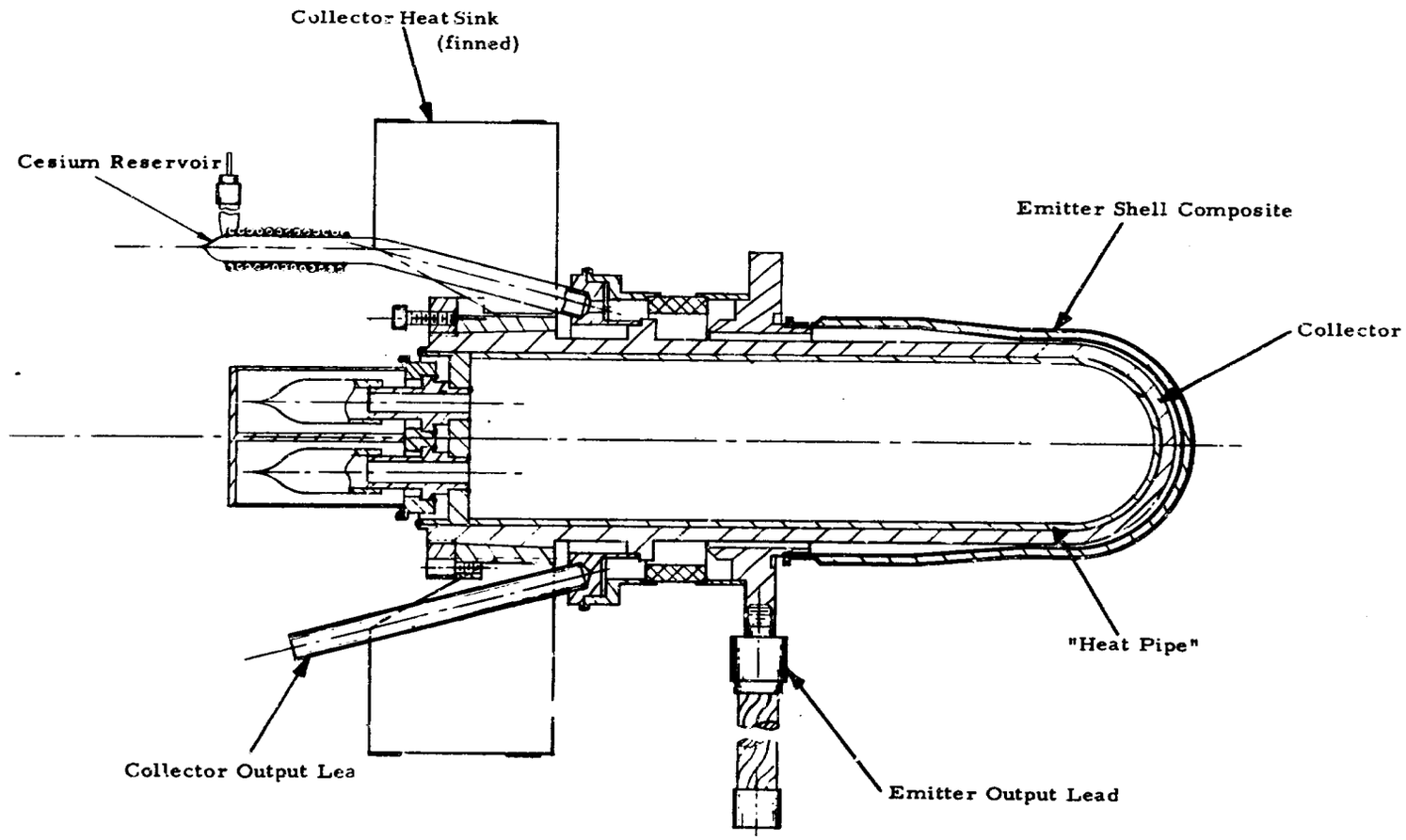

THERMO ELECTRON
ENGINEERING CORPORATION
85 FIRST AVENUE · WALTHAM, MASS. 02154

SK-574-12066
REV-B-

Figure III-17. Detail Drawing of Experimental Hydrocarbon-Fired Thermionic Converter, Series VI-S.

THERMO ELECTRON CORPORATION
8227

Figure III-18. Flame-Heated Thermionic Converter with Sodium-Molybdenum Heat Pipe for Collector Heat Dissipation.

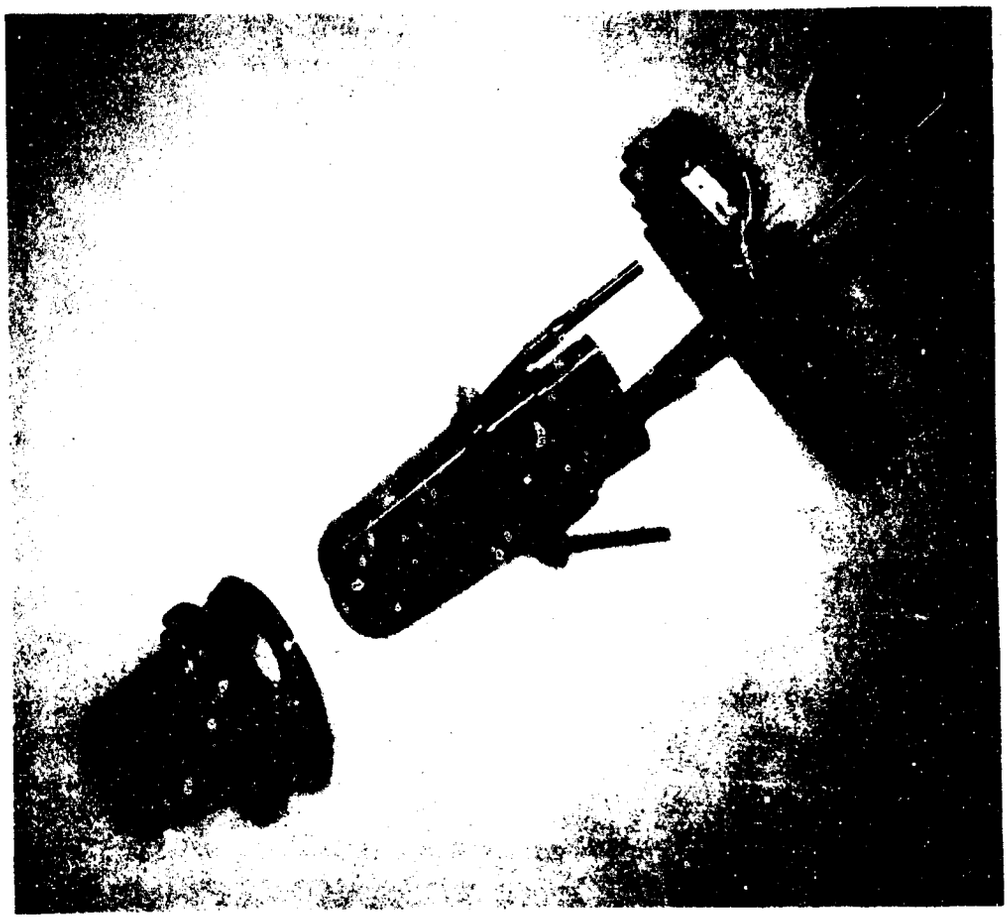

Figure III-19. Exploded View of Diode VI-S.

that a crack-free silicon carbide covers the carbon mandrel completely. In addition, to avoid outgassing of the porous carbon into the diode's volume and possible migration of carbon through cracks in the tungsten to the emitter surface, the tungsten shell has to be crack-free.

To establish whether the silicon carbide and the tungsten were crack-free, a dye penetrant was used (Zyglo) with which minute cracks in the SiC or W were visible under ultraviolet light.

A typical cracked tungsten surface, as received, is shown photographed with ultraviolet light in Figure III-20.

Since in certain cases not cracks but small pinholes were causing leaks, an additional leak-checking was used when the ultraviolet dye penetrant check did not show any cracks. The technique consists of evacuating a shell and back-filling with helium. If cracks exist in the tungsten the helium will penetrate in the porous carbon interlayer. When subsequently the shell is placed over a leak detector's evacuation port the presence of the helium in the carbon's pores becomes noticeable as a sustained background signal. A similar technique is used to detect minute cracks and pinholes on the silicon carbide that could not be detected by Zygloing

The dimensional checking of the assemblies was necessary because of the dependence of the final spacing of the diode on the initially set spacing between the emitter and collector hemispheres at the apex. The spacing was accomplished by selective machining of each structure. To obtain the exact dimensions and actually measure the "cold" spacing just before the final closure of the diode, the special tooling shown in Figures III-21 to III-25 was designed. Simulating the collector, an

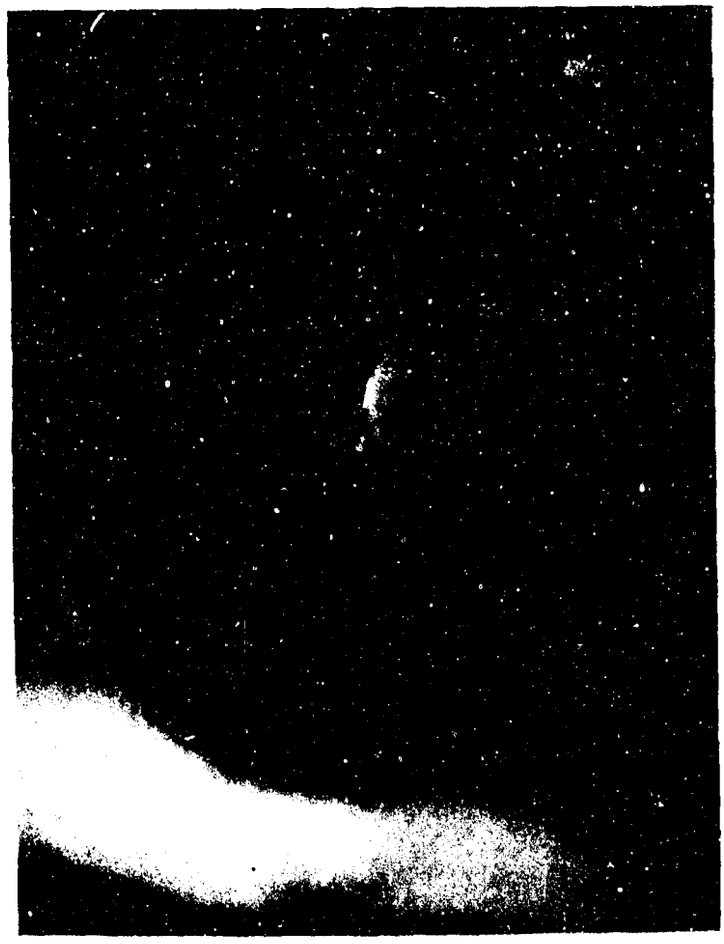

Figure III-20. Cracked Shell as Received and Zygloed.

Figure III-21. Emitter Depth Gauge.

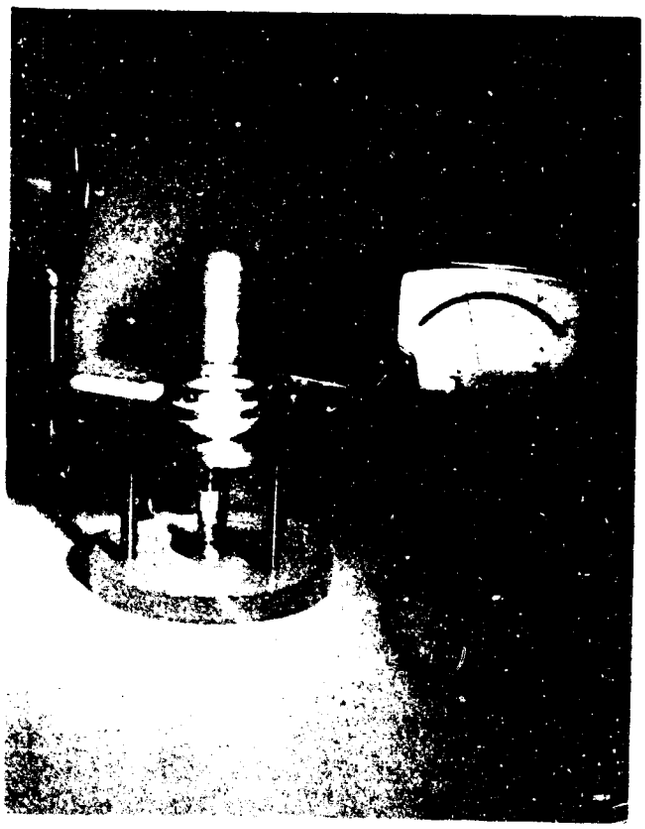

Figure III-22. Measuring Emitter Depth.

Figure III-23. Collector Length Gauge.

Figure III-24. Collector Length Measurement.

Figure III-25. Collector Concentricity Measurement.

axially movable part is raised inside the emitter until the contact is detected by an ohmmeter connected to the emitter and the simulated collector structures. The measurement of the exact length of the collector is done with another specially designed tool shown in Figure III-23, which fits exactly where the emitter assembly would fit. Measurements can then be performed to determine the exact length of the collector in the emitter and its eccentricity, if any. From these measurements exact information on the cold spacing is available. This combined with the exact temperature profile of the emitter structure during operation, permits a better estimate of the emitter-to-collector spacing during operation of the diode.

The following operations were performed before Diode VI-S-03 went into testing:

1 By a combination of thermocouple and optical temperature measurements, an accurate temperature profile of the emitter structure was established.

2. A series of tests were performed to establish the relationship of the collector temperature at the hemispherical end to the temperature indicated by a thermocouple located in the base of the collector heat pipe.

From the performance of these tests, the following results were obtained:

1. The heat conducted from the wall of the emitter shell was far lower than the designed value. As a result, the seal of the emitter shell to the molybdenum adapter plate was operating at temperatures much lower than the calculated 500°C. The true temperature profile is shown in Figure III-26.

2. A temperature difference as high as 75°C exists between the hemispherical end of the collector (Figure III-27) and the base of the collector heat pipe structure where the "collector" thermocouple is located. Although the main structure of the heat pipe does not show gradients higher than 15°C for the heat fluxes anticipated in this diode, the base of the heat pipe at the point where the finned structure is attached, located well in the condenser section, presents a ΔT of approximately 75°C from the temperature of the hemispherical end.

TESTING OF SERIES VI-S DIODES

Incorporating the above test results, Diode VI-S-03 was assembled and tested. The first tests on Diode VI-S-03 showed the validity of the chosen solutions and geometries, as can be seen from the typical temperature distribution chart shown in Figure III-26. The measured cold spacing of 0.026 was verified in addition to measurement of the parts, by an x-ray of the diode prior to its test. The actual spacing was measured under a shadowgraph-microscope and could be determined with an accuracy of ± 0.002. Under these conditions, the diodes in this series have an average operating spacing, at the hemispherical end, of 0.010 ±2.

The performance obtained from the diodes was lower than that expected, based on data obtained on research-type vehicles with the same emitter material. This is attributed to a random temperature distribution that exists on the emitter shell as a result of the geometry and the type of burner used (methane-oxygen test burner). It is estimated that only one-third of the emitter area is at the rated temperature (1400°C to 1450°C), while a very large temperature drop exists on the rest of the area, where temperatures as low as 1250°C and 1200°C have been measured. To correct this, modifications were made on the burner configuration.

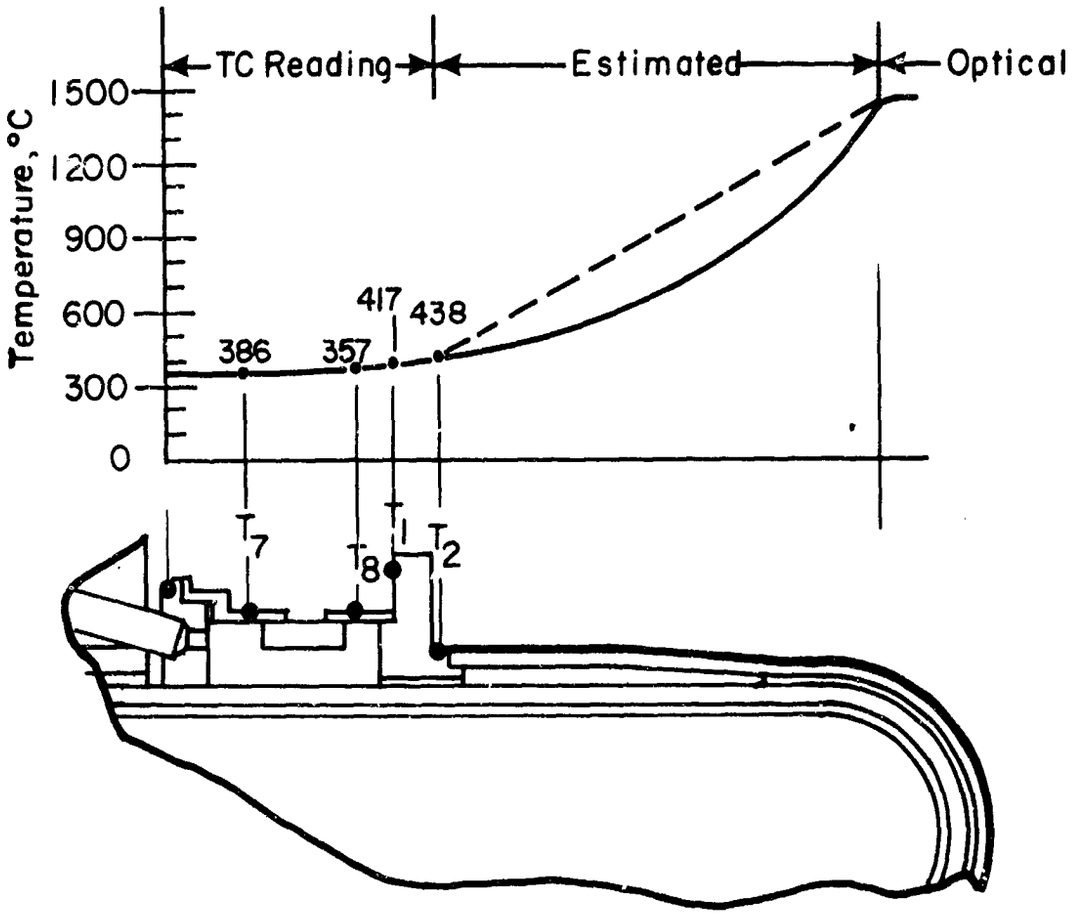

Figure III-26. Temperature Profile.

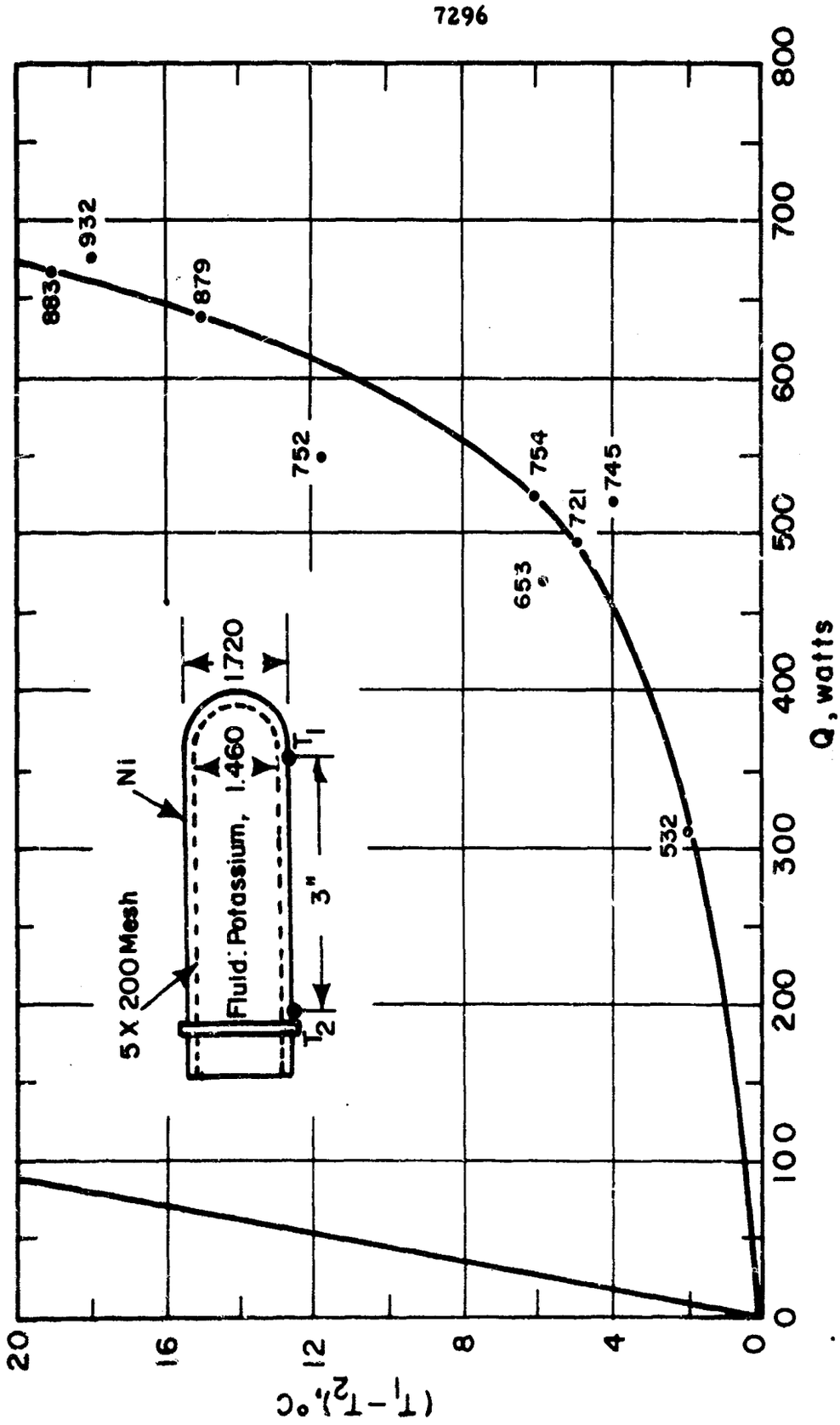

Figure III-27. Collector Heat Pipe Test Data.

HEAT-PIPE - COLLECTOR

The complete collector assembly incorporating the heat pipe cooling technique was tested successfully, and the test data is shown in Figure III-27. The collector-heat pipe assembly is made of a cup-shaped nickel piece with a long tubular section in which successive layers of wire mesh form the capillaries. It is interesting to note here that in this assembly the capillaries extend also to the hemispherical portion of the collector. In constructing this assembly, several wraps of fine-mesh stainless steel wire-cloth were used in the cylindrical and the hemispherical parts of the collector. The hemispherical layers were made after annealing and press-forming the wire-cloth so that it assumes a hemispherical shape, and is in direct contact with the wall of the heat pipe. Finally, to retain the fine-mesh wire-cloth in place and in good contact with the walls of the pipe, for uninterrupted capillary flow, a heavier-mesh wire-cloth as a structural member is used as the last inside layer. Components and a complete heat pipe are shown in Figure III-28.

The working fluid in the collector heat pipe is potassium; 20 grams are used for this assembly. Potassium is distilled into the assembly, and extreme care is taken that complete outgassing of both the metal parts and the working fluid is accomplished.

Performance testing of the heat pipe is done with the help of a pre-calibrated calorimeter in a set-up shown in Figures III-29 and III-30. The calorimeter consists of a cylinder of molybdenum carrying on one end a resistance heater, while the other end is water-cooled. A cylindrical section of known cross-sectional area and length carries two thermocouples, located at a predetermined distance, on which a ΔT can be measured. A calibration of that assembly established the relationship of heat to the ΔT

on the wall given in Figure III-31. Every effort has been made, through shielding and polishing surfaces, to minimize radiation losses. During the calibration, heat input is measured in terms of voltage and current supplied to the resistance heater at the top of the calorimeter, and the resulting ΔT's are measured by the two thermocouples on the wall of the calorimeter's cylinder.

For performance testing, the heat pipe structure is installed at the top of the calorimeter, where a good contact is achieved by virtue of differential expansions between the heat pipe-collector structure and the calorimeter. Thermocouples are installed on two locations on the heat pipe, one near the hemispherical end and one near the liquid-vapor interface (this level established after x-raying the assembly), to measure the ΔT along the wall. Heat input to the assembly is accomplished by induction heating of the hemispherical end, and the heat transfer capacity is measured by the ΔT of the pre-calibrated calorimeter section at the base. Figure III-32 shows the heat through the heat pipe vs ΔT along the wall during these tests. A complete heat pipe-collector structure is shown in Figure III-33.

TEST RESULTS

After the necessary modifications were made to the burner head to obtain an improved temperature distribution on the emitter, a number of diodes were assembled and were set up for life tests.

Two life-test setups had to be constructed for that purpose, equipped with the required number of automatic control devices so that failure of the converter from services interruption (water, gas, oxygen, electric power) would be avoided. At the same time the life-test units were so designed

Figure III-28. Components and a Complete Heat Pipe.

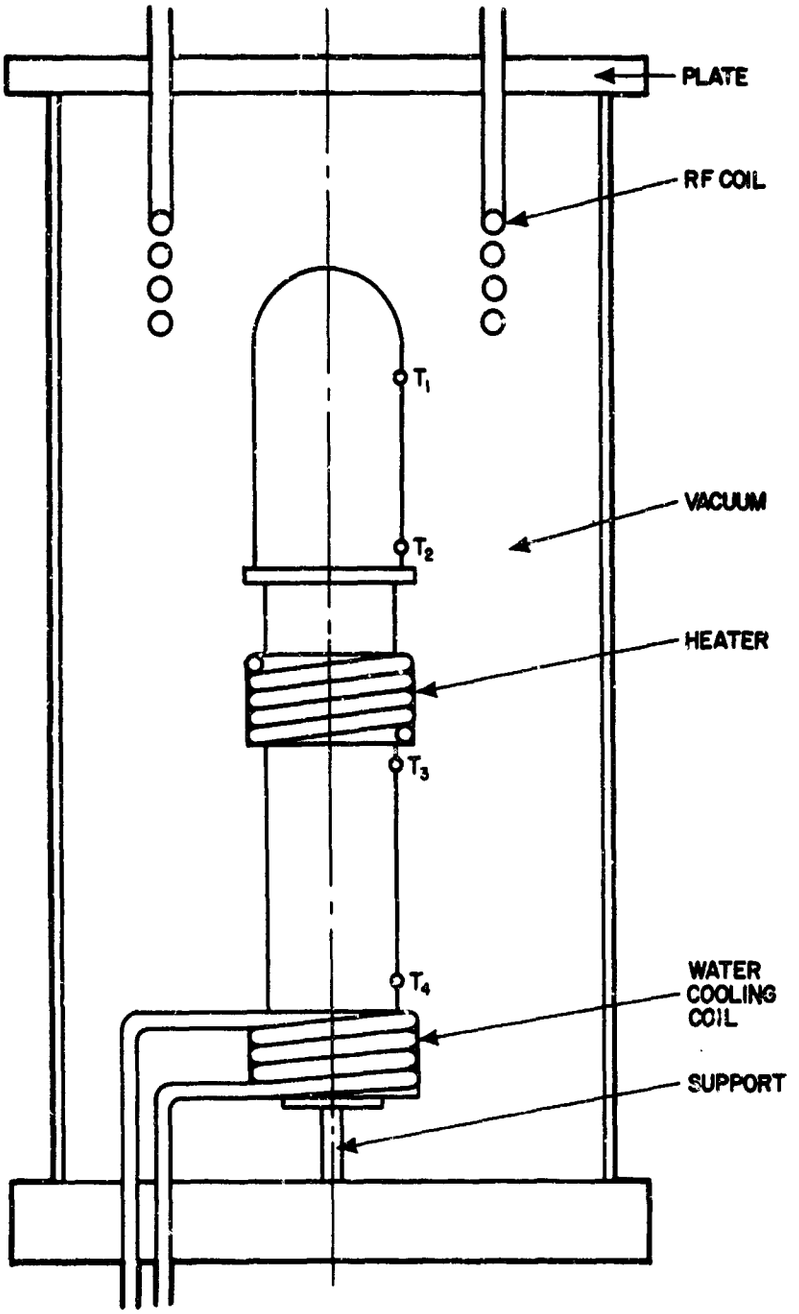

Figure III-29. Schematic of Precalibrated Calorimeter.

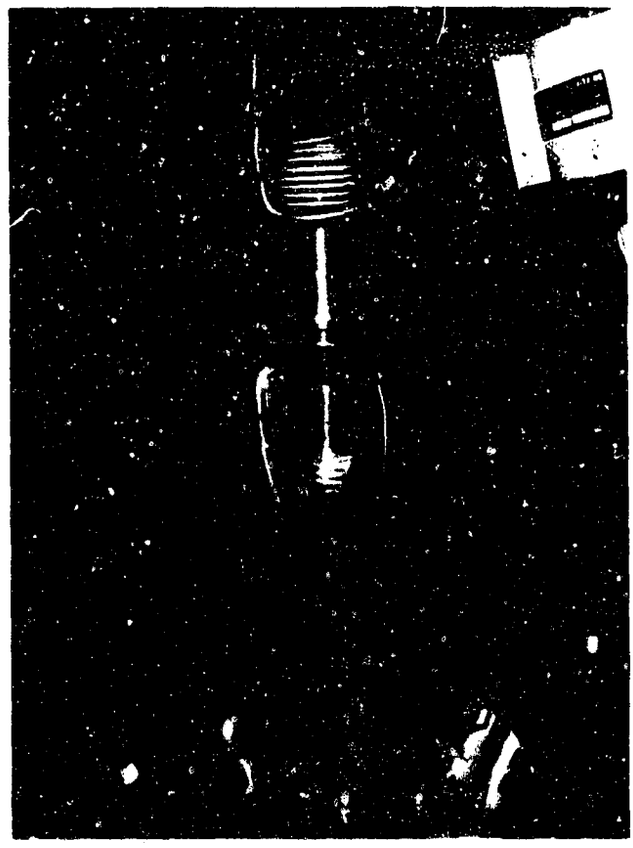

Figure III-30. Calorimeter Set-Up.

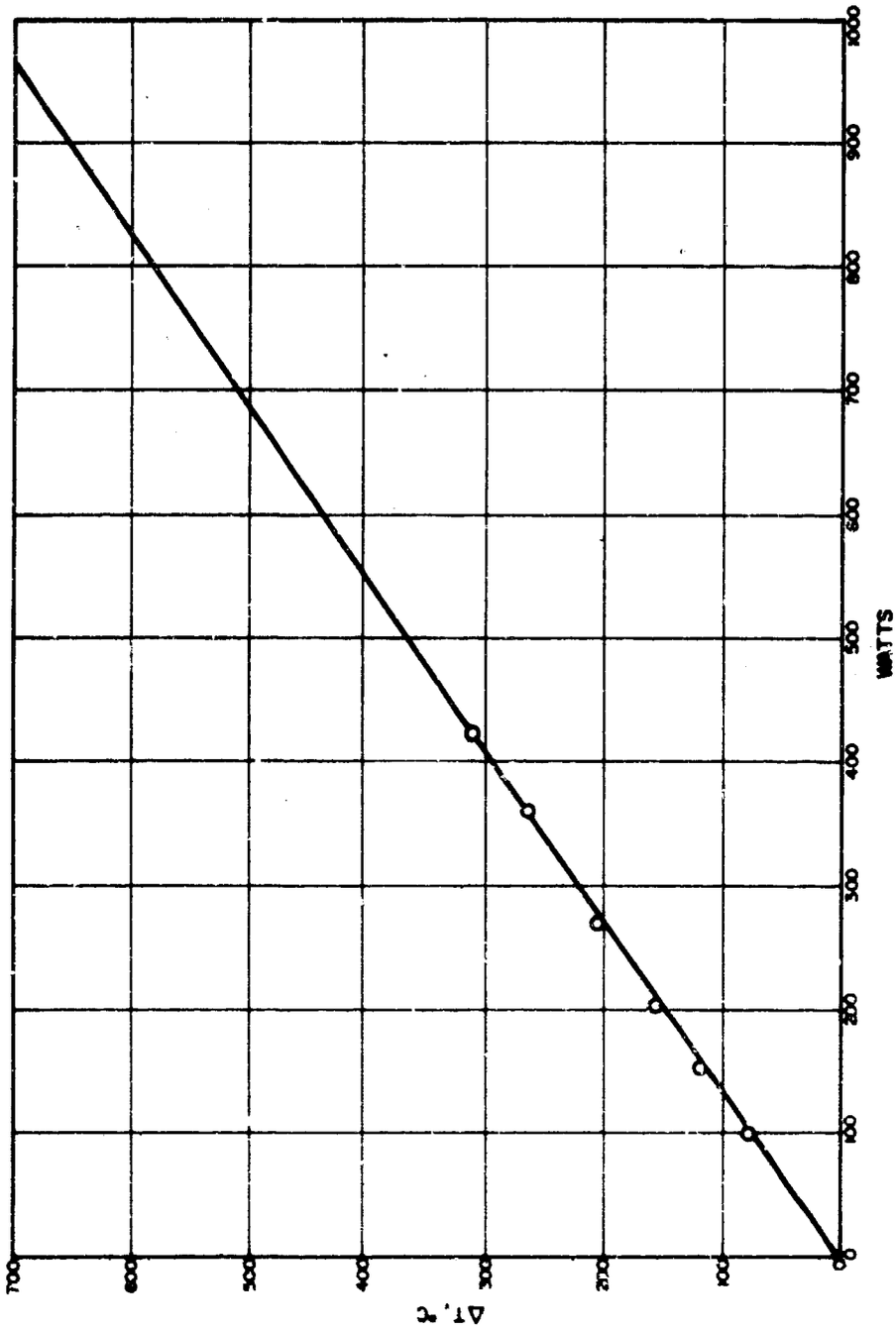

Figure III-31. Calorimeter Calibration.

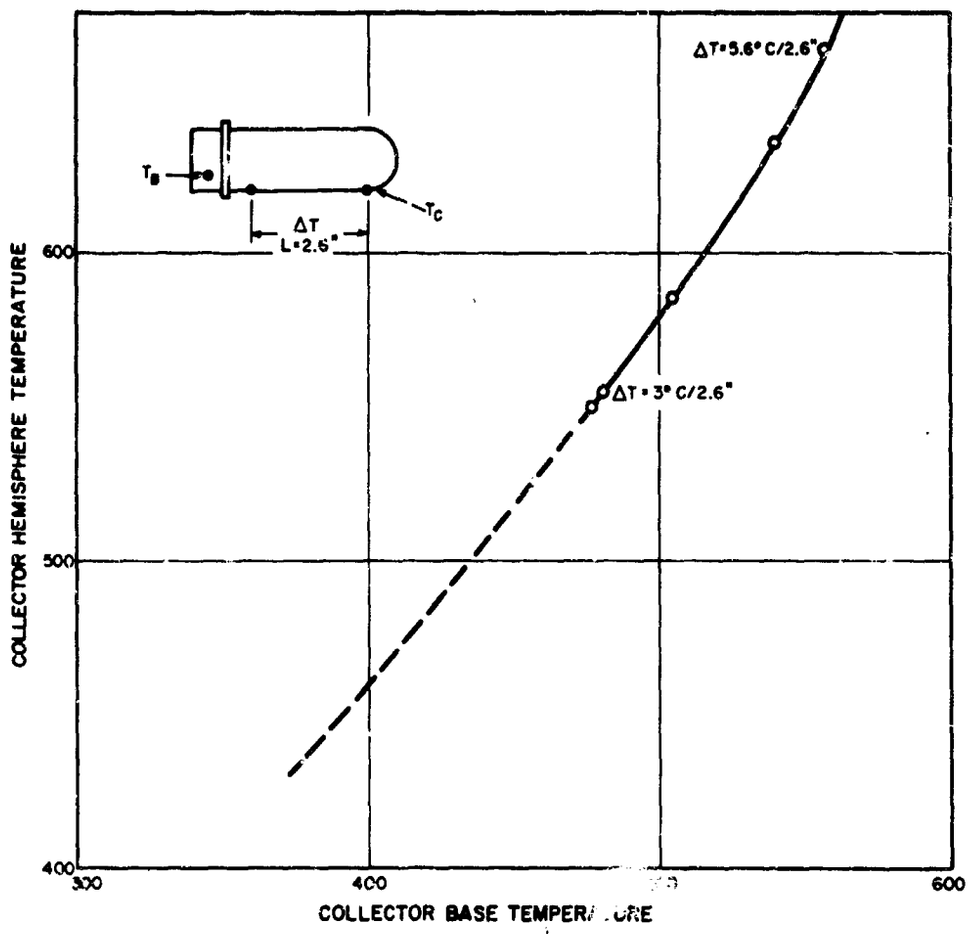

Figure III-32. Collector Tip versus Heat Pipe Condenser Temperature Plot.

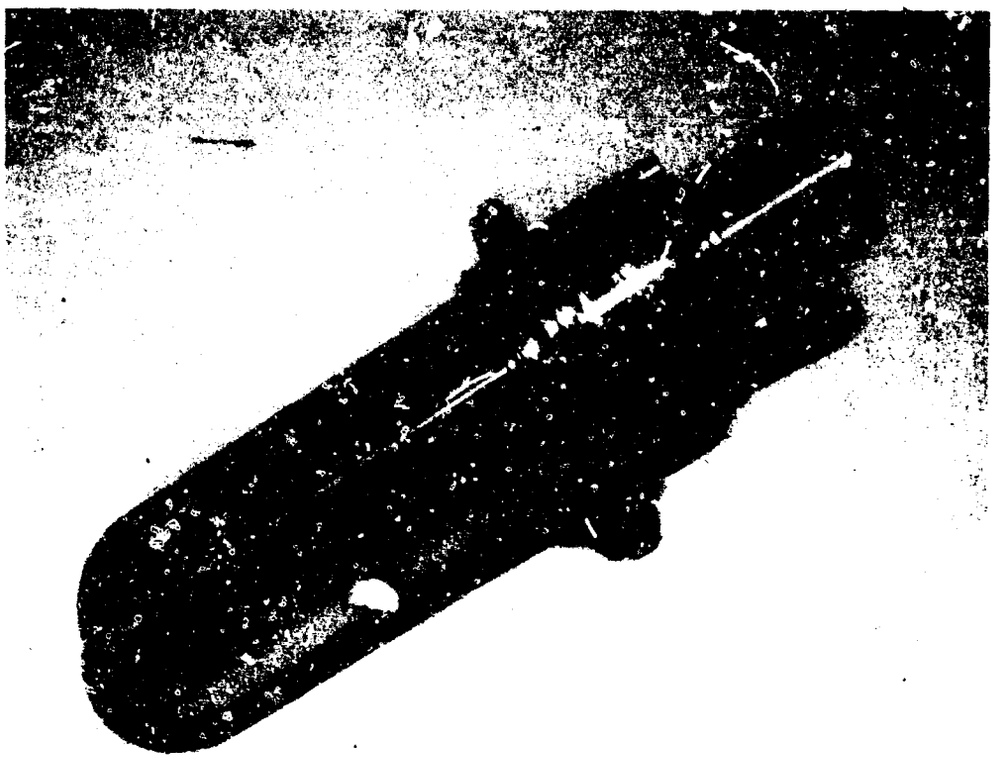

Figure III-33. Complete Heat Pipe - Collector Structure.

that, if variations in the performance of the diode indicated that a diode failure was approaching, the operation of the burner would be interrupted, together with the other services to the diode. In this way complete destruction of the diode is avoided and useful conclusions for future units can be drawn.

A typical life-test setup is shown in Figure III-34, where the main safety panel controls the gas and oxygen solenoid valves, which in turn are controlled through a sureflow switch so that the burner cannot be operated if the pressure of the water cooling is below a safe value. Pilot lights indicate the various functions. The diode safe shut-off panel is equipped with a time-delay switch which will turn off the burner a specific (set) time after the occurrence of the cause requiring the interruption of the test. In addition, to prevent destruction of the diode in the event that, due to malfunction of the burner and excessive emitter temperature, higher than normal current output is generated, the diode is open-circuited automatically when the set maximum current in the recorder is exceeded. This prevents overheating of the collector because of excessive electron heating and uncontrollable expansion of the collector which might cause ramming of the emitter and destruction of the diode.

Several diodes were tested, and for simplicity the shells used for the construction of the diodes have been numbered in consecutive numbers as they were manufactured. At that time a subcontract with Battelle Memorial Institute was started for the manufacture and metallographic examination of shells used in the life-test diodes. The shell type manu-

factured for the VI-S diodes was the FL type of shell. The heat pipe number was also introduced into the number of the diode, since each heat pipe had to be numbered and calibrated individually. Therefore the first diode to be life-tested was Series VI-S #9FL-01, i.e., shell #9FL and heat pipe #01.

This diode was tested for 26.7 hours at an emitter temperature of 1450°C, under a natural gas-oxygen burner and was subjected to eight cycles, during which it was allowed to cool to room temperature for inspection. At the end of the eighth cycle cracks were detected on the silicon carbide shell, and the test was discontinued. During the test of the diode, static and dynamic data were taken, and a set of I-V curves obtained from this diode is shown in Figure III-35.

The construction of shells and diodes continued, and a number of improvements in the deposition technique were made (see Section II) before the second life-test diode, #66FL-08, was ready. In the interim period improvements were also made in the diode construction techniques, and in particular on the collector assembly. The closure of the diode with a nickel to nickel-iron alloy inert gas weld caused a number of problems.

A side test effort was started in which a number of geometries, materials and equipment were tested. Finally a new piece of equipment for inert gas welding, which could be evacuated to 10^{-4} mm Hg before backfilling with high-purity argon, was used with successful results. It should also be mentioned here that a number of these problems which stemmed from impurities in the nickel used for the diode construction were later eliminated with the introduction of strict material quality control.

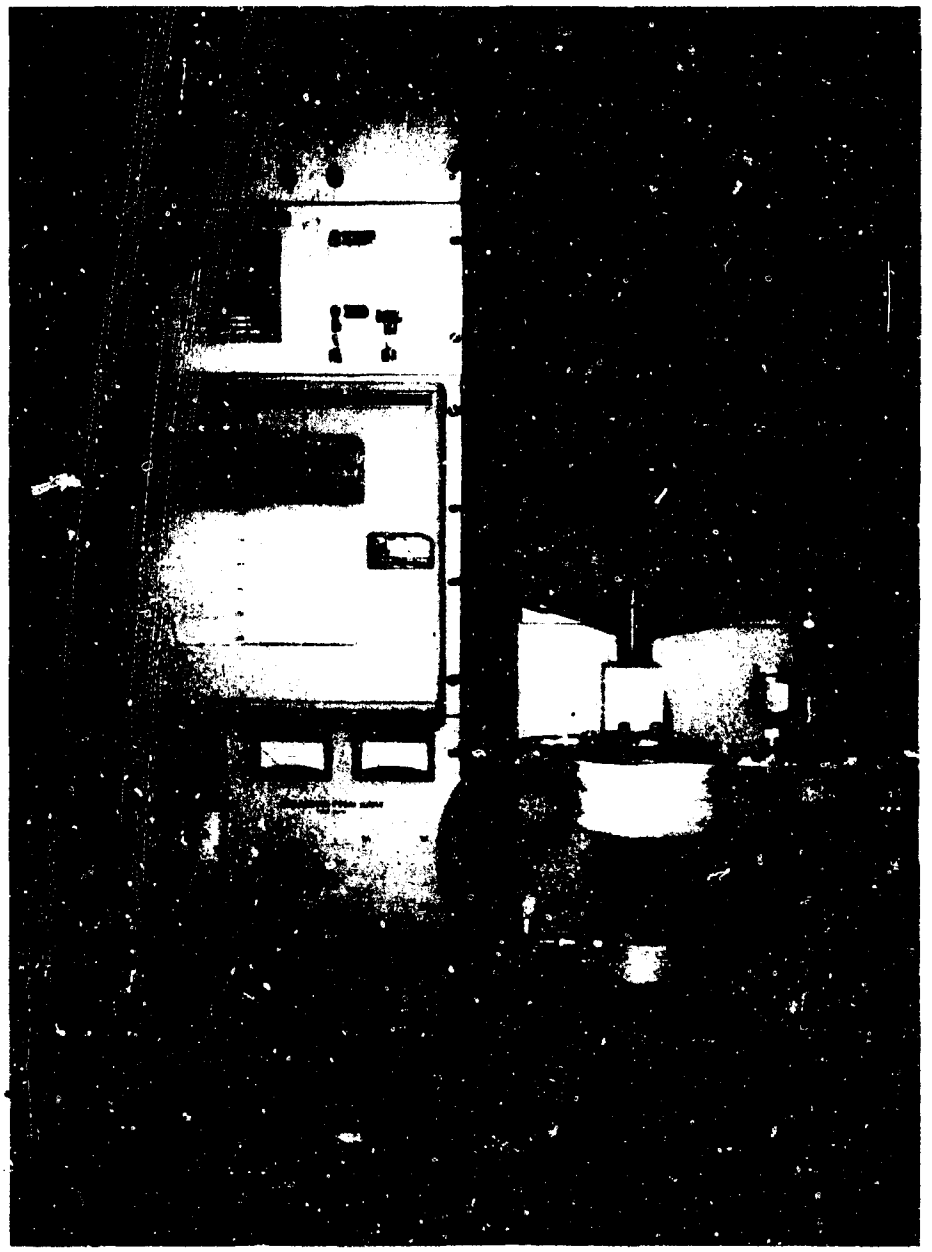

Figure III-34. Typical Life Test Set-Up.

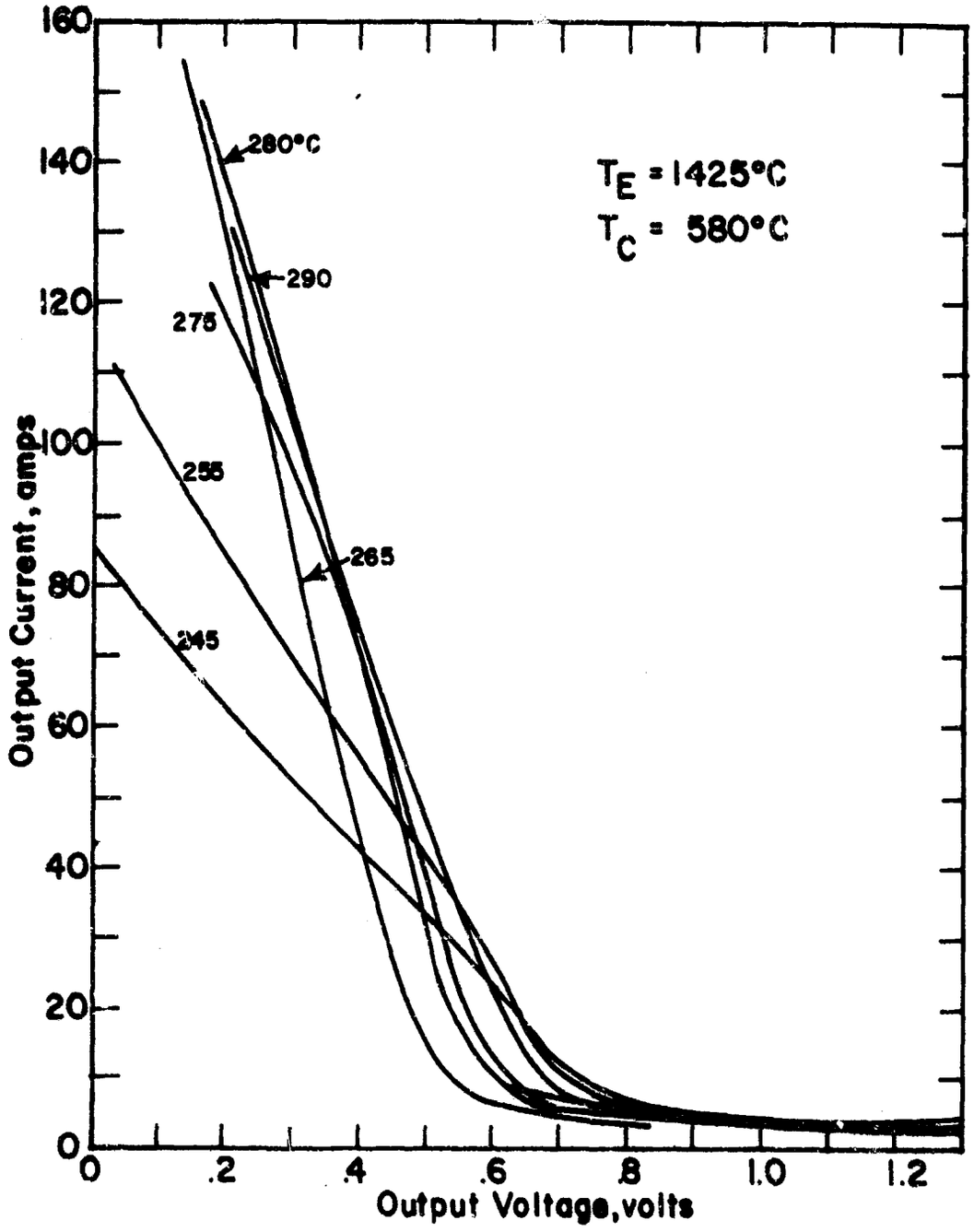

Figure III-35. Diode I-V Curves from VI-S.

Diode #66FL-08 was tested and failed after 170 hours of operation with one cycle at the 100-hour mark. The failure of this diode was attributed to erosion of the silicon carbide by a high-velocity jet of the methane-oxygen burner. As can be seen from Figures III-36, III-37 and III-38, considerable cratering occurred on one side of the diode, while the other side had a normal appearance. The diode was operated at a temperature of 1440° to 1400°C, and it yielded an output of 20 to 30 watts.

A second diode, #62FL-12, was tested in a similar setup but with an improved burner. It was run at a lower temperature, and its power output was approximately 25 watts at emitter temperatures of 1340° to 1375°C.

IMPROVED SERIES VI DIODES

In the beginning of 1967 several shells were made incorporating the improvements made in the vapor-deposition techniques of both silicon carbide and tungsten.

The major improvement was a uniformity in the texture of SiC with the new techniques of heating the carbon mandrel. In addition, considerable improvement was made in the surface finish of the tungsten with the resistance-heated tungsten vapor deposition equipment. The surface irregularities which were the major problem in the earlier stages of the shell development, in accomplishing the desired interelectrode spacing, were almost completely eliminated. Also, improvements were made in the mechanical and electrochemical techniques for the finishing of the emitter surface quality.

Figure III-36. Diode 66FL-08 After 170 Hours Test. Cratering on One Side of Diode.

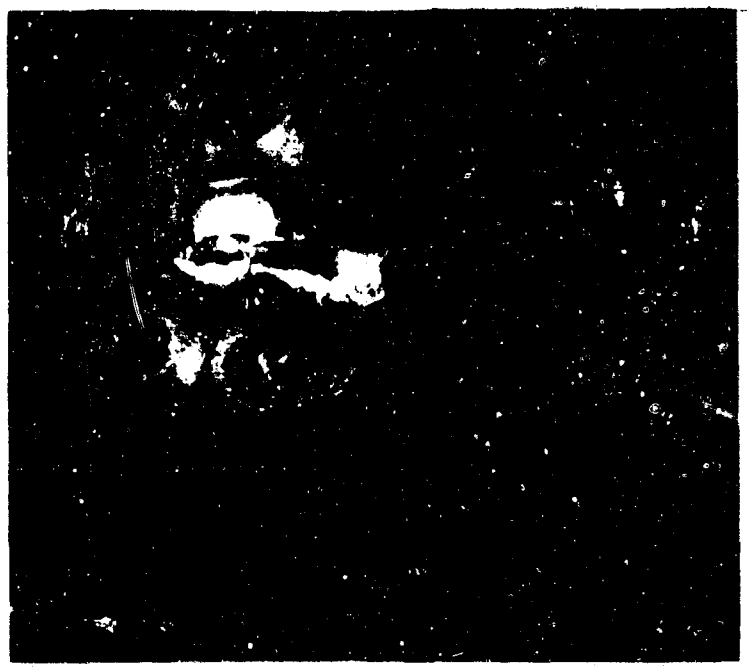

Figure III-37. Area of Jet Erosion of Diode 66FL-08 Resulting in Failure.

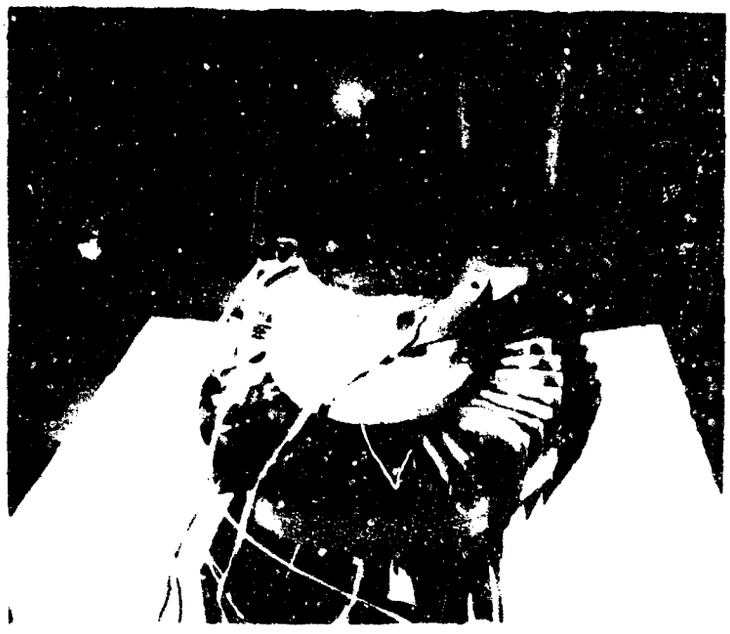

Figure III-38. Cratering on One Side of Diode.

A new diode, #74FL-17, was assembled with an improved shell, and the characteristic I-V curves obtained are given in Figure III-39. For comparison purposes Figure III-40 shows the envelope of these curves compared with I-V curves obtained from thermionic converters built at the beginning of 1966.

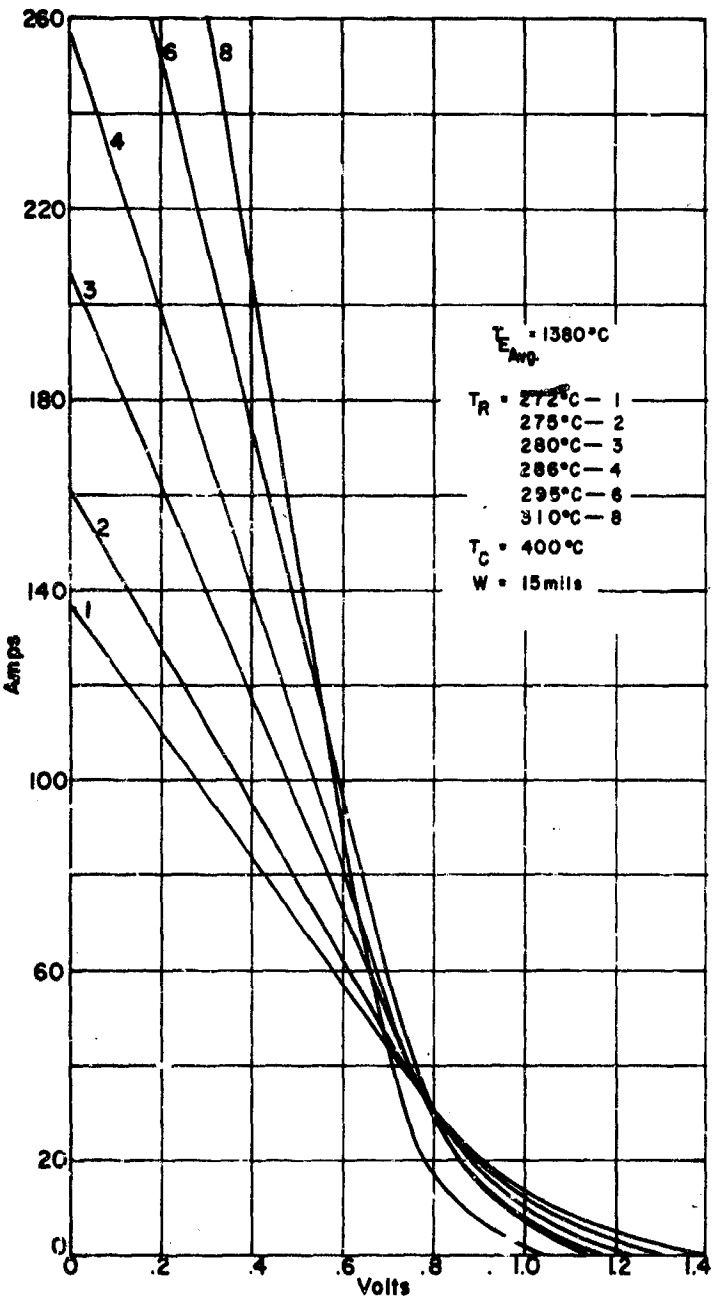

Figure III-39. Flame-Heated Diode I-V Curves for 74FL-17.

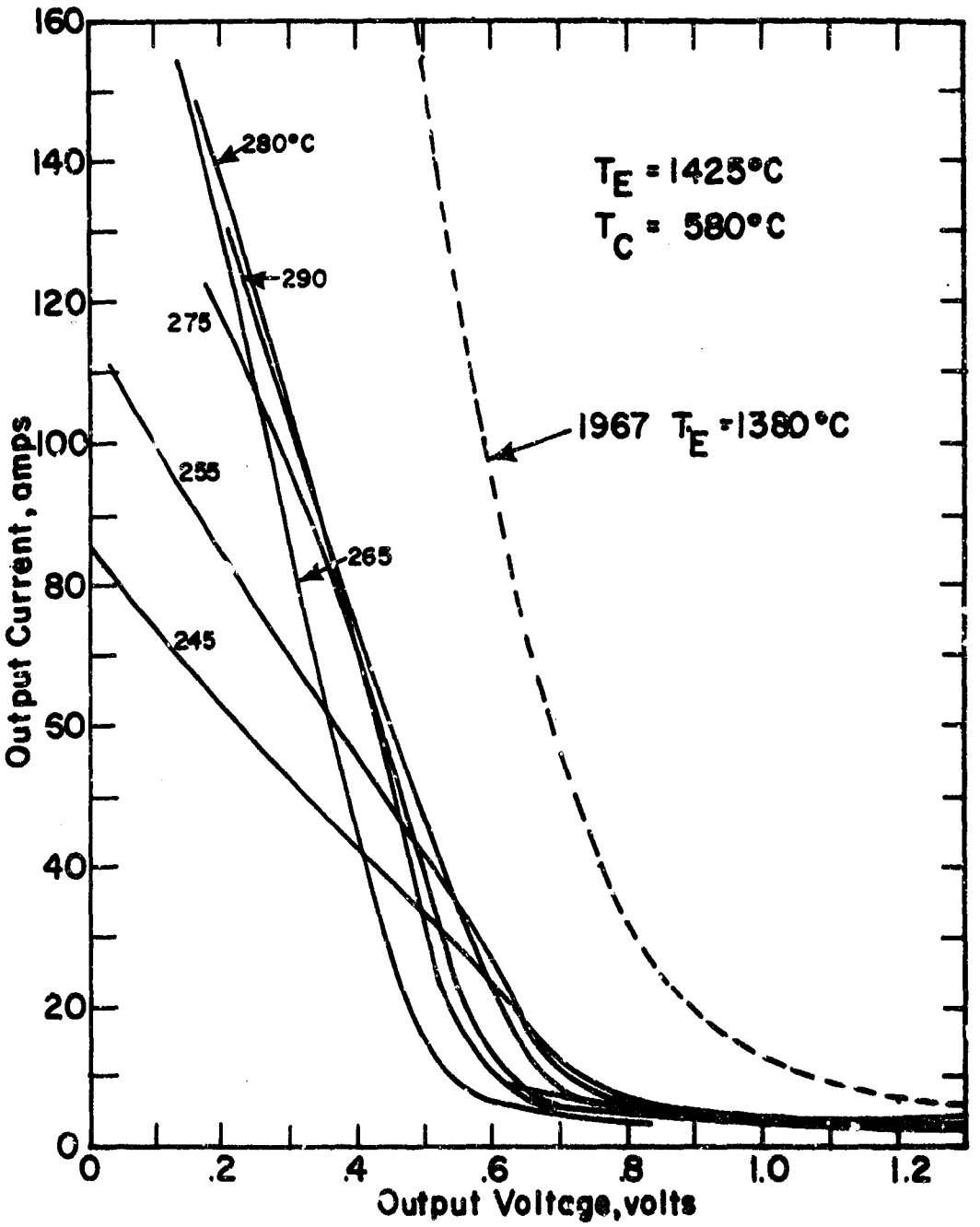

Figure III-40. Envelope of 74FL-17 Curves Compared with Curves Obtained in 1966.

IV. COMBUSTION SYSTEM

One of the first major problems which had to be solved before the feasibility of a hydrocarbon-fueled thermionic engine could be demonstrated was the development of a combustion system which could produce the heat necessary to drive a thermionic diode. Basically, the problem involved in the design of the combustion system is that the rate of heat transfer from a gas to a solid is notoriously slow, and that cesium diodes require high heat transfer rates to surfaces in the temperature region of 1350 to 1800°C. At first, it appeared that these two factors could only be reconciled by using enormously high air pressures and air flow rates through the burner.

Beginning in mid-1959, some basic burner configurations were experimentally evaluated, ranging from the pebble-bed burners, with their very high pressure losses and low heat flux densities delivered by convection, to multi-tube burners with flames inside the boundary layer delivering heat by radiation to the simulated diodes. These efforts were unproductive, although some variations that were tested met a few of the burner's technical requirements. By mid-1960 it was obvious that the basic problems preventing solution of the burner program were lack of effective heat recovery and thick boundary layers on the combustion gas side of the simulated emitter shell.

A burner with unique features for solving both of these problems was first conceived and built in 1960. The first configuration attempted to solve only the thick-boundary-layer problem, because the heat recovery problem would require the use of expensive materials which were extremely hard to fabricate. One of the first of these burners is shown on test in Figure IV-1. Although its initial pressure loss was high, the design could easily be modified to reduce the pressure loss.

The technical performance characteristics of the design are shown graphically in Figures IV-2, IV-3, and IV-4 as Model I data. A total of about 80 different variations of the same principle were investigated, and about 156 hours of hot time were accumulated on this burner. During the latter stages of the investigation, tests performed on a few jury-rig configurations with improved heat-recovery equipment indicated very strongly that major improvements in pressure drop and maximum simulated diode temperature were possible.

On this basis, a Model II burner was designed and built. The main features of this design included the use of the best available materials for the burner proper, better exhaust-heat recovery equipment, and larger cross-sectional areas for gas flow consistent with material availability. This burner was also better instrumented than Model I. It is shown in Figure IV-5 before its first firing and in Figure IV-6 driving a simulated emitter. After five months of development effort, the burner demonstrated the ability to deliver 41.1 w/cm^2 to a surface at a temperature of 1430°C, as shown in Figure IV-2. The complete technical performance of this burner is shown in Figures IV-2, IV-3, IV-4, and IV-7 as Model II data. Five basic variations in burner geometry were combined with up to eight different lengths of heat exchanger during approximately 250 hours of hot-testing time.

The first attempt by Thermo Electron to combine a high-performance cesium-vapor diode with a burner was made in the Model III burner. The new design features of this burner were the use of molded silicon carbide (which allowed intricate parts fabrication

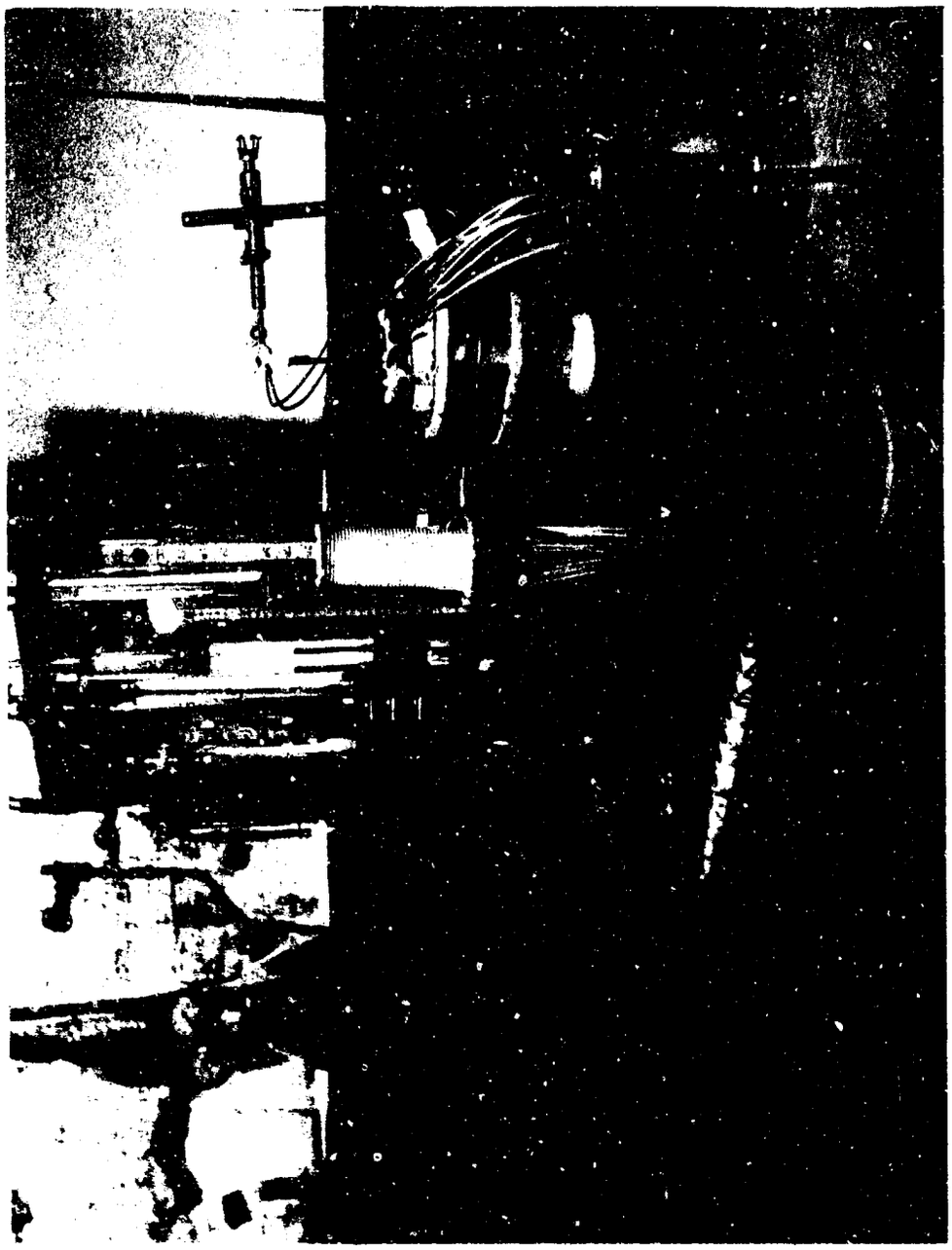

Figure IV-1. Experimental Set-Up for Evaluation of Model I Burners.

7367

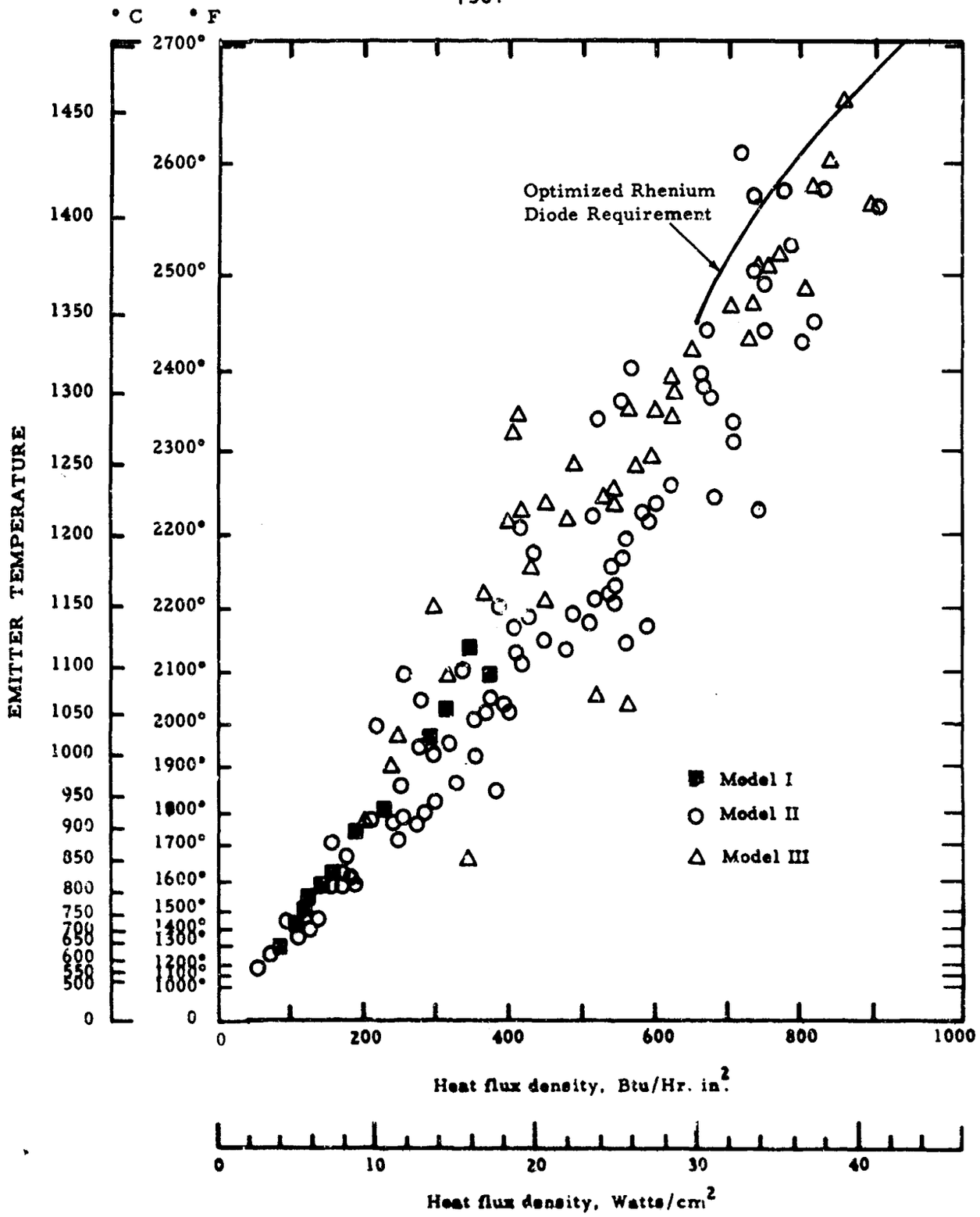

Figure IV-2. Heat Flux Density versus Simulated Emitter Temperature.

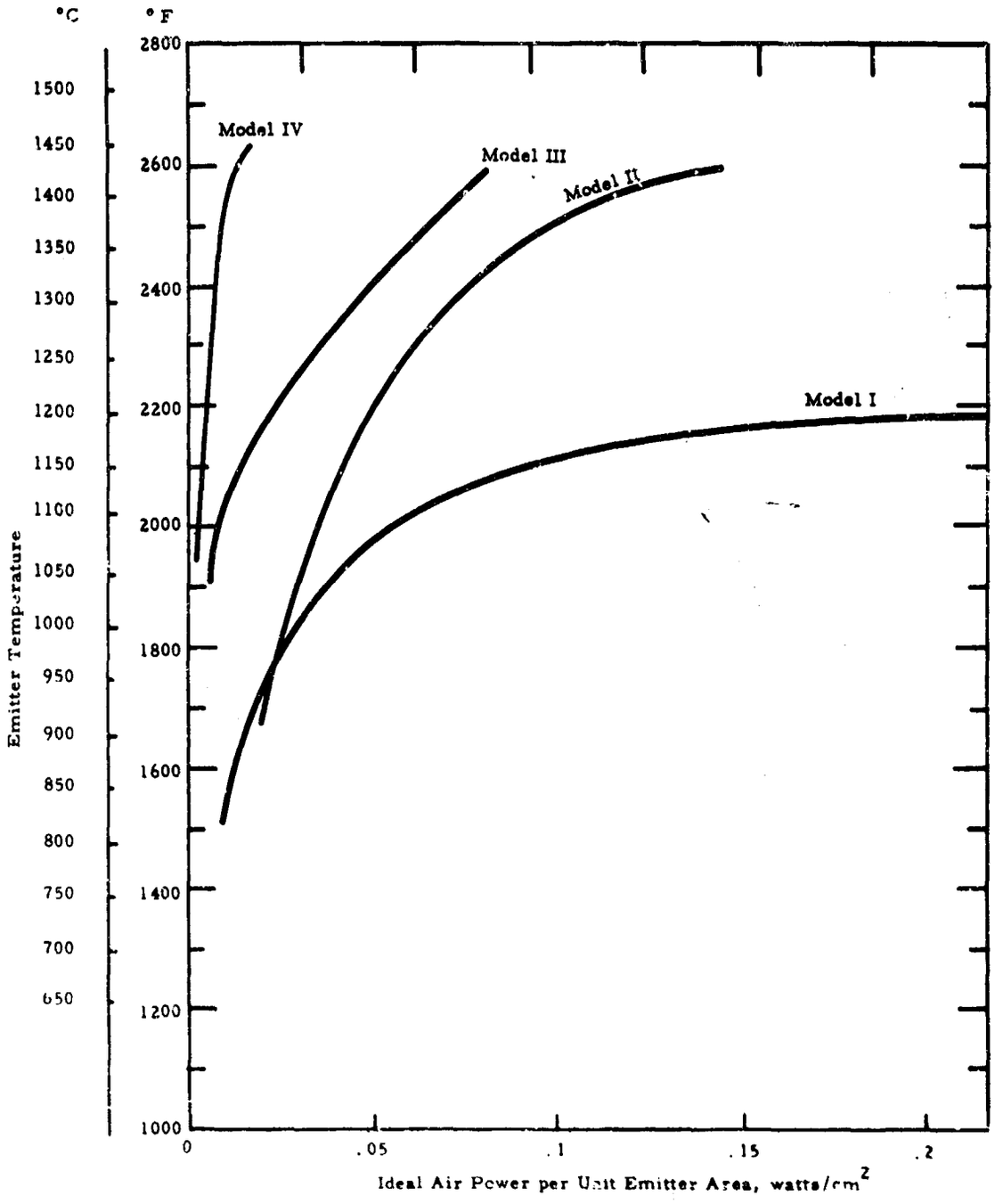

Figure IV-3. Emitter Temperature versus Ideal Air Power per Unit Heated Area.

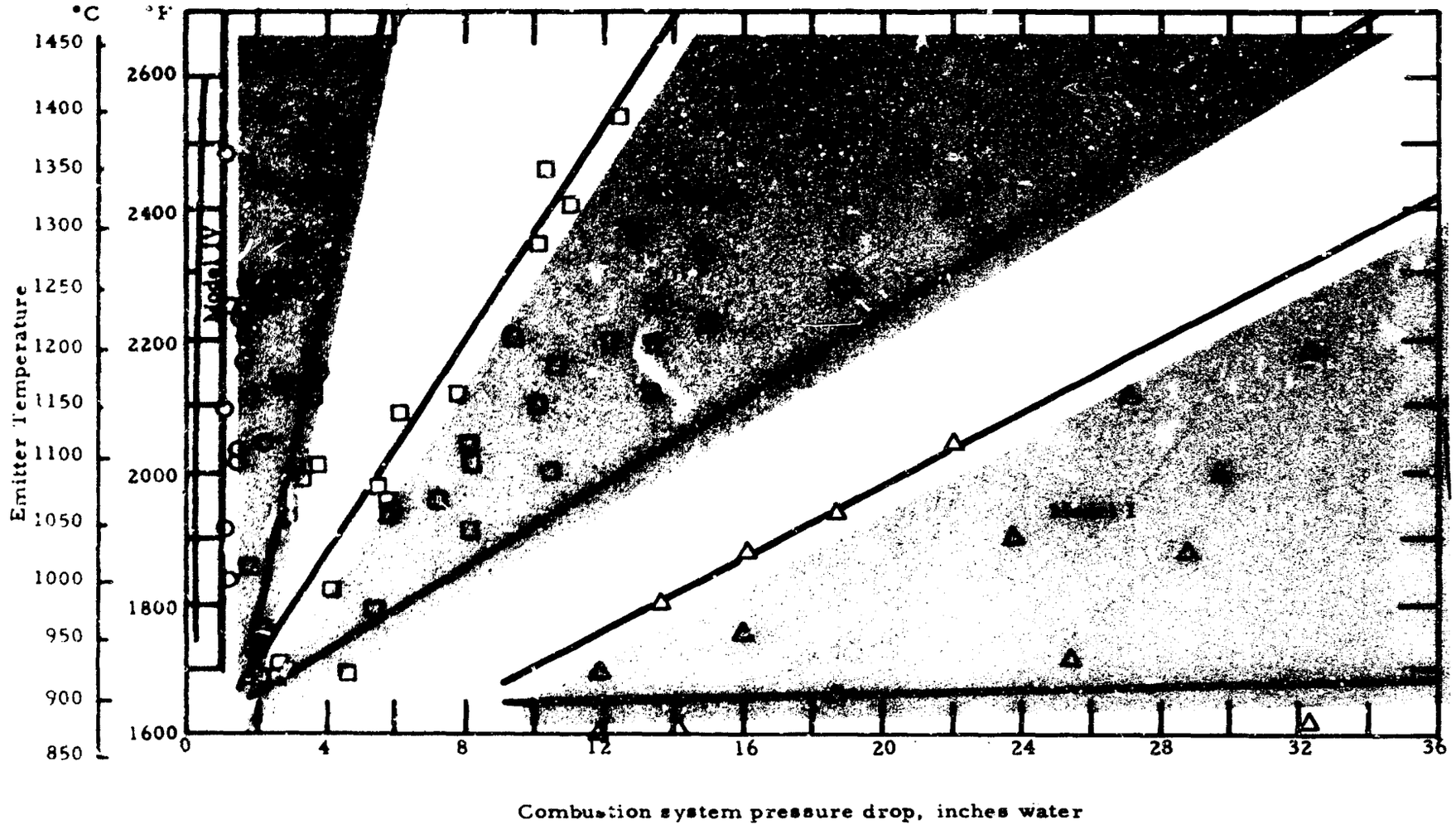

Figure IV-4. Combustion System Pressure Drop.

7369

Figure IV-5. Model II Burner Before Initial Test

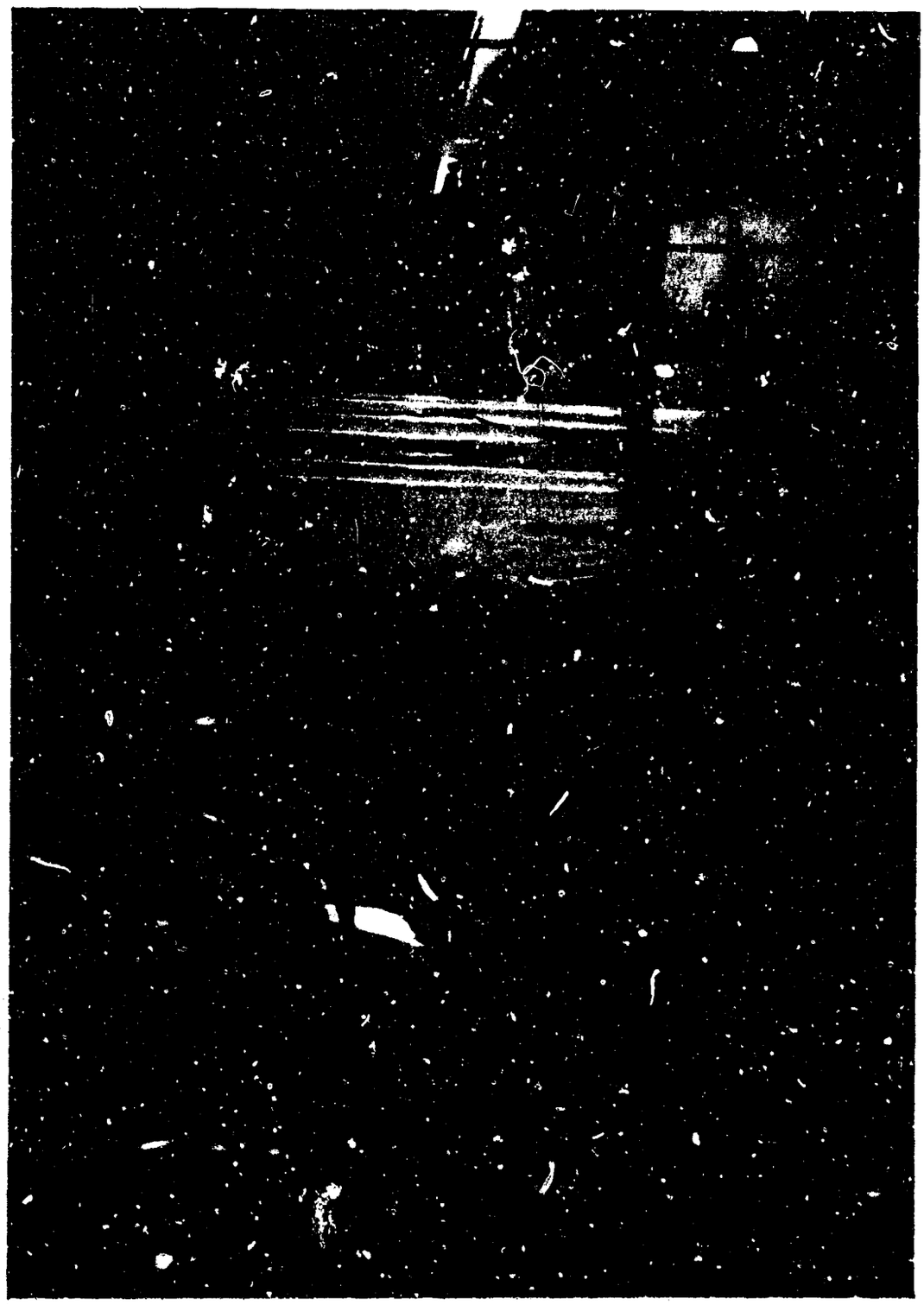

Figure IV-6. Model II Burner Under Test.

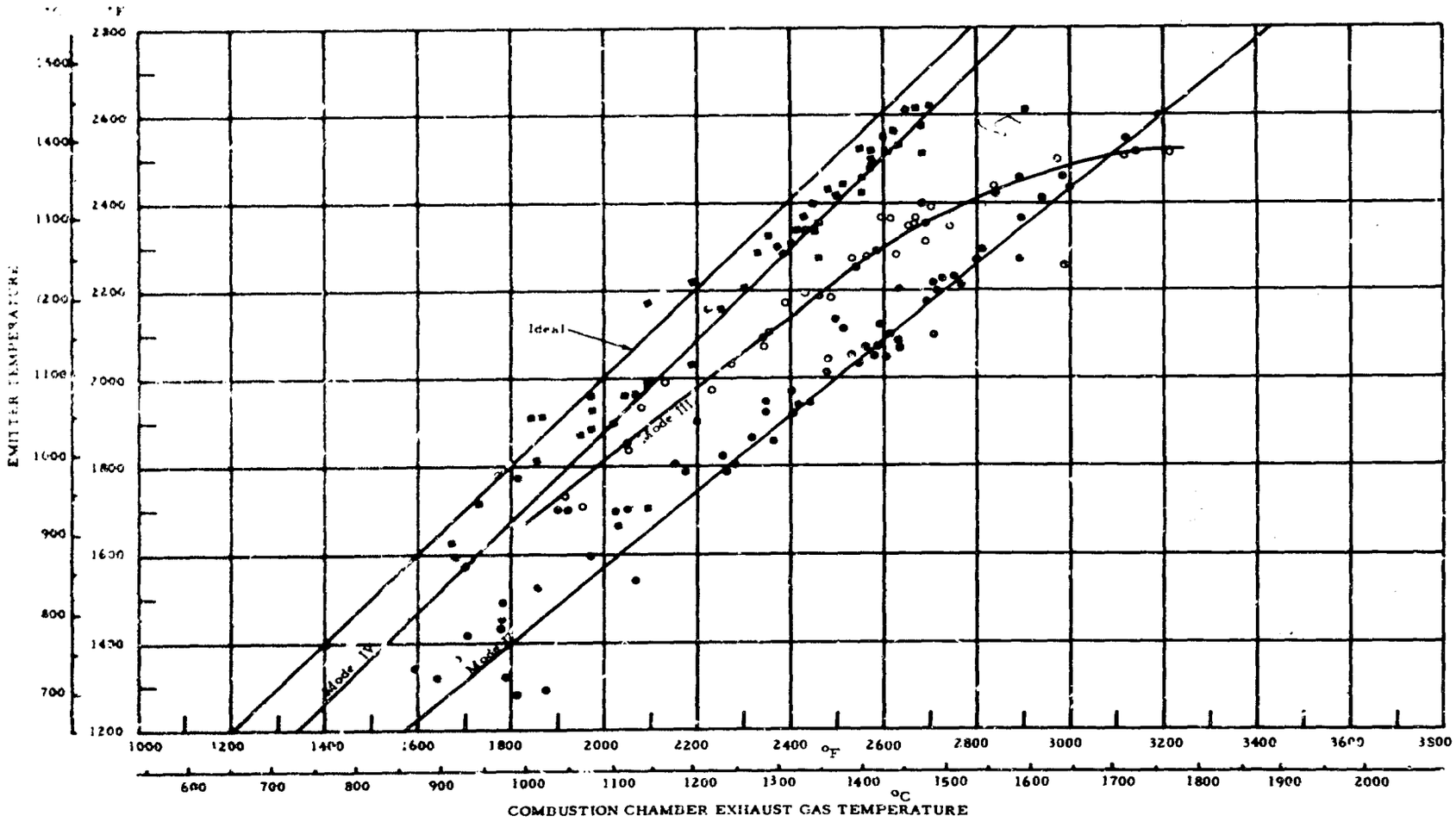

Figure IV-7. Emitter Temperature versus Combustion Chamber Exhaust Gas Temperature.

with a minimum of grinding), large gas passages, and a metallic air preheater. The burner for the modular diode-burner unit, wherein each diode is fitted with its own internal burner, was first fired on 16 October 1961 and reached fully developed status during June of 1962. The technical performance characteristics of this burner are shown in Figures IV-2, IV-3, IV-4 and IV-7 as Model III data. Over 2960 hours of hot time were accumulated on this burner, and another identical burner was built during September 1962. The burner could be ignited by means of a safety match, a high-tension spark and a cigarette lighter. It was so quiet that, at rated conditions, it could not be heard in a quiet room. This burner is shown in Figure IV-8 powering a diode whose maximum power density was 2.85 w/cm^2 (electrical) at 1430°C.

The first prototype of a combustion system design which would heat several diodes is shown in Figure IV-9. In this design, twelve thermionic diodes were located radially around a central combustion chamber. The system was equipped with a gas-air heat exchanger capable of heating the pre-combustion air temperature to 2250°F, and the gas velocities, as well as the pressure losses in the entire system, were minimized. It was designed to burn ordinary low-octane automotive-type leaded gasoline.

At the outset, the burner was operated on natural gas. Then a vaporizer was designed for use with gasoline. Basically, the vaporizer consisted of a stainless steel mesh heated by the burner's exhaust. Liquid fuel was fed to the mesh, where it vaporized. A small amount of air was used to carry the vapor through the fuel injectors and into the combustion area. This burner was continuously operated silently

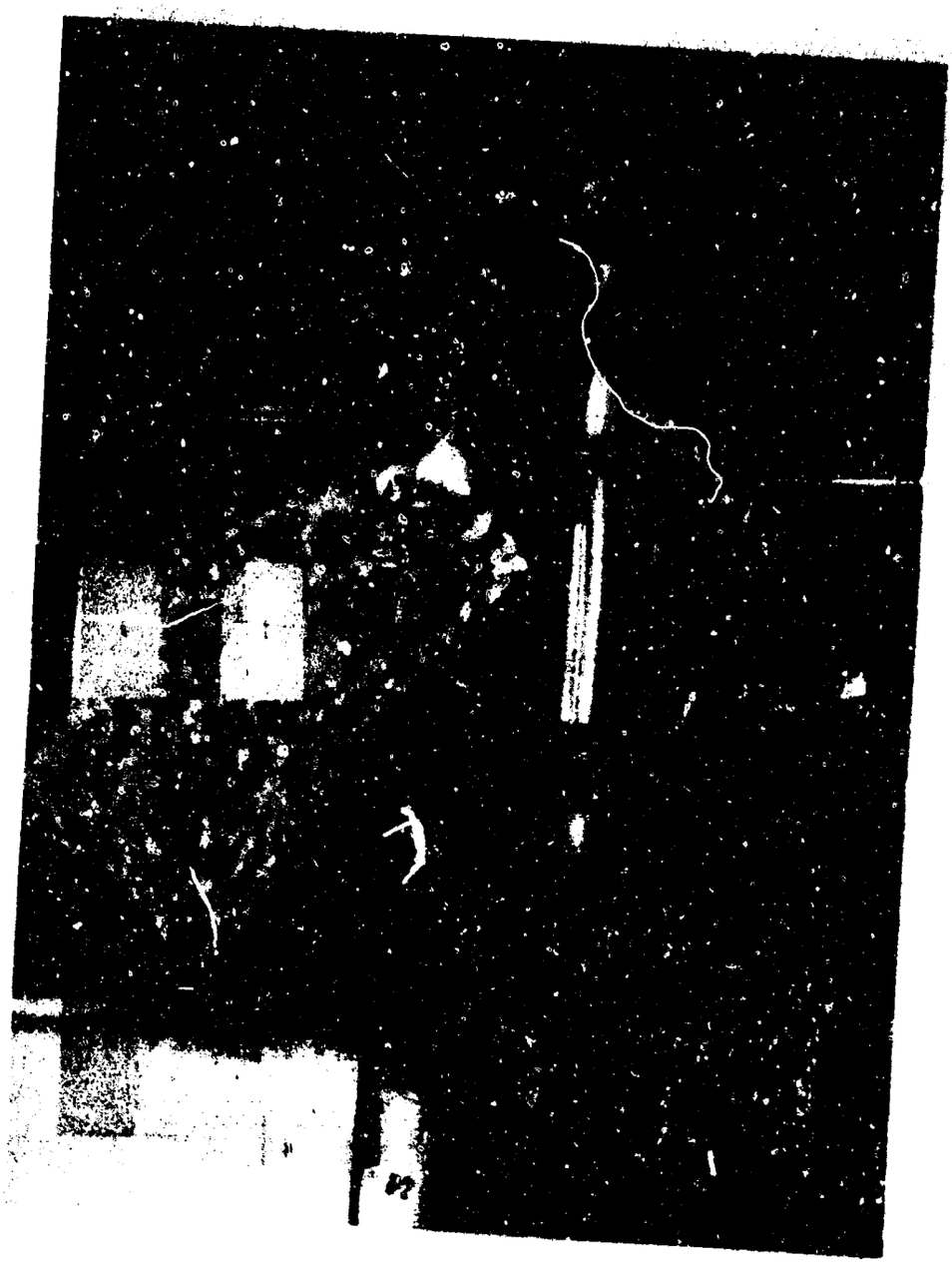

Figure IV-8. Model III Burner Driving Diode II-29.

Figure IV-9. Model IV Burner on Test.

at an emitter temperature of 1400°C using regular-grade leaded gasoline with extremely low pressure losses and gas velocities, and with the potential of generating a simulated diode temperature of 1600°C at a heat flux density of 60 - 70 w/cm^2.

The latest performance characteristics of this burner are shown in Figures IV-3, IV-4, and IV-7 as Model IV data. It should be noted that further developments are expected to produce higher preheat temperatures, as well as the ability to operate closer to the ideal fuel-air mixture. These improvements will be reflected in higher efficiency and lower scrubbing velocities.

Figure IV-10 shows data generated for the purpose of choosing the optimum thermionic engine operating point. This data shows the variation of "combustion efficiency"* with emitter temperature.

A number of major improvements were more recently incorporated into the burner to improve performance and reduce weight and volume. First, the design of the heat exchanger was modified to increase its effectiveness. The previous heat exchanger, shown on the burner in Figure IV-9, demonstrated an overall coefficient of heat transfer of only 8 Btu/hr ft^2 °F, a maximum outlet air temperature of 2200°F, and a pressure loss of 0.75 inch of water. In its initial development tests the revised design, shown in Figure IV-11 as Model V, demonstrated an overall coefficient of heat transfer of 40, a maximum outlet air temperature of 2250°F, and lower pressure losses.

---

*$\frac{\text{Heat delivered to diode}}{\text{Heating value of supplied fuel}}$

Finally, the exchanger effectiveness as a function of air flow rate and the number of stages is shown in Figure IV-12.

A second advantage of the Model V design was a reduction in the length of the overall engine, and therefore lower structural weight and volume. Furthermore, the combustion efficiency was higher because of reduced radiation from the hottest portion of the burner. With the diodes installed, no visible radiation emanates from the burner.

This burner was also operated on gasoline using a vaporizing carburetor.

One of the life-limiting elements of the burner, until recently, was the air swirler which is installed at the junction of the air preheater and the combustion chamber. Although the burner, as originally designed, was to be equipped with a silicon carbide swirler, vendors were unable to fabricate this part. As a poor substitute, swirlers were fabricated from Inco 702, one of the best oxidation-resistant high-temperature alloys available. These parts had a life expectancy no greater than 50 hours. In order to eliminate this problem, a swirler was machined from silicon carbide rings at Thermo Electron by electrical-discharge machining. This part was tested for well over 250 hours and showed no sign of deterioration. It is estimated that this part should have an actual lifetime of well over 5000 hours. Designs yielding the same aerodynamic results have been made using cast blades cemented in place.

The large amount of development testing to date has conclusively demonstrated that the combustion system can meet the requirements

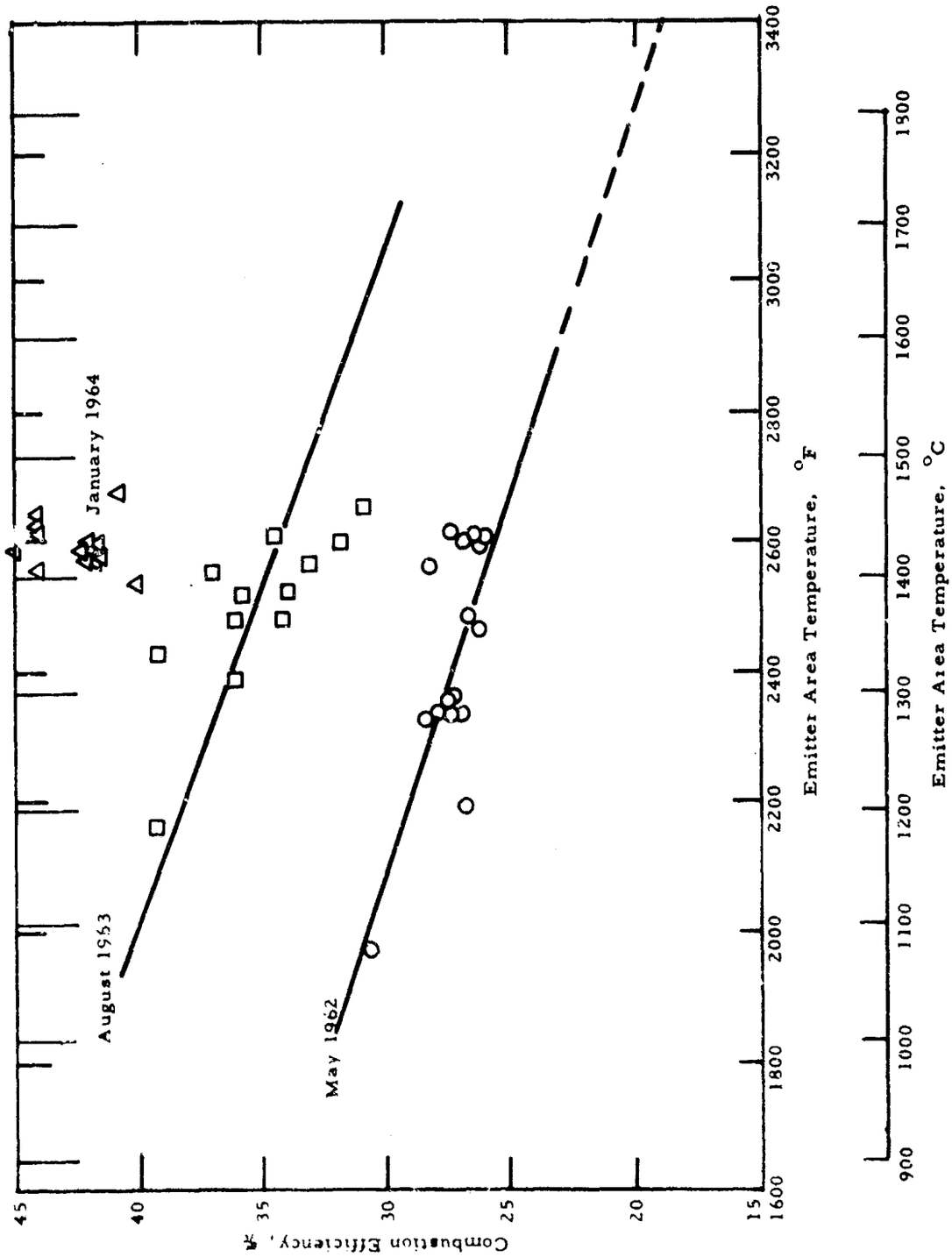

Figure IV-10. Combustion Efficiency versus Emitter Temperature.

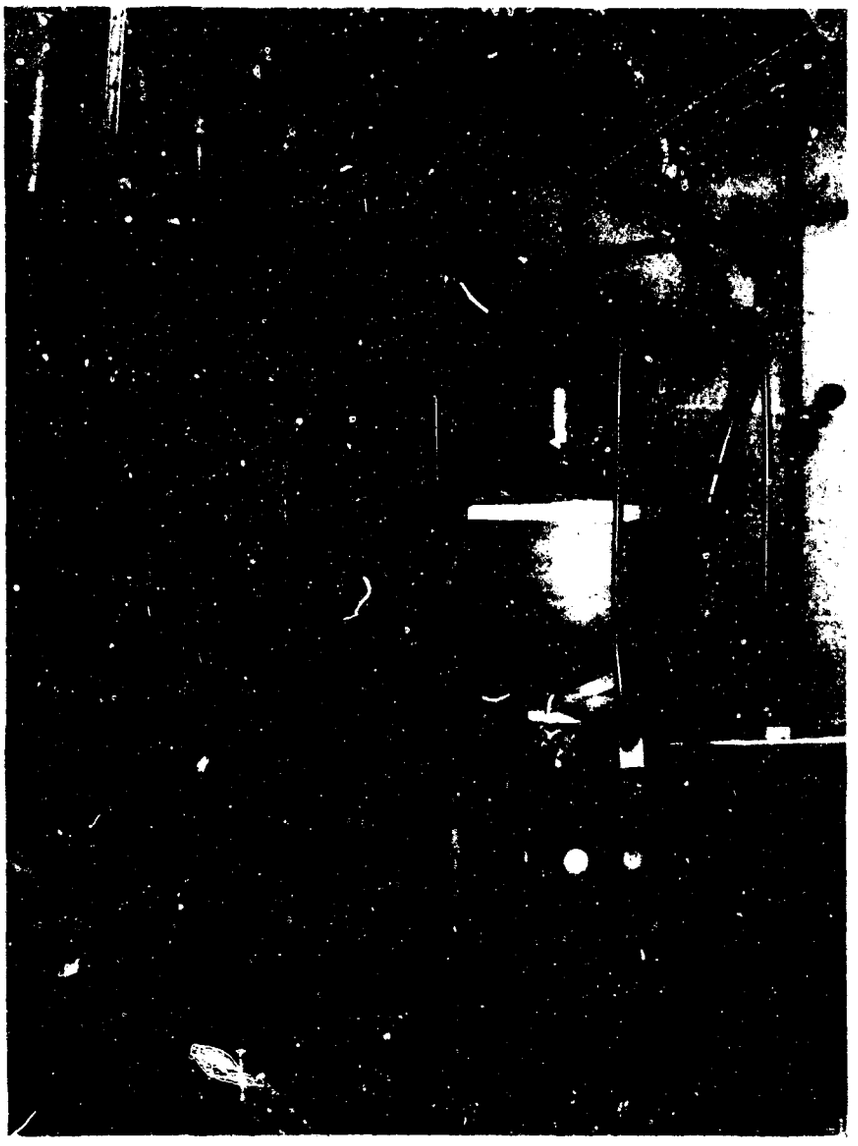

Figure IV-11. Model V Burner with Jet-Impingement Heat Exchanger.

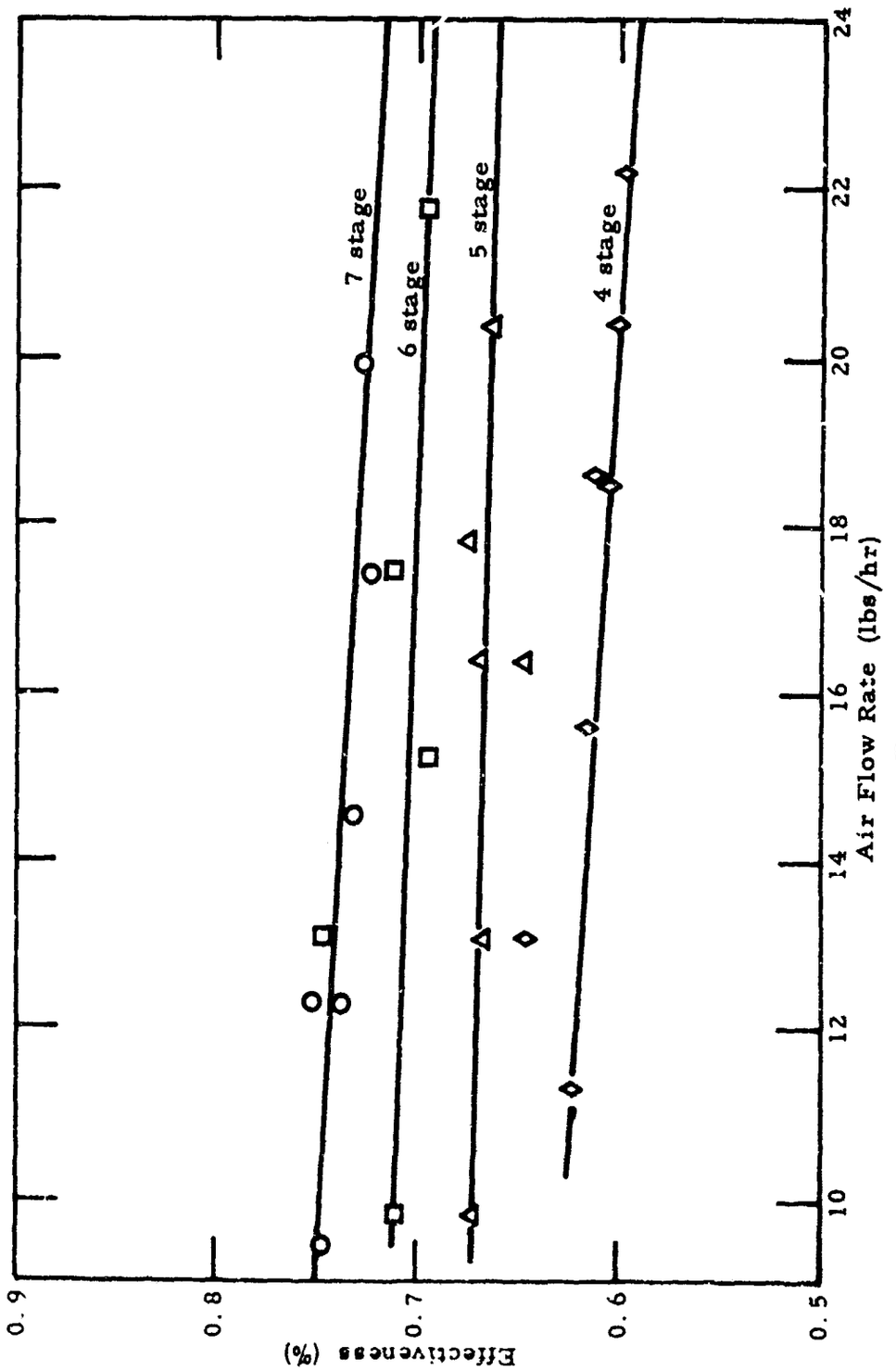

Figure IV-12. Effectiveness versus Pounds per Hour.

of a practical, lightweight hydrocarbon thermionic power supply. Future work should be directed toward further increases in combustion efficiency and toward the development of suitable ancillary components.

APPENDIX A

SYSTEM ANALYSIS

An analysis of the 45-watt thermionic engine was conducted in 1963 to compare the complexity, manufacturing cost, and weight as a function of the number of diodes used in the engine. Component performance data were generated which reflected the current state of technology and also that expected in late 1965.

Each engine configuration was assumed to consist of all the critical components required by a complete self-sustaining unit. These components are the diode or diodes, a dc-dc converter for all engines with less than 12 diodes, a combustion system, fuel, a fan driven by an electric motor, and the other accessories. The different arrangements considered are shown schematically in Figure A-1. These ranged from the single-diode engine, feeding a dc-dc converter which in turn drove the accessory system and load (72 watts total) with 6-volt power, to a 4-diode engine whose accessories were fed 2-volt power and whose dc-dc converter was rated at 45 watts output, and finally to a 12-diode engine with no dc-dc converter whose accessories again were rated at 6-volt input.

DIODES

All 1963 thermionic diodes were assumed to be of the same general type as currently being assembled, i.e., silicon carbide-tungsten hot shell, spherical emitting surface, conduction-cooled collector face, free-convection-cooled fins brazed to the collector stem, the ordinary type of brazed leadthrough, and the usual spacing

technique. The Series V diode was used as the basis for all weight and size calculations. Its weight was calculated as 0.52 lb, and its design output was 6 watts at 0.5 volt. Its calculated efficiency was 5.75% at an emitter temperature of 1400°C.

In order to arrive at the correct size of diode required by any specific configuration of engine, it was necessary to evaluate the performance of all the components in the engine. As will be shown later in this appendix, the estimated gross effect of other components (which might be used in a large variety of different engine configurations) was such that the range of diode generating capacity was between 6 and 105 watts gross output per diode. This variation in diode generating capacity required a variation in diode diameter between approximately 0.5" and 2.0". The smaller diode would be used in an engine with no dc-dc converter and having 12 diodes connected electrically in series. The larger diode would be required when one diode was connected directly to the dc-dc converter. The difference in the total generated power of these extreme configurations resulted because the increase in efficiency of the larger diodes was more than offset by the interposition of the dc-dc converter efficiency. Therefore, as the number of diodes in the system decreased, the gross diode power to be generated increased.

Because of the ambient pressure environment in which the diode must operate, the optimum trade-off between hot shell heat conduction losses and I^2R losses could not be achieved. Furthermore, current diodes required heavy-walled hot shells (10 mils of pyrolytic tungsten coated with 30 mils of pyrolytic silicon carbide), regardless of the diameter of the diode.

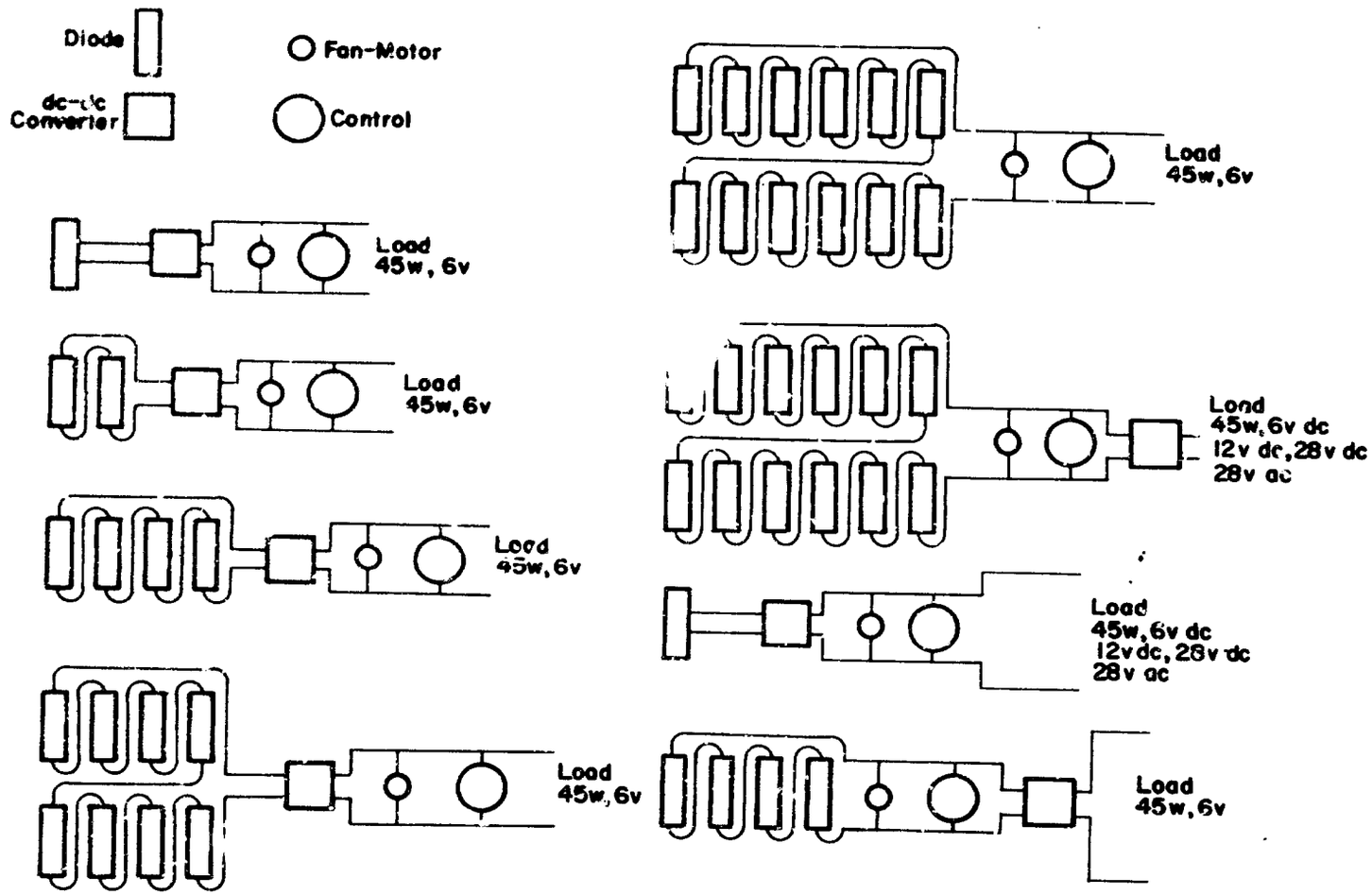

Figure A-1. Schematic Diagram of Possible Hydrocarbon-Fired Thermionic Engine Configurations.

Plans in 1963 called for the development of a diode in 1965 which was approximately 1/3 to 2/5 of the weight of the current diode. This weight reduction was to be accomplished primarily by replacing the massive collector stem and the free-convection-cooled fins to which the collector stem was attached with a hollow, thin-walled collector stem and aluminum tubing. This aluminum tubing would conduct air from the fan outlet and cool the air side of the thin-walled collector shell by forced convection.

Since approximately 67% of the weight of the Series V diode was concentrated in the subassembly of collector stem and cooling fins, elimination of these parts would have a large effect on diode weight. In addition, information supplied by fabricators of hot shells indicated that it should be possible to manufacture hot shells with the same thickness of pyrolytic silicon carbide, but with a 3-mil wall of pyrolytic tungsten. This design change would also reduce diode weight and increase efficiency.

A further basis for reduction in diode weight for 1965 was the expectation that thermionic research would continue to find means of improving performance. A 20% improvement was assumed. Calculations of the weight and efficiency of each diode are provided in Table A-1 for the 1963 diode and Table A-2 for the 1965 diode and are shown graphically in Figures A-2, A-3, A-4, and A-5. The estimates were based on reasonable engineering assumptions which account for the gross effects and were subject to revision based upon detailed analysis.

TABLE A-1

WEIGHT AND EFFICIENCY OF
1963 HYDROCARBON-FIRED DIODE

Gross Generated Power, watts	6.0	10.6	21.5	44.5	105
Efficiency, percent	5.75	6.42	7.22	7.74	8.25
Weight, lbs	.52	.78	1.41	2.78	6.18

TABLE A-2

WEIGHT AND EFFICIENCY OF
1965 HYDROCARBON-FIRED DIODE

Gross Generated Power, watts	6.0	9.58	20.2	41.4	100
Efficiency, percent	7.6	7.82	8.61	9.42	
Weight, lbs	0.18	0.208	0.29	0.45	0.89

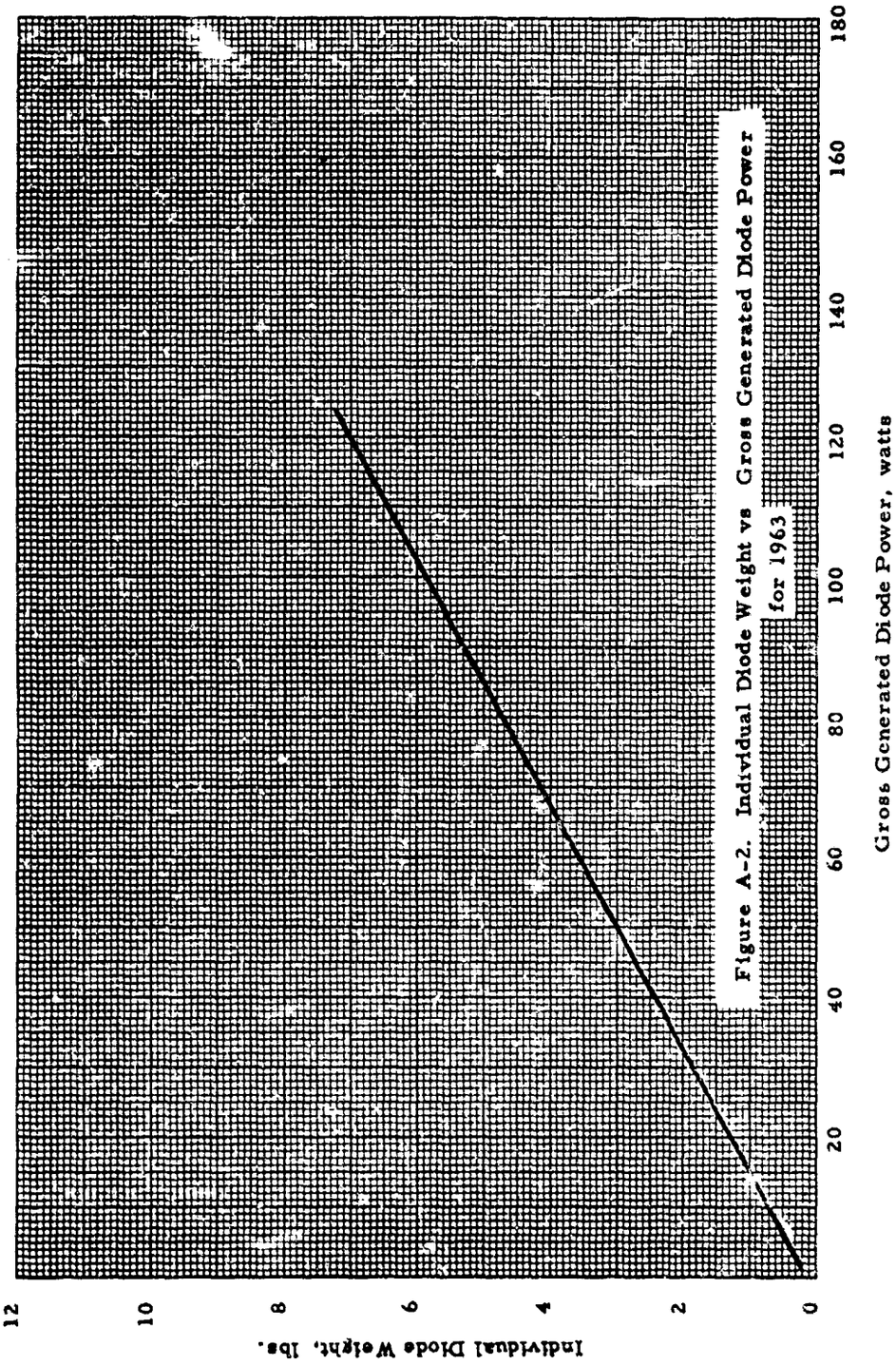

Figure A-2. Individual Diode Weight vs Gross Generated Diode Power for 1963

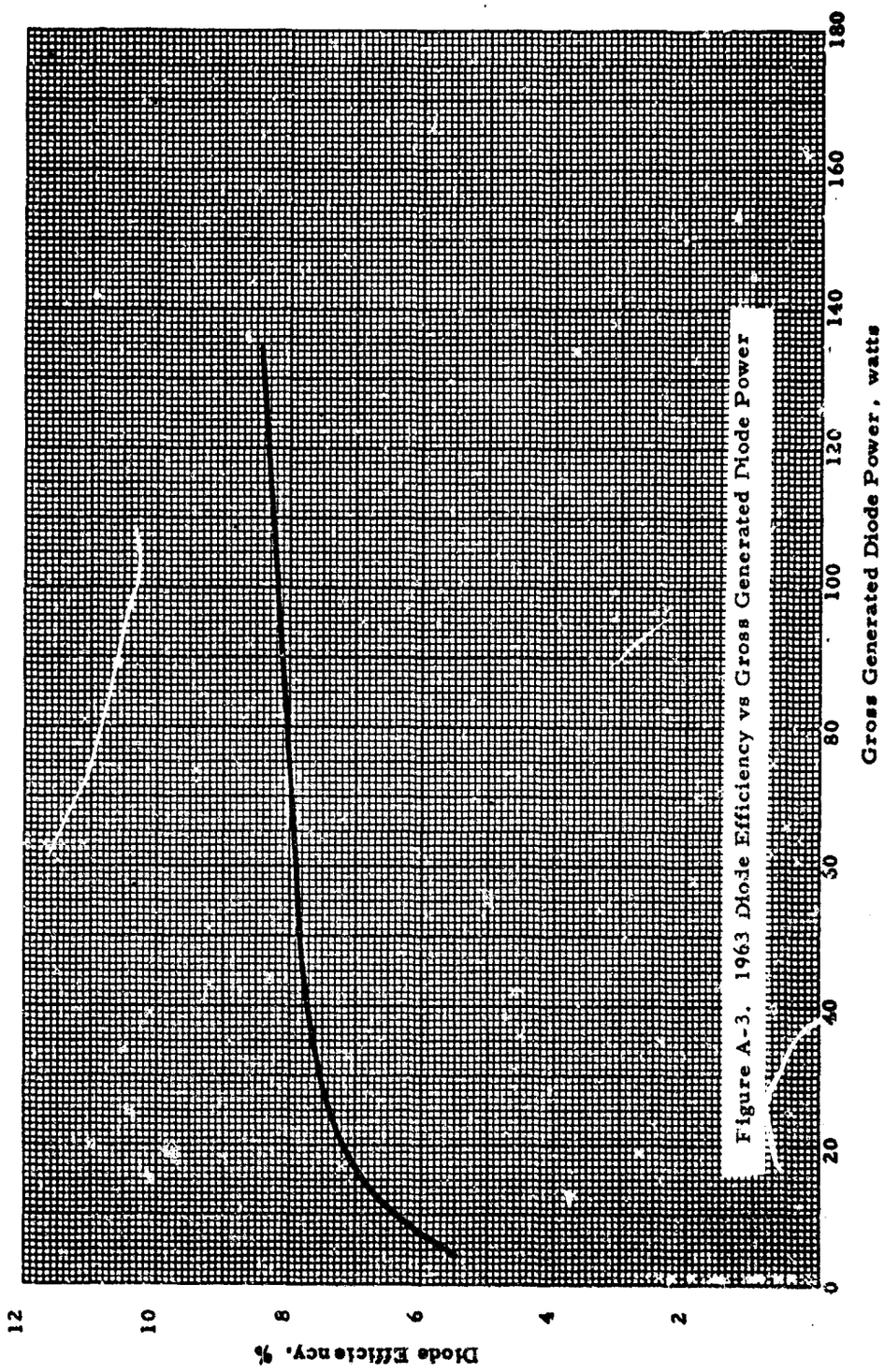

Figure A-3. 1963 Diode Efficiency vs Gross Generated Diode Power

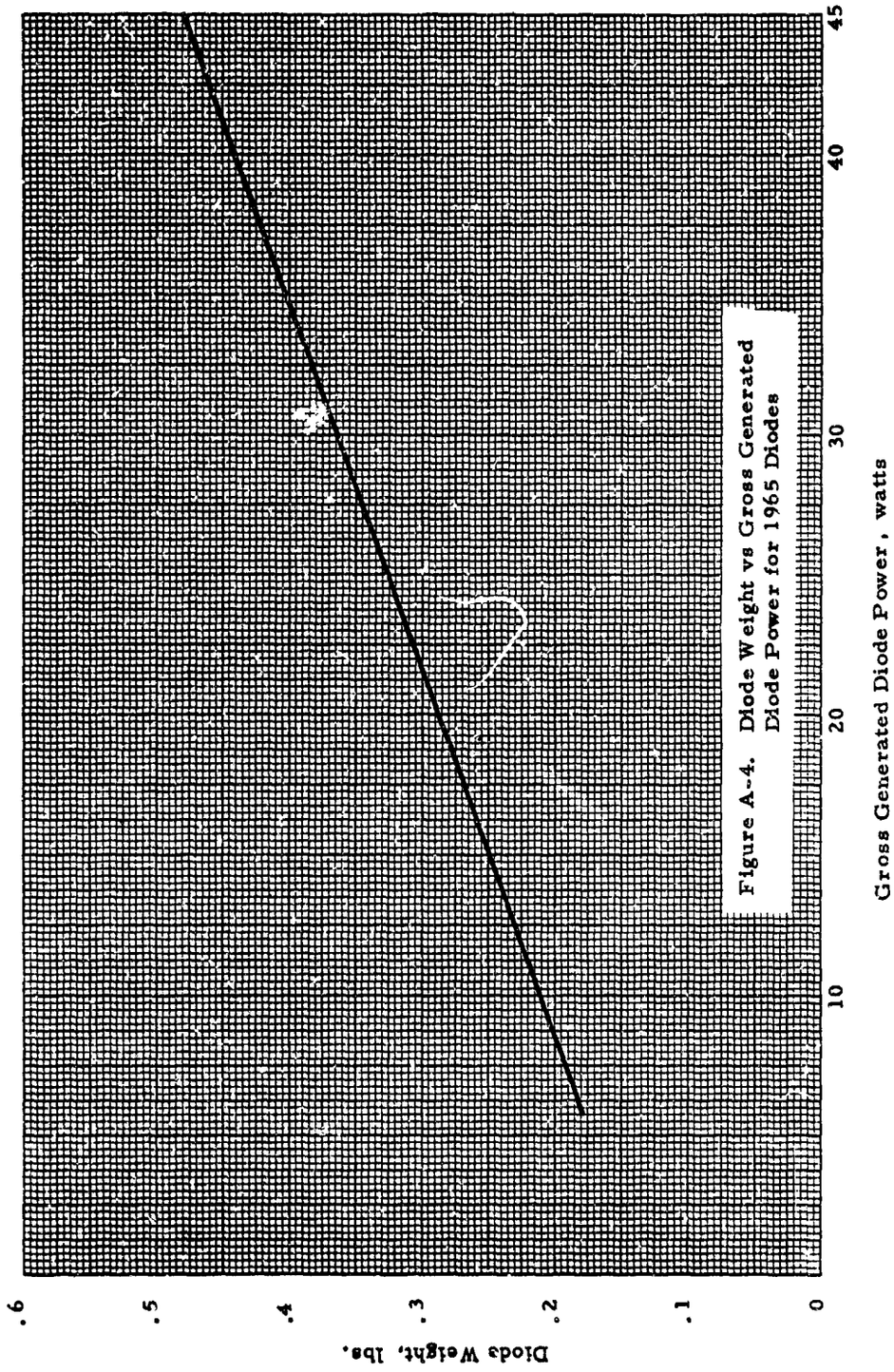

Figure A-4. Diode Weight vs Gross Generated Diode Power for 1965 Diodes

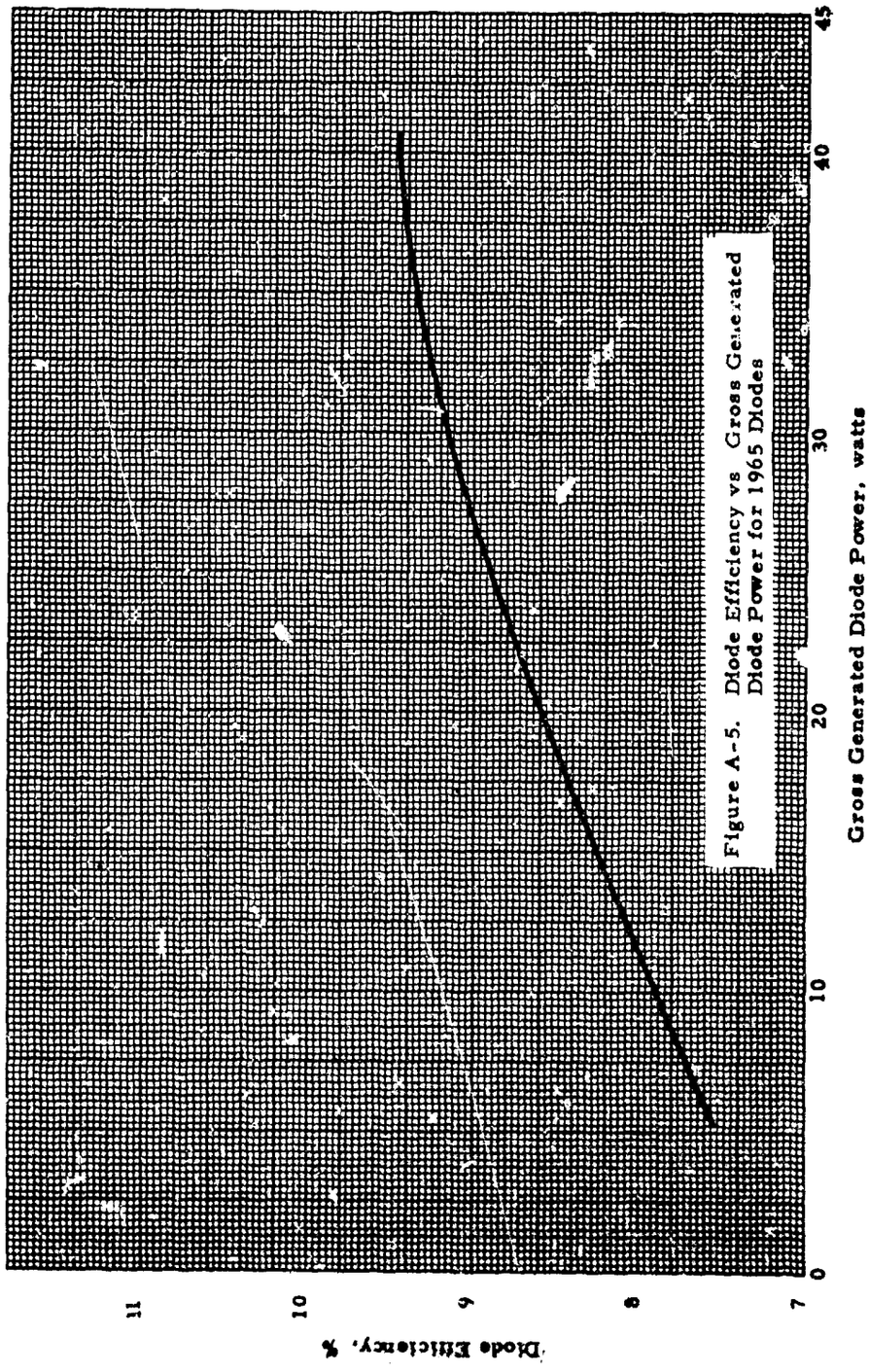

Figure A-5. Diode Efficiency vs Gross Generated Diode Power for 1965 Diodes

DC-DC CONVERTER

For any engine configuration with less than 12 diodes, and consequently with less than 6 v dc of output voltage, a dc-dc converter was required. In order to obtain data in this area, a specification was prepared calling for the conversion of 1.0, 2.0 and 4.0 volts dc to 6.0 volts dc. Output voltage ripple was to be held to 1% of mean, and each converter was to be specifically designed for its assigned input voltage. Output power was initially specified at 72 watts to account for the 45 watts delivered to the load, 15 watts to the fan, with an additional 12 watts allowed for automatic engine control, automatic cesium temperature controllers, and accessories. Various manufacturers of dc-dc converters were contacted, given the specifications, and asked to supply their estimates of overall efficiency, weight, volume and cost for 1963 and 1965 units. The component data supplied are shown in Tables A-3 and A-4 and Figures A-6 and A-7.

The weights and efficiencies quoted by the various organizations covered an extremely wide range. Since it was not clear which one to pick for analyzing a given system, the extreme values were chosen.

After the first results of the study were apparent, it was decided to investigate the 0.5-volt input system, a multi-valued dc-dc converter output (6, 12 and 28 v dc and 400 cps ac), and some systems calling for a 45-watt gross output dc-dc converter. In these latter systems only the load power passes through the converter. The accessory power is taken directly from the series-connected diodes.

FUEL LOAD

The next most important variable in the system was the weight of fuel, since it is the heaviest single item of the basic engine. A 12-diode engine was calculated to consume fuel at the rate of 0.5 lb per

TABLE A-3

WEIGHT AND EFFICIENCY OF

1963 DC-DC CONVERTER

Gross Output Power = 72 Watts at 6.0 Volts

Converter No. 1

Converter Input Voltage, volts	1.0	2.0	4.0
Efficiency, percent	70	77	85
Weight, lbs	4.5	4.0	3.5

Converter No. 2

Converter Input Voltage, volts	1.0	2.0	4.0
Efficiency, percent	82	85	92
Weight, lbs	6.5	6.25	5.7

Gross Output Power = 45 Watts at 6.0 Volts

Converter Input Voltage, volts	2.0
Efficiency, percent	86
Weight, lbs	5.5

TABLE A-4

WEIGHT AND EFFICIENCY OF

1965 DC-DC CONVERTER

Gross Power Output = 72 Watts at 6.0 Volts

Converter No. 1

Converter Input Voltage, volts	1.0	2.0	4.0
Efficiency, percent	73.5	81.0	89.2
Weight, lbs	4.05	3.6	3.15

Converter No. 2

Converter Input Voltage, volts	1.0	2.0	4.0
Efficiency, percent	87	89.3	94
Weight, lbs	6.0	5.77	5.3

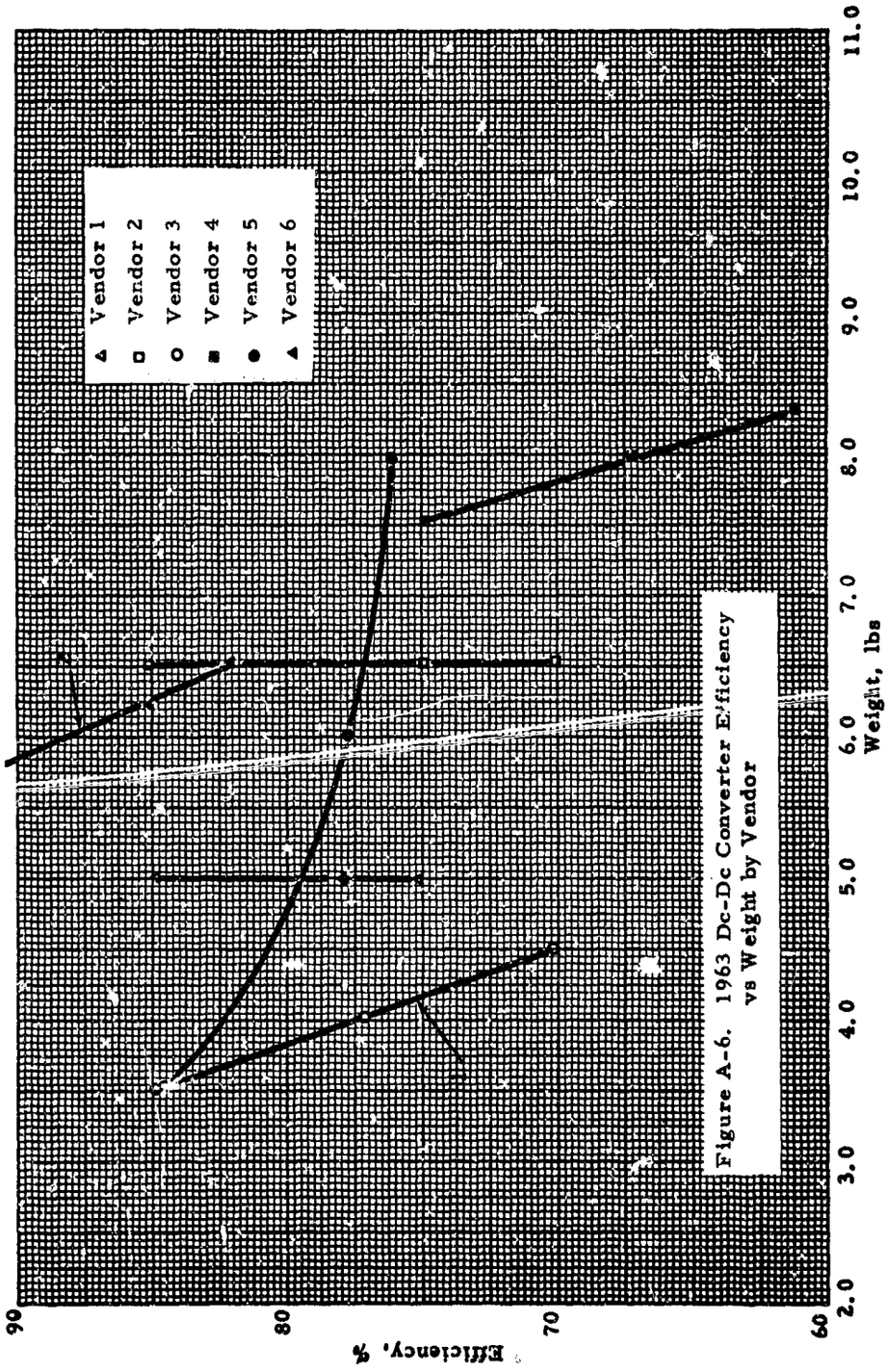

Figure A-6. 1963 Dc-Dc Converter Efficiency vs Weight by Vendor

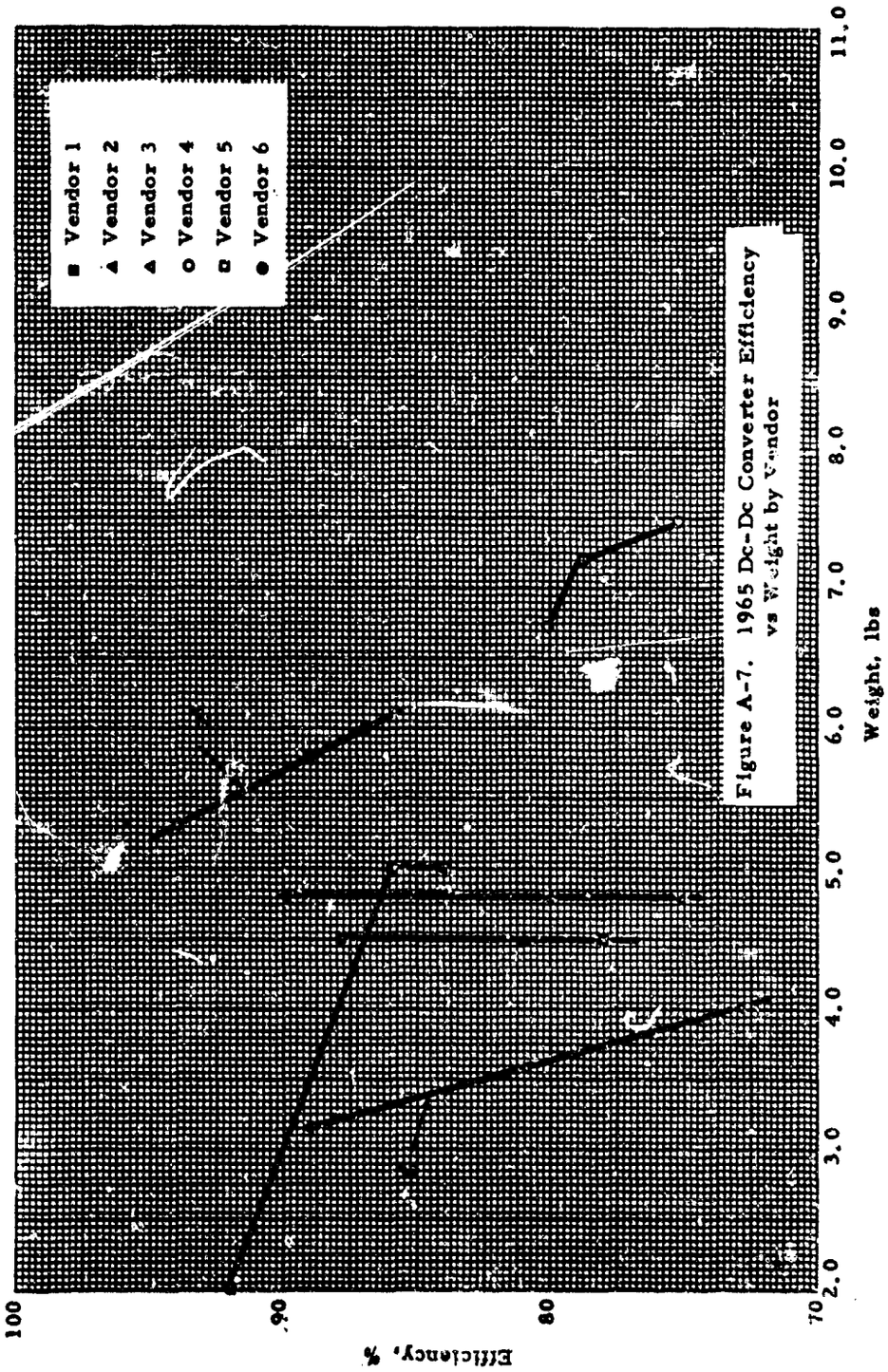

Figure A-7. 1965 Dc-Dc Converter Efficiency vs Weight by Vendor

hour for a gross output of 72 watts when the diodes were 5.75% efficient. In order to arrive at the fuel load for 12 hours for the other configurations, the combined efficiencies of the diode and converter were calculated. This value was ratioed to 5.75 and multiplied by 6.0 lbs (the basic engine fuel load).

COMBUSTION SYSTEM

The combustion system, i.e., the preheater, combustion chamber, fuel manifolds, injectors and thermal insulators, were sufficiently versatile so that it was assumed that neither weight nor efficiency would change by any significant margin for any system. The combustion system, therefore, was assigned a weight of 2.0 lbs (the calculated weight of the 12-diode engine) for all systems considered.

ACCESSORY SYSTEM

An interesting point became apparent during this study of the accessory system, namely, the possibility of using an ac electric motor to drive the fan when using a dc-dc converter in the engine. A form of ac power can be tapped from the output of the transistor used in the dc-dc converter and then fed into the electric motor. Unfortunately, it was not possible in the time available for this study to evaluate thoroughly all of the resulting possibilities in accessory system configuration.

One point in favor of an ac electric motor was its inherent low radio noise level. On the other hand, there seemed to be some reason to believe that the efficiency of a small ac motor would be lower than that for a dc motor, especially if the waveform of the supplied power was not truly sinusoidal. A dc motor would probably have to be shielded to avoid radio noise.

The radio shield would have a certain weight, which might or might not counteract any of the other advantages of a dc motor. Another factor in the choice of motor power requirements was that engine starting required a battery. If an ac motor was required this battery power would have to be fed through the dc-dc converter transistor, with a certain loss in power before going to the electric motor. It was assumed that the weight of each accessory system for all engines considered was equal to 1.5 lbs. This is the calculated weight of the system for an engine equipped with 12 series-connected 6-watt diodes.

RESULTS

The results of this system analysis can be summarized as follows: First, under any set of consistent assumptions, a system using 12 series-connected diodes had a lower weight than any other system. This is illustrated in Figure A-8, which compares the most significant possibilities (72 watts, dc-dc converter output, all accessories operating at 6-volt dc power, the number of diodes varying between 1 and 12). Second, the trade-off between a low-efficiency, low-weight dc-dc converter and a high-efficiency, high-weight dc-dc converter favors the lighter-weight unit for the component performance used. This conclusion certainly applied to 12-hour missions, but was probably not valid for much longer missions. None of the other allowable variations in engine configuration had any significant effect on total system weight.

Quite different conclusions were reached from the standpoint of cost. The cost of a 12-diode engine would be much higher than that of a one-diode engine with a converter. As a first example of cost savings, it was estimated that there was only a small difference in cost between a diode capable of generating 6 watts and one capable of generating

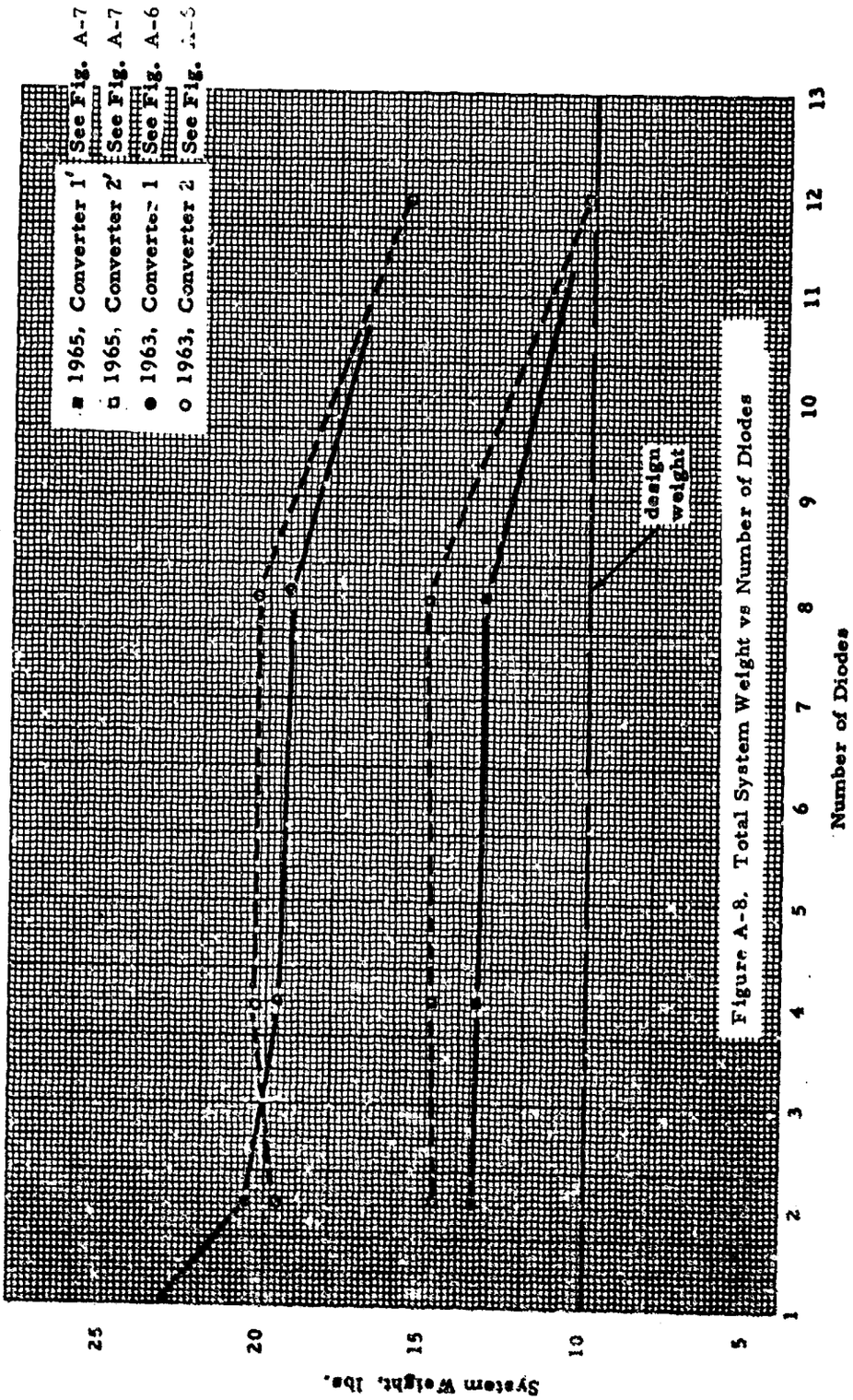

Figure A-8. Total System Weight vs Number of Diodes

100 watts. The cost of the dc-dc converter added to the cost of a 100-watt diode was lower by a factor of 3 to 5 than the 12 six-watt diodes this combination replaced. Obviously, the larger diode was also more useful in larger engines.

In view of the expectation that thermionic power supplies of a wide range of output powers would be useful to the Army if the developmental problems were solved, clearly a lower overall cost to the government would result when engines were purchased in one modular size. This advantage appeared to outweigh the somewhat greater weight at the 45-watt level, and consequently the program was redirected toward an engine using only one diode followed by a dc-dc converter.

APPENDIX B

SINGLE-DIODE 45-WATT ENGINE DESIGN

The comparison of a multi-diode versus a single-diode system for the 45-watt power supply (Appendix A) showed the single-diode approach to be best. Consequently such an engine was designed and is described here.

SUBSYSTEM DESCRIPTION

Figure B-1 shows the complete 45-watt generator in cross section. The thermionic converter (Series VI) is located at the bottom of the combustion chamber. Its emitter is at the top and the heat rejection fins are at the bottom.

The combustion system consists of a combustion chamber; an exhaust gas-to-air heat exchanger, which preheats the intake air; and a fuel injection system. The latter includes a carburetor using a stream of hot air tapped off one of the later stages of the heat exchanger to vaporize the fuel. The fuel then enters the combustion chamber through fuel injectors.

The accessory package consists of the following components: two electrically operated fans, one of which provides low-pressure air for the combustion system and the other cools the diode; a battery; an ignition coil; an engine control; a gasoline storage tank shaped to fit over the combustion system; a lightweight transport case; and various valves and ducts used for fluid transfer.

SYSTEM OPERATION

During steady-state operation, gasoline is gravity-fed from the storage tank into the carburetor, which, as indicated above, is also supplied with hot (1150° C) air tapped off the heat exchanger. This hot air is metered by a valve actuated by a bi-metallic helix. Another air line coming directly from the fan conducts cold air into the carburetor. The two air streams meet inside the carburetor, and the mixture enters the fuel-vaporizing section. At the interface between the air mixer and vaporizer, the bi-metallic helix senses mixed air temperature and adjusts the hot-air valve setting to hold the mixed air temperature at about 300° C.

The vaporizing section of the carburetor consists of a bank of horizontal fine-mesh stainless steel screens about 1/2 inch wide and 2 inches long, stacked vertically with 1/16-inch air gaps between each. The liquid fuel is distributed in a large tube above these screens so that fuel drops over the length of the upper screen. The tempered (300°C) air flows around and through the cascade of fuel-soaked screens and vaporizes the fuel.

The fuel-air ratio of the carburetor exit stream is about 10 times the stoichiometric value (fuel-rich). This stream is ducted into an insulated circumferential manifold which leads to the radial fuel injectors.

The fuel rate to the carburetor is metered by a standard shallow angle (1°) needle valve. A float valve holds a constant head of liquid fuel on this metering valve so that the effective area of the

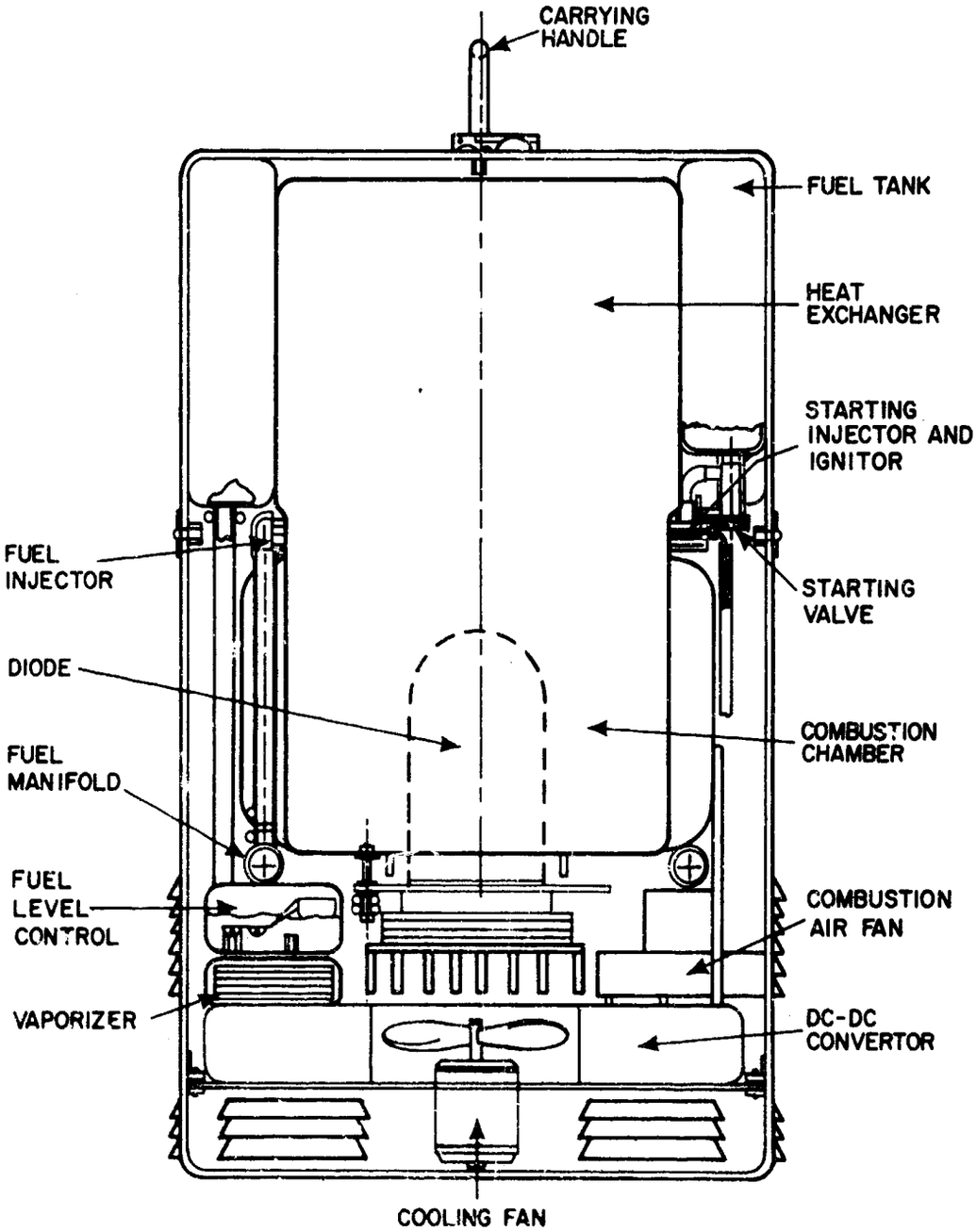

Figure B-1. Cross Section of Complete 45-Watt Generator.

orifice is the only variable affecting liquid fuel flow. The chamber of the float valve is equipped with a vent connected directly to the carburetor exit so that vapor lock cannot occur.

The output of a cooling fan is ducted into the finned region of the diode. After cooling the collector, the air is discharged. This fan is located within and also cools the dc-dc converter. A second fan provides combustion air. After traversing a part of the exchanger, when the combustion air reaches 1150° C, approximately 3 to 5% of it is diverted to the carburetor and then ultimately through the fuel injector. The remainder flows directly into the combustion chamber. There the highly preheated air and fuel are mixed and burn.

Diode operation at a given operating point can be optimized by controlling the temperature of the cesium reservoir, which determines the cesium pressure in the interelectrode spacing. Control of the cesium temperature is achieved with a thermal shunt between the burner and the cesium reservoir, designed to supply slightly less than the required amount of heat to the reservoir when the diode is at operating temperature and maximum ambient temperature conditions exist. An auxiliary electrical resistance heater supplied with 6 volts of power and controlled by a small solid-state amplifier is used. An increasing amount of electrical power is used as the ambient temperature drops. The maximum power requirement of this system is expected to be of the order of 0.5 - 2.0 watts.

The power generated by the diode is fed directly into the dc - dc converter adjacent to it, which then produces the required 6-volt output voltage.

The procedure for starting the engine is as follows: The operator throws a switch which connects a 6-volt battery to the input leads of the fan motors. The combustion air fan has a rating of 4-1/2 volts and 2 amperes at 15,000 rpm and can deliver 16 lbs of air per hour against a back pressure of 2 inches of water. During the start cycle, when 6 volts are applied to the motor and the pressure drop through the burner is relatively low, the air flow delivery will be about 50 lbs per hour. Then another switch will be thrown, and the battery will also power an integral breaker-point ignition coil which will supply a spark for ignition. A starting fuel injector is provided which combines a liquid-fuel injector and high-tension spark leads. When the spark is established, the operator will turn the fuel control to the "start" position, which will meter the correct amount of fuel to the burner. This fuel flow will be of the order of 3 to 4 times the steady-state value, since the air flow is about 3 times greater during the start cycle and the f/a will be very close to the value yielding the maximum flame temperature.

This mode of operation will be held for approximately 2 to 2-1/2 minutes, during which time the unit will be driven to approximately half its rated emitter temperature. At the end of this 2 to 2-1/2 minute period, the air outlet temperature of the preheater will be high enough to operate the vaporizing carburetor. The operator then turns the fuel control to the intermediate indent, and the same total amount of fuel will be divided between the carburetor and the starting fuel injector. The temperature of the unit will then rise very rapidly to design emitter temperature. At this point an "on-off"

indicator will show the operator that the diode is producing rated power. He will then turn the fuel control to the "run" position, reducing the fuel flow to its nominal value of 0.5 lb/hour, and simultaneously switch the electric motor to draw 4-1/2 v of power from the converter. Steady-state full-power operation will then have been established in a minimum period of time.

For starting under the extremely low ambient temperature, the engine accessory system will be equipped with a large-diameter fan which can generate the required pressure at a speed of approximately 4500 rpm. Instead of using battery power, a speed-increasing gear train will be driven by the operator through a manual crank. Instead of an integral breaker-point ignition coil, a mechanical breaker point will be driven off the cranked shaft, and electric power for the spark will be generated by the permanent-magnet electric motor operating as a low-efficiency dc generator. All other functions will be identical to that described above.

Shut-down is accomplished simply by shutting off the supply of gasoline to the carburetor. Air will continue to circulate through the heat exchanger and combustion chamber so that the unit will gradually be cooled to ambient temperature. For transport, a clam-shell Fibreglass case is closed and latched. As shown in Figure B-1, this case consists of three pieces of molded Fibreglass, hinged together with waterproof rubber seals at all interfaces. Military-type latches provide the pressure required to make the unit completely submersible in water.

UNCLASSIFIED

Security Classification

DOCUMENT CONTROL DATA - R&D

(Security classification of title, body of abstract and indexing annotation must be entered when the overall report is classified)

1. ORIGINATING ACTIVITY *(Corporate author)* Thermo Electron Corporation, 85 First Avenue, Waltham, Massachusetts	2a. REPORT SECURITY CLASSIFICATION Unclassified 2b. GROUP

3. REPORT TITLE

DEVELOPMENT OF A GASOLINE-FIRED THERMIONIC POWER SUPPLY

4. DESCRIPTIVE NOTES *(Type of report and inclusive dates)*

Final Report November 1961 - July 1966

5. AUTHOR(S) *(Last name, first name, initial)*

Lazaridis, Lazaros J.
Pantazelos, Peter G.

6. REPORT DATE January 1968	7a. TOTAL NO. OF PAGES 160	7b. NO. OF REFS
8a. CONTRACT OR GRANT NO. DA36-039-SC-87341(E) b. PROJECT NO. 1T6-22001-A-053 c. Task No. 1T6-22001-A-053-01 d. Subtask No. -09	9a. ORIGINATOR'S REPORT NUMBER(S) TE4017-40-68 9b. OTHER REPORT NO(S) *(Any other numbers that may be assigned this report)* ECOM-87341-1	

10. AVAILABILITY/LIMITATION NOTICES

11. SUPPLEMENTARY NOTES	12. SPONSORING MILITARY ACTIVITY U. S. Army Electronics Command Ft. Monmouth, N. J. (AMSEL-KL-PE)

13. ABSTRACT

~~This~~ report summarizes the work performed by ~~Thermo-Electron Corporation~~ to develop a gasoline-fired thermionic power supply. The work is divided into three phases:

1. The development of a gasoline burner capable of providing the high temperatures and high heat fluxes required by the thermionic converters.

2. The development of a thermionic converter with the required power output, efficiency, weight and life.

3. The design of a power supply utilizing the above two components and including power conditioning, controls and packaging.

The development of suitable oxidation protection for the converter's refractory-metal emitter is described, as well as the experimental evaluation of a variety of materials under conditions simulating a flame-heated thermionic converter. The development work on a flame-heated thermionic converter culminated in the recently completed Series VI-S Converter. The design, construction, and test of the potassium heat pipe used for collector cooling are also described. Test data is given, and a system design is presented.

DD FORM 1 JAN 64 1473

UNCLASSIFIED

Security Classification

UNCLASSIFIED

Security Classification

14. KEY WORDS	LINK A ROLE	LINK A WT	LINK B ROLE	LINK B WT	LINK C ROLE	LINK C WT
Thermionics						
Thermionic Power Supply						
Silent Power Supply						
Multi-fuel Silent Power Supply						
Power Supply						
Energy Converter						
Battery Charger						
Oxidation Resistant Coating						
Compact Heat Exchanger						
Heat Pipe						
Silicon Carbide						
Vapor Deposited Tungsten						
Vapor Deposited Silicon Carbide						
Recuperative Burner						

INSTRUCTIONS

1. ORIGINATING ACTIVITY: Enter the name and address of the contractor, subcontractor, grantee, Department of Defense activity or other organization *(corporate author)* issuing the report.

2a. REPORT SECURITY CLASSIFICATION: Enter the overall security classification of the report. Indicate whether "Restricted Data" is included. Marking is to be in accordance with appropriate security regulations.

2b. GROUP: Automatic downgrading is specified in DoD Directive 5200.10 and Armed Forces Industrial Manual. Enter the group number. Also, when applicable, show that optional markings have been used for Group 3 and Group 4 as authorized.

3. REPORT TITLE: Enter the complete report title in all capital letters. Titles in all cases should be unclassified. If a meaningful title cannot be selected without classification, show title classification in all capitals in parenthesis immediately following the title.

4. DESCRIPTIVE NOTES: If appropriate, enter the type of report, e.g., interim, progress, summary, annual, or final. Give the inclusive dates when a specific reporting period is covered.

5. AUTHOR(S): Enter the name(s) of author(s) as shown on or in the report. Enter last name, first name, middle initial. If military, show rank and branch of service. The name of the principal author is an absolute minimum requirement.

6. REPORT DATE: Enter the date of the report as day, month, year; or month, year. If more than one date appears on the report, use date of publication.

7a. TOTAL NUMBER OF PAGES: The total page count should follow normal pagination procedures, i.e., enter the number of pages containing information.

7b. NUMBER OF REFERENCES: Enter the total number of references cited in the report.

8a. CONTRACT OR GRANT NUMBER: If appropriate, enter the applicable number of the contract or grant under which the report was written.

8b, 8c, & 8d. PROJECT NUMBER: Enter the appropriate military department identification, such as project number, subproject number, system numbers, task number, etc.

9a. ORIGINATOR'S REPORT NUMBER(S): Enter the official report number by which the document will be identified and controlled by the originating activity. This number must be unique to this report.

9b. OTHER REPORT NUMBER(S): If the report has been assigned any other report numbers *(either by the originator or by the sponsor)*, also enter this number(s).

10. AVAILABILITY/LIMITATION NOTICES: Enter any limitations on further dissemination of the report, other than those imposed by security classification, using standard statements such as:

(1) "Qualified requesters may obtain copies of this report from DDC."

(2) "Foreign announcement and dissemination of this report by DDC is not authorized."

(3) "U. S. Government agencies may obtain copies of this report directly from DDC. Other qualified DDC users shall request through _____."

(4) "U. S. military agencies may obtain copies of this report directly from DDC. Other qualified users shall request through _____."

(5) "All distribution of this report is controlled. Qualified DDC users shall request through _____."

If the report has been furnished to the Office of Technical Services, Department of Commerce, for sale to the public, indicate this fact and enter the price, if known.

11. SUPPLEMENTARY NOTES: Use for additional explanatory notes.

12. SPONSORING MILITARY ACTIVITY: Enter the name of the departmental project office or laboratory sponsoring *(paying for)* the research and development. Include address.

13. ABSTRACT: Enter an abstract giving a brief and factual summary of the document indicative of the report, even though it may also appear elsewhere in the body of the technical report. If additional space is required, a continuation sheet shall be attached.

It is highly desirable that the abstract of classified reports be unclassified. Each paragraph of the abstract shall end with an indication of the military security classification of the information in the paragraph, represented as *(TS)*, *(S)*, *(C)*, or *(U)*.

There is no limitation on the length of the abstract. However, the suggested length is from 150 to 225 words.

14. KEY WORDS: Key words are technically meaningful terms or short phrases that characterize a report and may be used as index entries for cataloging the report. Key words must be selected so that no security classification is required. Identifiers, such as equipment model designation, trade name, military project code name, geographic location, may be used as key words but will be followed by an indication of technical context. The assignment of links, rules, and weights is optional.

UNCLASSIFIED

Security Classification